https://doi.org/10.15388/vu.thesis.488
http://orcid.org/0000-0002-0853-6980

VILNIUS UNIVERSITY

Povilas Tarailis

Evaluation of electrical brain activity of the resting state: relation with subjective experiences

DOCTORAL DISSERTATION

Natural Sciences,
Biophysics (N 011)

VILNIUS 2023

The dissertation was prepared between 2018 and 2022 at Vilnius University.

Academic supervisor – Dr. Inga Griškova-Bulanova (Vilnius University, Natural Sciences, Biophysics – N 011)

This doctoral dissertation will be defended in a public/closed meeting of the Dissertation Defence Panel:

Chairman – Prof. Dr. Aidas Alaburda (Vilnius University, Natural Sciences, Biophysics – N 011).
Members:
Dr. Marek Binder (Jagiellonian University, Poland, Social Sciences, Psychology, S 006),
Prof. Dr. Aleksandr Bulatov (The Lithuanian University of Health Sciences, Natural Sciences, Biology – N 010),
Dr. Kastytis Dapšys (Vilnius university, Natural Sciences, Biophysics – N 011),
Dr. Grace Wang (University of Southern Queensland, Australia, Natural Sciences, Biophysics – N 011).

The dissertation shall be defended at a public meeting of the Dissertation Defence Panel at 10 hour on 4th of July 2023 in Room R-401 of the Faculty Life Sciences Center
Address: Sauletekio av.,7 No., Room No., Vilnius, Lithuania
Tel. +370 5 223 4419; e-mail: info@gmc.vu.lt

The text of this dissertation can be accessed at the libraries of Vilnius university, as well as on the website of Vilnius University:
www.vu.lt/lt/naujienos/ivykiu-kalendorius

https://doi.org/10.15388/vu.thesis.488
http://orcid.org/0000-0002-0853-6980

VILNIAUS UNIVERSITETAS

Povilas Tarailis

Smegenų ramybės būsenos įvertinimas: ryšys su subjektyviais potyriais

DAKTARO DISERTACIJA

Gamtos mokslai,
Biofizika (N 011)

VILNIUS 2023

Disertacija rengta 2018–2022 metais Vilniaus universitete

Mokslinė vadovė – dr. Inga Griškova-Bulanova (Vilniaus universitetas, gamtos mokslai, biofizika – N 011)

Gynimo taryba:
Pirmininkas (-ė) – **Prof. Dr. Aidas Alaburda** (Vilniaus universitetas, gamtos mokslai, biofizika – N 011).
Nariai:
Dr. Marek Binder (Jogailos universitas, Lenkija, socialiniai mokslai, psichologija, S 006),
Prof. Dr. Aleksandr Bulatov (Lietuvos Sveikatos mokslų universitetas, gamtos mokslai, biologija – N 010),
Dr. Kastytis Dapšys (Vilniaus universitetas, gamtos mokslai, biofizika – N 011),
Dr. Grace Wang (Pietų Kvynslando universitetas, Australija, gamtos mokslai, biofizika – N 011).

Disertacija ginama viešame Gynimo tarybos posėdyje 2023 m. liepos mėn. 4 d. 10 val. Vilniaus universiteto Gyvybės mokslų centro R-401 auditorijoje. Adresas: Saulėtekio al. 7, Vilnius, Lietuva, tel. +370 5 223 4419; el. paštas: info@gmc.vu.lt.

Disertaciją galima peržiūrėti Vilniaus universiteto bibliotekoje ir VU interneto svetainėje adresu: *https://www.vu.lt/naujienos/ivykiu-kalendorius*

CONTENTS

ABBREVIATIONS

ARSQ – Amsterdam Resting State Questionnaire

BF – Bayes Factor

EEG – Electroencephalography/Electroencephalogram

DAN – Dorsal Attention Network

DMN – Default Mode Network

FFT – Fast Fourier Transform

fMRI – functional Magnetic Resonance Imaging

f-PCA – frequency Principal Component Analysis

GEV – Global Explained Variance

GFP – Global Field Power

GFS – Global Field Synchronization

GMD – Global Map Dissimilarity

MEG – Magnetoencephalography

MDS – Multi Dimensional Scaling

LORETA - Low Resolution Electromagnetic Tomography

PET – Positron Emission Tomography

TMS - Transcranial Magnetic Stimulation

1. INTRODUCTION

Resting state is a brain mapping method to evaluate brains activity which happens when no task is performed (Rosazza and Minati, 2011). During last three decades resting state brain imaging approach gained a lot of attention and popularity in cognitive and clinical neuroscience, due to its simplicity for patients, straightforward standardization, and sensitivity to brain disorders. Research using this approach showed that instead of being inactive, brain works in self-organized manner and shows high activity. Various data acquisition and analysis methods are used to investigate this constant activity, leading to different interpretations regarding brain's spatial and temporal organization. Early functional magnetic resonance (fMRI) studies showed that during resting state sessions brain displays synchronous activity, similar to the one observed while participants were engaged in a task (Biswal et al., 1995; Raichle et al., 1996).

Despite the easy implementation, the resting state approach can be sensitive to the potential phenomenological heterogeneity of subjective experiences, which can differ between and within people (Hurlburt et al., 2015; Smallwood and Schooler, 2015, 2006; Weinstein, 2018). Unlike the participants' experience during studies implementing tasks where it is generally assumed that all participants are engaged in the same mental activity, mind – wandering or daydreaming occurring during resting state session is unconstrained and can be driven by both internal and external sources (Gorgolewski et al., 2014; Smallwood and Schooler, 2015). This spontaneous activity fluctuates from one moment to the next and participants find themselves drawn into thoughts about the past, plans for the future, or self- and other-directed reflection (Smallwood and Schooler, 2006; Zanesco et al., 2021a).

Different analysis methods are applied to evaluate resting state activity obtained using different brain imaging modalities. Among these modalities, electroencephalography (EEG) has been widely applied. EEG reflects the electrical brain's activity and the signal carries the information about power, phase, complexity, spatio-temporal patterns.

Most common way to evaluate resting state EEG is power analysis. Unfortunately, the boundaries between frequency ranges are arbitrary set (Newson and Thiagarajan, 2019) which can affect the interpretation the the results and comparison between the studies. Thus, to overcome this problem frequency principal component analysis was suggested as a way to decompose EEG signal into meaningful distinct components with the inherent advantage of providing a data-driven approach across the traditional bands (Barry and

De Blasio, 2018; Dien, 2012). The method has been applied in several healthy and clinical populations.

To asses functional connectivity between brain areas, certain phase evaluation methods has been introduced (for review (Van Diessen et al., 2015)). Unfortunately, these parameters suffer from certain methodological challenges which most of the time are ignored. Lehmann and colleagues (Lehmann et al., 2006) showed that significant relationship between the electrodes changes by changing the reference electrode. Thus, the need to evaluate phase synchronization, which is not dependent on reference electrode is crucial. Koenig et al., (Koenig et al., 2001) introduced references independent parameter to evaluate global functional connectivity – global field synchronization. The method was successfully applied in both – clinical and healthy -populations.

Another popular way to evaluate resting state EEG is microstate analysis (Khanna et al., 2015). With the microstate approach, the recorded electrical signal is defined by non-overlapping distinct topographies (Khanna et al., 2015; Koenig et al., 2002) which, through competitive fitting based on spatial correlation, are fitted back to the original signal. Unfortunately, most of the time, number of microstates to extract is predefined, which can cause spatially similar but functionally different microstate be merged into one cluster (Custo et al., 2017), which can cause the misattribution of the functional roles. Thus, estimation of the optimal number of microstates is crucial for analysis.

It is evident, that constantly changing mentation makes it challenging to relate ongoing subjective mental activity with observed biological signals. Several different approaches to measure and quantify mind – wandering exist for both, task related and resting state sessions (Weinstein, 2018). The objective/indirect approach measures behavioral aspects such as reaction times (Cheyne et al., 2006) or eye movements (Reichle et al., 2010), while subjective/direct approach focuses on self-reports of participants' internal states. Subjective/direct approach can be further divided into self – caught, where participants at any moment in time can report their subjective experience or when their attention has shifted away from that task, and probe – caught, where participants are stopped or indicated to remember the subjective experiences and mind-wandering, approaches.

Despite these approaches being popular, they require more elaborate experiment design. Thus, to collect retrospective experiences over a short period of resting state using a specified questionnaire is easier and faster way. Several different resting state questionnaires were developed and used in brain imaging and behavioral studies (Delamillieure et al., 2010; Diaz et al., 2014,

2013; Gorgolewski et al., 2014). These self – report questionnaire covers several aspects of mind – wandering and gives a standardized way to quantify the ongoing experience. Balancing groups based on their cognitive states could lead to bigger group differences which would help to improve the interpretation of the findings and increase the sensitivity and specificity of neuroimaging biomarkers in clinical and pharmacological studies (Diaz et al., 2013).

1.1 Aim and objectives

This work aimed to investigate the relationship between subjective experiences reported by the participants during the resting state session and neurophysiological indices of brain activity measured with EEG with the focus on power, phase synchronization and topographical aspects. The objectives were as follow:

1. To relate subjective experiences of participants with the loadings of frequency principal components of the resting-state EEG power.
2. To relate subjective experiences of participants with the global field synchronization of the resting-state EEG.
3. To relate subjective experiences of participants with temporal parameters of EEG microstates.

1.2 Scientific novelty

1. For the first time subjective experiences were related with the data-driven method in a frequency domain using frequency principal component analysis.
2. For the first time subjective experiences were related with global functional connectivity assessed using global field synchronization.
3. For the second time subjective experience was related with temporal parameters of the data-driven EEG microstates.

1.3 Practical implications

1. Global field synchronization in alpha (8-13 Hz) and beta (13-30 Hz) frequency ranges can be used to quantify subjective experience of Comfort as measured with Amsterdam Resting State Questionnaire.
2. Neural activity in alpha (9 Hz) and theta (5.5 Hz) ranges can be used to quantify subjective experience of Comfort and Sleepiness as measured with Amsterdam Resting State Questionnaire.

3. Coverage of microstate F can be used to quantify subjective ratings of Somatic Awareness; occurrence rate of microstate B and duration of microstate D can be used to quantify subjective ratings of Self related thoughts; occurrence rate of microstate C can be used to quantify subjective ratings of Comfort; duration of microstates E and G can be used to quantify subjective ratings of Comfort as measured with Amsterdam Resting State Questionnaire.

1.4 Statements to be defended

1. Global Field Synchronization values of alpha (8-13 Hz) and beta (14-30 Hz) frequency ranges correlate with subjective rating of Comfort.
2. Loading scores of principal components of theta and alpha frequency correlate with subjective levels of sleepiness and comfort.
3. Temporal parameters of EEG microstates are related with distinct domains of Amsterdam Resting State Questionnaire.

2. LITERATURE REVIEW

2.1 Electroencephalography

Electroencephalography (EEG) is a powerful and one of the most used brain imaging method for noninvasive studies of the electrophysiological dynamics of the brain and for linking those dynamics to cognition, disease and (dys)functions (Michel and Murray, 2012). EEG signal consists of different oscillating electrical voltages - brain waves - reflecting brain's electrical activity. The method has a variety of research and clinical applications in humans and animals: it is used to monitor alertness (Bréchet et al., 2020; Brodbeck et al., 2012; Massimini et al., 2005), coma states and brain death (Binder et al., 2020; Gobert et al., 2018); to investigate and monitor changes in neurological and psychiatric disorders (Koenig et al., 2001; Nishida et al., 2013; Smailovic et al., 2019); to monitor sleep disorders (Tan et al., 2012; Wei and Van Someren, 2020); to locate areas of damage following head injury (Haveman et al., 2019), stroke (Zappasodi et al., 2017); to assess cognitive functions (Beppi et al., 2021); to assess influence of drugs and pharmacological substances (Prashad et al., 2018; Vejmola et al., 2021; Yoshimura et al., 2007); to monitor brain development (Angelini et al., 2023; Bagdasarov et al., 2022); as a tool in brain-computer interface or biofeedback setups (Asai et al., 2022; Diaz Hernandez et al., 2016).

EEG reflects changes of the electrical potentials occurring in a large number of synchronized cortical pyramidal neurons (Cohen, 2017; Jackson and Bolger, 2014). For EEG signal to be recorded, these neurons must be arrange 1) in parallel fashion, otherwise, the individual dipoles' positive and negative ends will sum and cancel each other out, and 2) work synchronously, in order to produce a large enough signal to be measured on a scalp surface (Cohen, 2017; Jackson and Bolger, 2014) (Figure 1).

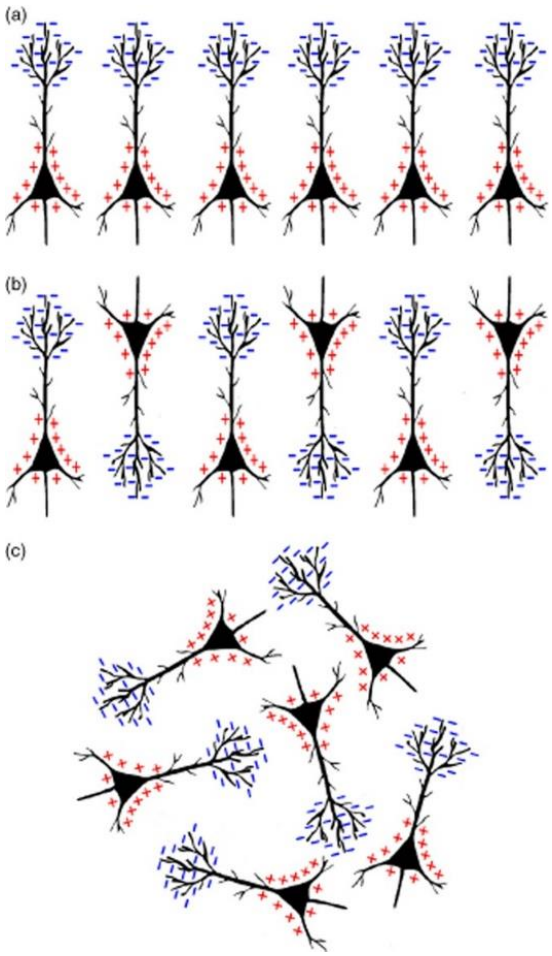

Figure 1. Neurons arraignment and synchronous activity allows electrical signal to be recorded (a); Dyssynchronous activity cancel each other out (b); No clear dipole emerges from random arrangement of positive and negative charge pools, so no signal is measurable at the scalp (c) (Jackson and Bolger, 2014)

EEG has many advantages over other brain imaging methods, including high temporal precision, low maintenance cost, ability being portable (LaRocco et al., 2020; Looney et al., 2012). However, it is generally stated that EEG lacks substantial spatial resolution due to the fact that electrical signal must go through different resistive layers (cerebrospinal fluid, skull, skin) which provides a distorted view of the brain activity resulting in a spatial resolution of around 5 to 9 cm (Burle et al., 2015; Nunez et al., 1994). However, using sophisticated source localization algorithms combined with high density EEG systems (64 or more channels) and anatomical information

of the head, EEG provides a sufficient information about the underlying sources (Brunet et al., 2011; Ferree et al., 2001; Hedrich et al., 2017; Michel et al., 2004; Michel and Brunet, 2019) making it an important and affordable brain imaging tool.

2.2 Spectral properties of EEG

The recorded EEG signal is a complex signal, that contains frequencies, amplitude, phase, global activity patterns, complexity, morphology information. Thus, EEG signal can be analyzed using different analysis approaches focusing on these features. Furthermore, each of these features can be analyzed applying different mathematical procedures. For instance, to assess connectivity between the regions or between the electrodes phase lag index (Stam et al., 2007), phase lag value (Lachaux et al., 1999) or coherence (Bowyer, 2016) methods can be used.

The power spectral analysis of EEG is well established and one of the most commonly applied methods for the EEG analysis. (Bai et al., 2017). The power spectral analysis uses signal decomposition methods, for example, Fast Fourier Transform (FFT), to convert EEG signal from time domain (amplitude vs. time) to frequency domain (amplitude vs. frequency) which reflects the magnitude of the frequency components (Liu et al., 2021) and can be interpreted as the amount of the activity in certain frequency or frequency bands (Xiao et al., 2018).

The frequencies are divided into distinguished frequency bands: delta (0.5–3.5 Hz), theta (4-7.5 Hz), alpha (8-13 Hz), beta (14-30 Hz) and gamma (30-100 Hz). Each of these frequency bands are associated with distinct functions and can be affected by various neuropsychiatric disorders and vigilance states. Changes of frequency bands properties can be used as a biomarker for certain neurophysiological disorders such as Parkinson's disease (Miladinovic et al., 2021; Vecchio et al., 2021), schizophrenia (Boutros et al., 2007; Koenig et al., 2012b), depression (Grin-Yatsenko et al., 2009; Knott et al., 2001) and many more. For instance, a commonly reported phenomena is reduced complexity of the EEG signal (Tait et al., 2020) and the slowing of resting state EEG or MEG activity measured as a decrease in alpha and increase in theta band activity (Babiloni et al., 2016; Grunwald et al., 2002; Montez et al., 2009; Simpraga et al., 2017) in Alzheimer's disease.

The boundaries between the different frequency bands can vary across studies and labs, with some bands further being divided into sub-bands with distinct sources and functions (Groppe et al., 2013; Newson and Thiagarajan, 2019; Tenke and Kayser, 2005). For instance a review paper by Newson and

Thiagarajan (Newson and Thiagarajan, 2019) revealed big variability and confusion as to the specific frequency range that defines each band. Out of 184 clinical studies reviewed in their paper, across all bands the most frequently used range was found in only 30- 50% of studies depending on the particular band. While theta and alpha were more or less consistent, delta band could begin anywhere between 0 Hz to 2 Hz and end anywhere from 3.5 Hz to 6 Hz. Meanwhile, beta band could begin anywhere between 12 Hz and 15 Hz and end anywhere between 20 Hz and 50 Hz. Thus, what one publication defines as 'delta' or 'beta' is therefore not necessarily the same as what is defined in another publication using the same terminology (Newson and Thiagarajan, 2019). Consequently, this kind of approach makes the evaluation process biased and results difficult to generalize.

2.3 Frequency-Principal Component Analysis

Principal component analysis (PCA), is a widely used data dimensionality reduction method, which increases interpretability of the data and minimizes information loss (Jollife and Cadima, 2016). PCA creates new variables that are linear functions of the original dataset variables. Thus, to overcome the high number of individual variables and rather than using simple mean measures of some sort, frequency PCA (f-PCA) was proposed to decompose the EEG frequency spectral structure into meaningful distinct components with the inherent advantage of providing a data-driven approach across the traditional bands (Barry and De Blasio, 2018; Dien, 2012; Tenke and Kayser, 2005). This approach has been successfully implemented in both healthy and clinical samples. Previous studies compared f-PCA outcomes in young and older subjects (Barry et al., 2019), and in young adults and children (Rodríguez Martinez et al., 2012), and attributed observed differences to the effect of brain maturation. Moreover, f-PCA has been suggested as a tool to identify response biomarkers for antidepressant treatment (Tenke et al., 2017, 2011). The association between f-PCA outcomes and state measures has also been shown: a negative relationship was reported between multiple alpha components and skin conductance level (Barry et al., 2020), pointing to the role of alpha activity as an index of brain arousal (Barry et al., 2005). Finally, the components and their topographies (electrical distribution on a scalp) are highly similar in both eyes open and eyes closed conditions (Barry and De Blasio, 2018; Karamacoska et al., 2019a; Tenke and Kayser, 2005). Thus, f-PCA provides a unique chance to identify the constituent components in frequency domain.

2.4 Global Field Synchronization

In 2001 Koenig and colleagues proposed a reference free, multichannel EEG analysis method to estimate large-scale synchrony – Global Field Synchronization (GFS) (Koenig et al., 2001). GFS evaluates the global phase (the position along the sine wave at any given time point) alignment between all channels and frequency ranges between 0 (no predominant phase) to 1 (perfect EEG phase (or anti-phase) among all channels. Higher GFS values indicate increased global functional connectivity of brain processes (Achermann et al., 2016; Koenig et al., 2001). The common phase between the channels implies that there are simultaneous synchronization patterns of large-scale functional brain network nodes (Achermann et al., 2016; Michel and Koenig, 2018; Seeber and Michel, 2021). Although, since the EEG signal is not produced by one spatially isolated source, spread in phase alignment across channels must have been generated by distinct intracranial electric sources that differ in phase (Achermann et al., 2016; Custo et al., 2014; Koenig et al., 2001). By assuming zero time lag between the different EEG channels, GFS is a measure of global connectivity (Rusterholz et al., 2017).

Using signal decomposition methods, multichannel EEG signal is transformed to frequency domain, providing information about the magnitude and the angle at a given frequency. These values can be visualized as cloud of data points in two-dimensional complex plot (Figure 2). The distance from the origin to the data point indicates the amplitude and the angle indicates the phase. The shape of the resulting data cloud indicates the amount of phase synchronization across channels: a very elongated cloud indicates that the EEG at the given frequency is dominated by a common phase or anti-phase. In contrast, if the cloud is shaped like a disk, no predominant phase is present (Koenig et al., 2001; Rusterholz et al., 2017). Horizontal and vertical lines indicate the explained variance of the first and the second principal components respectively. The ratio of the length of these lines yields the value of GFS (Koenig et al., 2001).

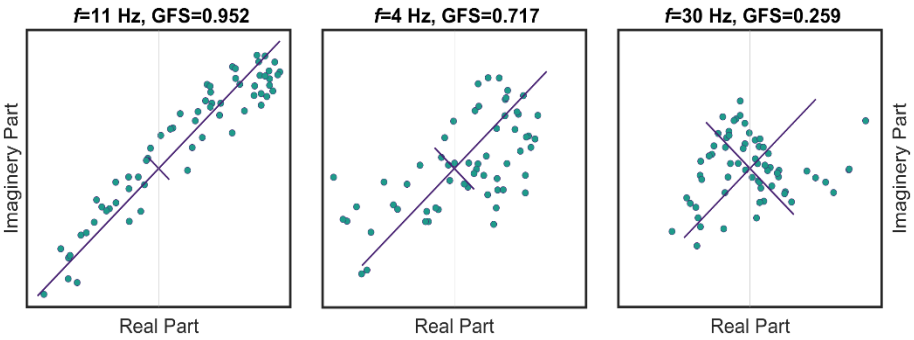

Figure 2. Illustration of GFS determination in the complex coordinates plain for 11, 4 and 30 Hz. Green circles: complex Fourier coefficients. Purple lines: two principal components with relative length of the two eigenvalues.

GFS was successfully applied in both resting state and evoked response EEG studies. Changes of global connectivity in several neuropsychiatric disorders were demonstrated using this approach: reduced GFS in theta range were reported in schizophrenia (Koenig et al., 2012a, 2001), decreased GFS values in delta, alpha, beta ranges observed in Alzheimer's disorder (Koenig et al., 2005; Ma et al., 2014; Park et al., 2008; Smailovic et al., 2018), decreased GFS values in delta and theta revealed in mild cognitive impairment (Smailovic et al., 2022), decreased GFS values in delta and broadband (0.5-70 Hz) ranges shown in obsessive-compulsive disorders (Özçoban et al., 2018). Finally, the measure appeared to be sensitive to the different vigilance (Achermann et al., 2016; Nicolaou and Georgiou, 2014; Rusterholz et al., 2017) and attention (Griskova-Bulanova et al., 2018) levels. Thus, making GFS a useful measure in assessing global functional connectivity and possible biomarker in certain neuropsychiatric disorders.

2.5 EEG Microstates

Multichannel EEG is used to assess the spatio-temporal dynamics of the brain's electrical activity. Although, traditionally, EEG is characterized by the temporal waveform morphology and/or frequency distribution of recordings at certain preselected electrodes, unfortunately, this type of analysis misses out a large part of information. In 1970's Dietrich Lehmann and colleges proposed a new method to quantify the information from all channels at once (Lehmann, 1971; Lehmann et al., 1987; Lehmann and Skrandies, 1980). The method was based on the segmentation of the ongoing EEG activity into non-

overlapping topographical map series, which remained stable for around 100 ms before transitioning into another stable topographical map, which is referred as a microstate.

Since the initial introduction of the method, it was improved, mostly from mathematical and computational perspective (Murray et al., 2008; Pascual-Marqui et al., 1995). The analysis starts with calculation of Global Field Power (GFP), which is a well-established quantifier of global scalp field strength and is used to decompose EEG into series of topographical maps (Lehmann and Skrandies, 1980; Murray et al., 2008; Skrandies, 1990; Zanesco, 2020). GFP is defined as the standard deviation of the power between all electrodes over a given time frame and it reflects the strength of synchronized (zero-lag) brain activity and is measured in microvolts (Seeber and Michel, 2021). It is well known that resting EEG has relatively low signal-to-noise ratio, thus only topographies at GFP peaks are extracted (Koenig and Brandeis, 2016; Michel et al., 2009; Zanesco, 2020) and submitted to clustering analysis. The clusterization algorithm groups topographies together based on their spatial similarity into a certain number of clusters, where each topography (brain's electrical distribution on a scalp) is assigned to only one cluster. The cluster analysis yields a set of the most dominant topographies for each subject. Then a set of single subject's topographies is submitted to the second round of cluster analysis to determine a set of the most dominant group level topographies. Finally, group level topographies are fitted back into the original EEGs, where the momentary maps of the of EEG are labelled according to the label of the most similar group level topographical map (winner-takes-all approach (Gschwind et al., 2016; Michel and Koenig, 2018)). EEG microstates are defined as continuous time periods where all momentary maps are assigned to the same cluster (Figure 3).

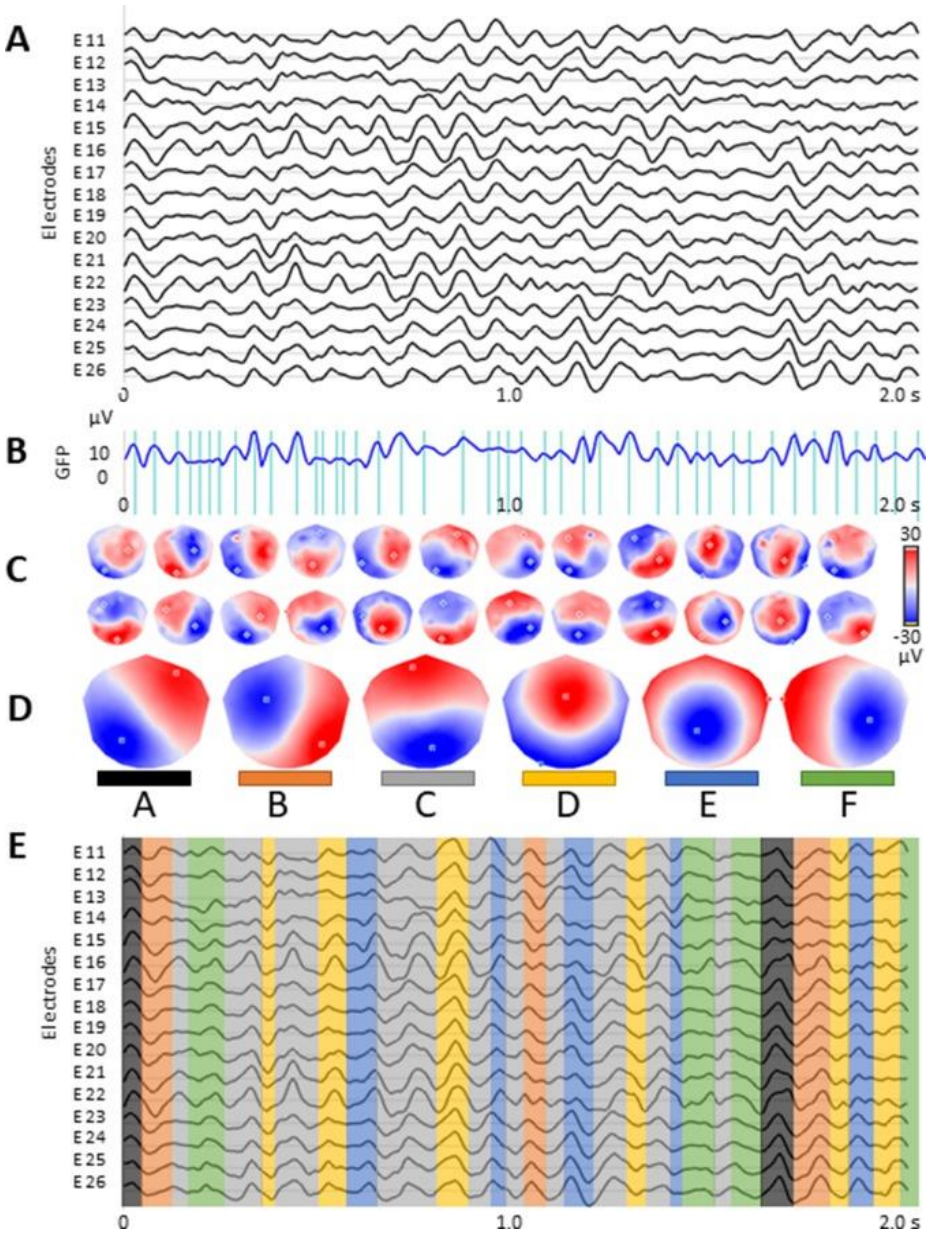

Figure 3. Visualization of the EEG microstate analysis steps (Damborska et al. (2019)). 2 seconds of the ongoing EEG (A). GFP as a time-varying function (blue line) and GFP peaks (vertical lines) (B). Topographies from GFP peaks (C). Group level topographies determined by cluster analysis (D). Topographies from (D) fitted by to the original signal using winner-takes-all approach (E).

The obtained topographies are reliable, comparable between the studies and independent from the number of electrodes used to record the signal (Khanna et al., 2014; Zhang et al., 2021), analysis frequency ranges (Férat et al., 2022) and algorithms used to clustered the data (Khanna et al., 2014; von Wegner et al., 2018). Based on the physical laws, distinct topographies are generated by spatially distinct neuronal sources (Michel and Koenig, 2018; Vaughan, 1982), that are approximately simultaneously active (Seeber and Michel, 2021) thus being potentially related to different functional/physiological processes.

After the fitting procedure, temporal parameters are extracted. The most commonly assessed temporal and spatial parameters are described in Table 1. For the last several years, sequence analysis received a lot of attention, as the signal complexity parameters were adopted, implemented and applied for microstate analysis: Adjusted Mutual Information (Férat et al., 2022b), Hurst exponent (Liu et al., 2020; Van De Ville et al., 2010; von Wegner et al., 2018, 2017, 2016), Markov chain (Gärtner et al., 2015; von Wegner et al., 2017), Shannon's (information) entropy (von Wegner et al., 2018; Zhang et al., 2021), (partial) autoinformation/autocorrelation function (Al Zoubi et al., 2019; Liu et al., 2020; von Wegner et al., 2018, 2017), Lempel-Ziv complexity (Artoni et al., 2022; Tait et al., 2020), pairwise dissimilarities based on optimal matching (Takarae et al., 2022; Zanesco et al., 2021a). Changes in these parameters revealed that microstate time series show dependencies over long time ranges and can be changed in neuropsychiatric disorders, such as mood and anxiety disorder, Alzheimer's disorder. Thus, could possible serve as a biomarkers (Al Zoubi et al., 2019; Tait et al., 2020).

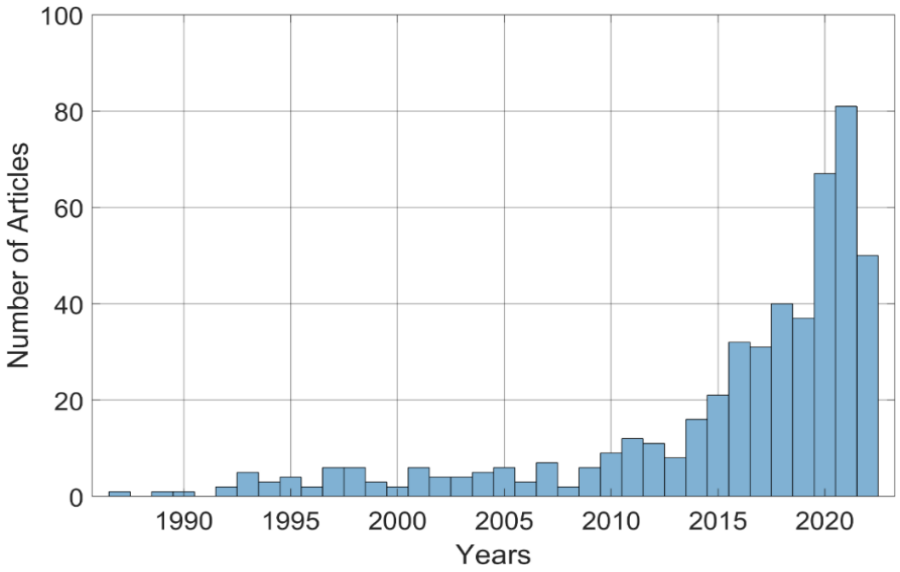

Figure 4. Number of articles per year from PubMed database search using keyword 'EEG microstat*', where '*' stands for any ending.

A growing body of clinical and cognitive neuroscience studies is applying the broadband EEG microstate approach to evaluate electrical activity of the large-scale cortical networks (Figure 4). Microstate analysis is applied to evaluate activity of the brain networks in different psychiatric and neurologic disorders such as schizophrenia (da Cruz et al., 2020; Kindler et al., 2011; Koenig et al., 1999; Rieger et al., 2016; Tomescu et al., 2014) , psychosis (de Bock et al., 2020; Mackintosh et al., 2020; Murphy et al., 2020a), Alzheimer's and/or dementia (Nishida et al., 2013; Smailovic et al., 2019; Tait et al., 2020), epilepsy (Liu et al., 2021; Raj V et al., 2018), bipolar disorder (Damborská et al., 2019a; Vellante et al., 2020), autism spectrum disorders (Bochet et al., 2021; Jia and Yu, 2019; Nagabhushan Kalburgi et al., 2020), mood and anxiety disorders (Al Zoubi et al., 2019; Atluri et al., 2018; Damborská et al., 2019b; Murphy et al., 2020b), obsessive compulsive disorder (Yoshimura et al., 2019), Parkinson's disease (Chu et al., 2020; Ignacio Serrano et al., 2018), multiple sclerosis (Gschwind et al., 2016), panic disorder (Galderisi et al., 2001; Kikuchi et al., 2011), tinnitus (Cai et al., 2019; Cao et al., 2020), insomnia (Wei et al., 2018), narcolepsy (Drissi et al., 2016; Kuhn et al., 2015), sleep apnea (Xiong et al., 2021), stroke (Zappasodi et al., 2017), migraine (Li et al., 2022), fibromialgia (González-Villar et al., 2020), Huntington's desease (Faber et al., 2021), methamphetamine addiction (T. Chen et al., 2020), gaming disorder (Cui et al., 2021; L. Wang et al., 2021),

lower limb amputation patients (Shan et al., 2021), psychosocial stress (Kadier et al., 2021), post-traumatic stress disorder (Terpou et al., 2022), attention - deficit/hyperactivity disorder (Férat et al., 2021). The method is also used to test activity in different wakefulness and sleep stages (Bréchet et al., 2020; Brodbeck et al., 2012; Diezig et al., 2022; H. Wang et al., 2021), in different age and gender groups (Koenig et al., 2002; Tomescu et al., 2018; Zanesco et al., 2020b), under the effect of pharmacological substances (Artoni et al., 2022; Schiller et al., 2021, 2019; Yoshimura et al., 2007), or meditation and hypnosis (Brechet et al., 2021; Faber et al., 2017; Katayama et al., 2007; Zanesco et al., 2021b).

The EEG microstate approach is also successfully implemented in combination with other brain imaging modalities, such as functional Magnetic Resonance Imaging (fMRI) (Abreu et al., 2021; Britz et al., 2010; Schwab et al., 2015; Van De Ville et al., 2010), functional Near-Infrared Spectroscopy (fNIRS) (Zhang and Zhu, 2019), Positron Emission Tomography (PET) (Rajkumar et al., 2021a, 2021b), Transcranial Magnetic Stimulation (TMS) (Croce et al., 2018b, 2018a; Qiu et al., 2020; Sverak et al., 2018), Magnetoencephalography (MEG) (Coquelet et al., 2022). The method was successfully used in neurofeedback studies (Asai et al., 2022; Diaz Hernandez et al., 2016) and tested in rodent models (Mégevand et al., 2008; Mishra et al., 2021).

Table 1. Most common microstate characteristics to evaluate.

Most common microstate characteristics	
Mean duration	The mean temporal duration of consecutive maps assigned to the same microstate class, interpreted to reflect its intracortical generators synchronously activity for each occurrence of a particular microstate configuration and is measured in milliseconds (ms) (Khanna et al., 2015).
Occurrence rate	The mean number of times a microstate occurred during one second period, interpreted as the tendency of intracortical sources to be synchronously activated and is measured in Hertz (Hz) (Khanna et al., 2015).
Coverage	The total percent of the time frames for which a microstate is accounted, it reflects the relative time microstate being activated (Khanna et al., 2015; Murray et al., 2008).
Global Explained Variance (GEV)	The sum of the explained variances weighted by the Global Field Power at each moment in time and is measured in percentages (Murray et al., 2008).
Global Field Power (GFP)	An average power standard deviation of the time frames for which a microstate is accounted and measured in microvolts (μV) (Murray et al., 2008; Skrandies, 1990).
Spatial Correlation (SC or C)	Defined as Pearson's product-moment correlation coefficient between the potentials of the two maps to be compared and ranges from -1 to 1, where values approaching 1 indicates topographical similarity and -1 indicates inverted polarity (Murray et al., 2008). To ignore polarity inversion, the absolute values are usually taken (Custo et al., 2017; Tarailis et al., 2021).
Global Map Dissimilarity (GMD or DISS)	Defined as an index of topographical differences between two electric fields scaled to unitary strength (normalized by their GFP) and is bounded between 0 and 2, where the values closer to 0 indicates topographical similarity and 2 indicates inverted polarity. SC and GMD are invasively related (Brandeis et al., 1992; Brunet et al., 2011; Murray et al., 2008).
Microstate syntax/transition	Defined as transition counts among all microstates and normalized for the overall count of transitions and is characterize as the pattern of transitions between microstates when they occur, measured in probability (Lehmann et al., 2005).

Compared with more commonly applied EEG analysis methods that focus on the morphology of the waveform and/or frequency distribution over a small number of preselected electrodes, multichannel EEG approach has four main advantages:

1) Based on a volume conduction, the activity of a single source will simultaneously affect all scalp electrodes, resulting in an intrinsic correlation between the electrodes; since information from all electrodes are taken into account, the scalp field produced by difference source(s) is taken into account to its largest possible extent (Dien, 2012; Koenig et al., 2011; Michel et al., 2004; Michel and Murray, 2012).
2) An electrode at any given scalp location not only detects neuronal activity in area directly below it, but also simultaneously records activity from remote sources, since all sensors are being used, false negatives based on partially overlapping scalp fields are unlikely, and over-interpretation of spatial location is avoided (Dien, 2012; Koenig et al., 2011; Michel and Koenig, 2018).
3) Since there are different generators working independently in the same frequency (Custo et al., 2014), taken information from all electrodes into account, topographical display reflects the sum of the all momentary active neuronal populations in the brain, thus it makes it reference independent (Brunet et al., 2011; Koenig et al., 2011; Lehmann and Skrandies, 1980; Michel et al., 2004; Michel and Koenig, 2018; Murray et al., 2008).
4) Based on the physical laws, distinct topographies are generated by spatially distinct neuronal sources (Michel and Koenig, 2018; Vaughan, 1982), thus distinct topographies are directly related to different functional/physiological processes.

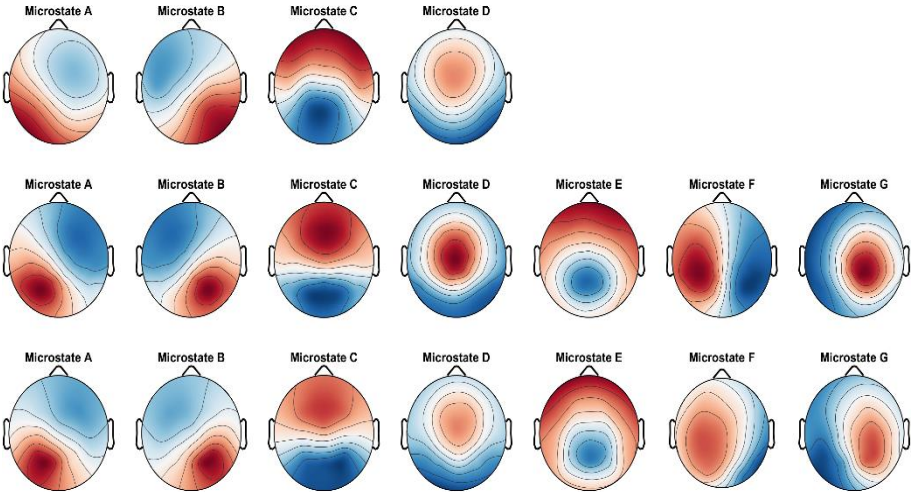

Figure 5. Electrical configuration of canonical four microstates reported by Koenig et al. (2002) from 496 participants (top row), seven microstate topographies obtained by Custo et al. (2017) from 164 participants (middle row) and by Tarailis et al., (2021) from 197 participants (bottom row)

Number of EEG studies has consistently reported similar looking four microstates, that explains majority of the ongoing activity (60 – 80 %) (Michel and Koenig, 2018) and comparable temporal parameters. These four microstates a referred as canonical EEG microstates (Figure 5 top row). Although, this a priori selection to extract only four microstates has been criticized (Custo et al., 2017; Michel and Koenig, 2018; Tarailis et al., 2021).It was noticed that topographies of microstate classes differs between studies to a certain degree (Michel and Koenig, 2018), with the most pronounced differences reported for microstate C: it displays anterior-posterior configuration in some studies and posterior maximum—in others. Custo et al.(Custo et al., 2017), and Tarailis et al. (Tarailis et al., 2021) (Figure 5 middle and bottom rows) showed, that spatially similar, but functionally different microstates can be merged into one microstate class, if a priori number of classes are selected this potentially could explain the functional heterogeneity of microstate C reported in the literature. Studies using optimization criteria most of the time report more than four microstates that display high spatial similarity independently of number of classes (Tarailis et al., submitted). Since there is no fixed number of microstates preselecting a number of microstates to extract can cause misattribution of the functional roles between spatially similar topographies (Custo et al., 2017; Michel and Koenig, 2018; Tarailis et al., 2021).

2.6 Resting State approach

Assessment of brain activity at rest is a classical data-collection setting used both in clinical and experimental studies. It does not require active participation of the subjects. Numerous studies showed that rather than remaining inactive until the upcoming stimulus, the brain at rest is very active, self-organized and the observed ongoing activity is not random (Fox et al., 2005; Fox and Raichle, 2007; Greicius et al., 2003; Van De Ville et al., 2010), thus providing a valuable information on the state of the brain.

However, despite its straightforward application, investigation of brain at rest presents conceptual and methodological challenges, compared with the responses to controlled stimuli (experimental paradigm) that is dominant in neuroscience. The results obtained by resting state approach can be sensitive to participant-, procedure-, and measurement-related factors such as sex, emotional state, body weight, state of vigilance, participant's body position, choice of the reference and frequency bands when the EEG is recorded, and extrenal irritants such as fMRI background noise, to name a few (Duncan and Northoff, 2013; Van Diessen et al., 2015). While a majority of these factors can be minimized or taken into account during statistical evaluation, the participants' mental activities, even during a brief resting-state session, cannot be precisely controlled, and the relationship between the ongoing experience of mind wandering and neurophysiological signals is still unclear (Gonzalez-Castillo et al., 2021; Hurlburt et al., 2015; Smallwood and Schooler, 2015). The knowledge on the relationships between subjective experiences and objectively observed physiological activity would help to improve the interpretation of the findings and increase the sensitivity and specificity of neuroimaging biomarkers in clinical and pharmacological studies (Diaz et al., 2013).

To overcome the problem of mind-wandering, several "resting-state" studies implemented task-initiated thoughts (Antonova et al., 2022; Bréchet et al., 2019; Faber et al., 2017; Milz et al., 2016; Roehri et al., 2022; Seitzman et al., 2017) or descriptive experience sampling, where participants are to attend to the experience that was ongoing at the moment of the onset of the auditory beep and describe their experiences after the session to the interviewer (Hurlburt et al., 2015; Hurlburt and Akhter, 2006).

2.7 Amsterdam Resting-State Questionnaire

To quantify participants' subjective experiences during the resting-state session, several resting state questionnaires were introduced. New York Cognition Questionnaire (NYC-Q) (Gorgolewski et al., 2014) separates mind wandering into categories of content (future, past, positive, negative, social) and form (words, images, specificity). The Resting-State Questionnaire (ReSQ) (Delamillieure et al., 2010) is a semi-structured, supervised and based on decision tree questionnaire, which focuses on inner speech/language and visual imaginary aspects. Diaz et al., (Diaz et al., 2014, 2013) introduced Amsterdam Resting-State questionnaire (ARSQ) as a tool to effectively quantify subjective experiences, emotions, and thoughts during the resting-state periods. ARSQ covers similar domains as NYC-Q and ReSQ but unlike ReSQ is based on self-report and self-assessments. Up to date ARSQ is the most commonly used questionnaire to asses subjective experience of mind wandering.

Initially, authors formulated more than 100 statements that participants might experience during the resting session and during a small-sample pilot study, statements that were too ambiguous (always rated 'strongly disagree') or too specific (always rated 'strongly agree') were eliminated. Additionally, participants could suggest statements that they felt were lacking (Diaz et al., 2013).

The ARSQ 1.0 questionnaire was developed to minimize the impact of the fading memory of the resting-state experience by keeping it short: the full ARSQ is usually completed in less than four minutes even when lying in an fMRI scanner (Diaz et al., 2013). The questionnaire contained 27 statements divided into seven domains of mind-wandering: Discontinuity of Mind (DoM), referring to the dynamics of the ongoing thoughts; Theory of Mind (ToM), referring to other people-related thoughts; Self, referring to self-related thoughts; Planning, referring to future directed thoughts; Sleepiness, referring to the level of drowsiness; Comfort, referring to the level of relaxation during the session; Somatic Awareness (SA), referring to the interoceptive awareness of one's own body. Five additional statements were included to assess response validity ('I felt motivated to participate', 'I have difficulty remembering my thoughts', 'I have difficulty remembering my emotions', 'I had my eyes closed', 'I was able to rate the statements').

Table 2. Ten domains model of ARSQ 2 (Diaz et al., 2014)

Discontinuity of mind	'I had busy thoughts.' 'I had rapidly switching thoughts.' 'I had difficulty holding on to my thoughts.'
Theory of Mind	'I thought about others.' 'I thoughts about people I like.' 'I placed myself in other peoples' shoes.'
Self	'I thought about my feelings.' 'I thought about my behavior.' I thought about myself.'
Planning	I thought about things I need to do.' I thought about solving problems.' 'I thought about the future.'
Sleepiness	'I felt tired.' 'I felt sleepy.' 'I had difficulty staying awake.'
Comfort	'I felt comfortable.' 'I felt relaxed.' 'I felt happy.'
Somatic Awareness	'I was conscious of my body.' 'I thought about my heartbeat.' 'I thought about my breathing.'
Health Concern	'I felt ill.' 'I thought about my health.' 'I felt pain.'
Visual Thought	'I thought in images.' 'I pictured events.' 'I pictured places.'
Verbal Thought	'I thought in words.' 'I had silent conversations.' 'I imagined talking to myself.'

However, the first iteration of ARSQ did not cover some domains that are important facets of mind-wandering, like visual or verbal imagery. The

authors improved and extended the original ARSQ to ten domains questionnaire, by adding Health Concern (HC), referring to general well-being; Visual Thought (Vis), referring to the visual imagery during mind-wandering; and Verbal Thought (VT), referring to the spontaneous thoughts formulated in words (Diaz et al., 2014).

Additionally, the domains were standardized by keeping the number of items per factor equal in order to avoid differences in the discreetness of the underlying scale. The statements of ARSQ 2.0 are presented in Table 2. Several EEG, fMRI and behavioral studies (Table 3) reported the relationship between ARSQ domains and physiological and/or psychological variables in healthy (Diaz et al., 2016, 2014, 2013; Marchetti et al., 2015; Pipinis et al., 2017; Portnova et al., 2019; Schiller et al., 2021; Stoffers et al., 2015; Tarailis et al., 2022, 2021; Tomescu et al., 2022; Zanesco et al., 2020a), and clinical cohorts. Moreover, the scores of domains of ARSQ correlated with well-established measures of general mental well-being, like Pittsburgh Sleep Quality Index, Insomnia Severity Index, Hospital Anxiety and Depression Scale, Center for Epidemiological Studies Depression Scale, Inventory of Depressive Symptomatology, Temporal Experience of Pleasure Scale-Anticipatory, Consummatory Pleasure, Research And Development 36, Dysfunctional Beliefs and Attitudes About Sleep Scale, Beck Depression Inventory, AQ-short (Diaz et al., 2013; Palagini et al., 2016; Simpraga et al., 2021).

Table 3. Studies that applied ARSQ.

EEG	fMRI	Behavioral
Diaz et al. 2013	Marchetti et al. 2015	Diaz et al. 2014
Diaz et al. 2016	Stoffers et al. 2015	Palagini et al. 2016
Pipinis et al. 2016		Simpraga et al. 2021
Portnova et al. 2019		
Schiller et al. 2021		
Tarailis et al. 2021		
Tarailis et al. 2022		
Tomescu et al. 2022		
Zanesco et al. 2021		

Studies using different brain imaging modalities and applying different analysis methods reported associations with the ARSQ domains. (DoM (Stoffers et al., 2015; Tomescu et al., 2022), ToM (Marchetti et al., 2015), Self (Tarailis et al., 2021; Tomescu et al., 2022), Planning (Portnova et al., 2019; Zanesco et al., 2021a), Sleepiness (Diaz et al., 2013; Stoffers et al., 2015),

Comfort (Stoffers et al., 2015; Tarailis et al., 2021; Zanesco et al., 2021a), Somatic Awareness (Pipinis et al., 2017; Tarailis et al., 2021; Tomescu et al., 2022; Zanesco et al., 2021a), Visual Thought (Stoffers et al., 2015), Verbal Thought (Tomescu et al., 2022). Most important, these results are overlapping and comparable between the studies and are supported by results reported in the literature. For instance, several studies (Pipinis et al., 2017; Tarailis et al., 2021; Tomescu et al., 2022; Zanesco et al., 2021a). were aiming to relate individual scores of ARSQ domains with broadband spatio-temporal parameters of EEG activity – EEG microstates. In all of these studies, domain of Somatic Awareness showed association with microstate activity which is related with interoception and emotional cognition. This result was confirmed by Schiller et al., (Schiller et al., 2021), where microstate related with interoception showed significant correlation with Somatic Awareness domain in alcohol intoxicated subjects. Other correlation were also observed between EEG microstates temporal characteristics and ARSQ domains. For instance. Tarailis et al (2021) also reported association between microstate B and domain of Self. In previous studies, microstate B was related with autobiographical memory, scene reconstruction and self visualization in the scene (Bréchet et al., 2019). Additionally, the activity of this microstate was reported to be reduced in bipolar patients, who has poor visualization of autobiographical memories (Damborská et al., 2019b; Vellante et al., 2020). Positive correlation between domain of Comfort and microstate G, which is related with sensorimotor network (Custo et al., 2017) was also reported (Tarailis et al., 2021), which falls in line with results reported in fMRI study by Stoffers et al., (Stoffers et al., 2015) where the individual scoring for domain of Comfort showed positive correlation with activity within sensorimotor network.

By applying different EEG spectral analysis, Diaz et al., (Diaz et al., 2016, 2013) and Tarailis et al., (Tarailis et al., 2022) reported relationship between activity in theta frequency band and ARSQ domain of Sleepiness. Additionally, Tarailiset al., (2002) reported theta activity in limbic lobe, the anterior cingulate gyrus, and Broadman area 24 and Broadman area 23 which corresponds with results reported in literature (Nishida et al., 2004; Scheeringa et al., 2008; Smith et al., 2020).

Portnova et al., (Portnova et al., 2019) reported positive relationship between high alpha (12 – 13 Hz) and domain of Planning, while activity in delta band had negative relationship with domain of Planning. Tarailis et al., (2022) reported association between activity in alpha frequency range (9 Hz) and domain of Comfort, while activity in delta frequency range did not displayed any relationship between domains of ARSQ.

3. METHODS

The study was approved by the Vilnius Regional Biomedical Research Ethics Committee (Nr. 2019/10-1159-649, date of approval: 8 October 2019) and all subjects gave their written informed consent to participate.

3.1 Participants

Data from two hundred and twenty-six participants was collected (Females=131; Males=95, mean age 23.41, standard deviation ±3.87). Participants aged from 19 to 35 years, with normal or corrected to normal vision were included. All subjects were Caucasians residing in Lithuania. All females were healthy, nonpregnant, not using hormonal contraception, and reported experiencing regular menstrual cycles. Based on self-reports, 107 females participated in the study during the early follicular phase (menses), 20 during the luteal phase, and 4 during the ovulatory phase. Eighteen participants were left-handed and the remaining were right-handed. Participants were asked not to consume nicotine and caffeine 2 h prior to the study. The description of the participant groups used for each analysis approach is summarized in Table 4.

Table 4. Descriptive statistics of participants for each analysis

	f-PCA and GFS	**EEG Microstates**
N	226	197
Males	95	94
Females	131	103
Mean age and standard deviation	23.41 (3.87)	23.97 (3.81)

3.2 Data collection

To avoid subjects falling asleep and ensure the sufficient amount and quality of the data (Jobert et al., 2012; Liu et al., 2020; Tagliazucchi and Laufs, 2014), five minutes of resting state EEG were recorded in the dim lighted, sound attenuated and electrically shielded room while participants were comfortably seated in the upright position. Before the start of the recording session participants were instructed to stay still with their eyes closed, not to think about anything in particular and not to fall asleep.

EEG data were collected using EEG equipment (ANT Neuro, The Netherlands) and 64 Silver/Silver Chloride electrodes placed according to

international 10-10 system and mounted of elastic WaveGuard EEG cap (Figure 6). All electrodes were referenced against mastoids (M1 and M2) and ground electrode was attached close to Fz. The impedance of electrodes was kept below 20 kΩ.

Two pairs of additional electrodes (VEOG and HEOG) were used. VEOG were placed above and below the right eye to record electrical muscle activity of vertical eye movements, while HEOG were placed approximately

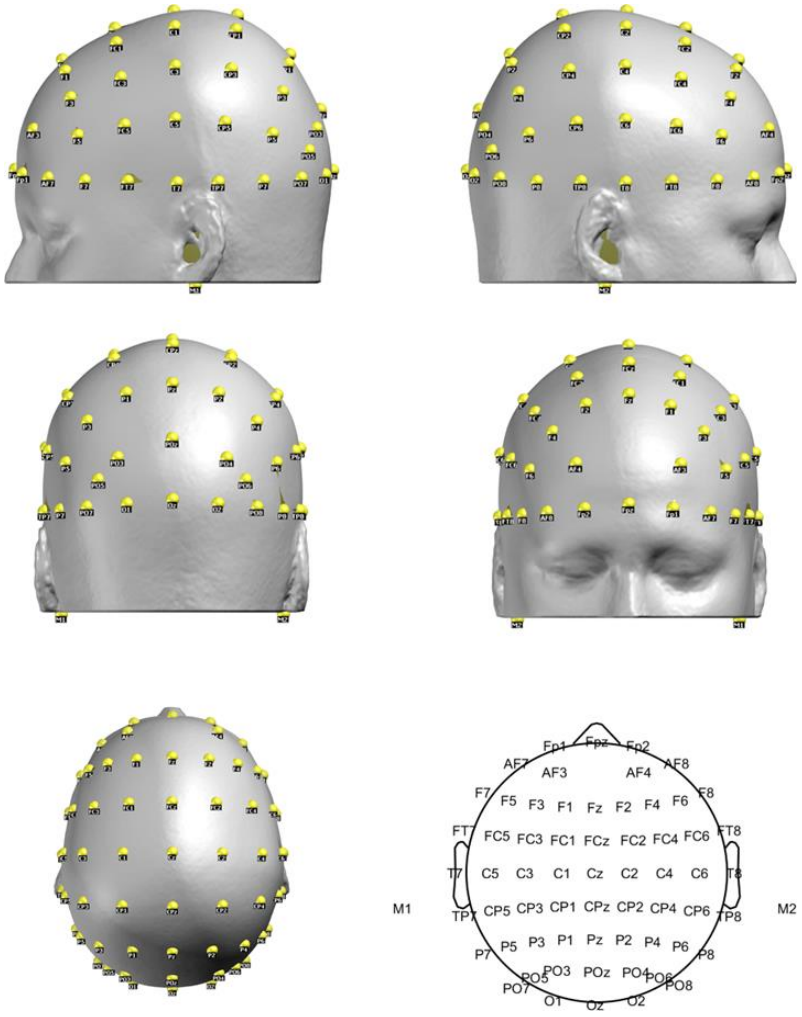

Figure 6. Electrodes layout used in the data collection.

2 cm from the right and left outer canthi to record electrical muscle activity of horizontal eye movements. Data was recorded with sampling rate of 2048 Hz. Right after the EEG recording session participants completed the Lithuanian version of ARSQ where they had to retrospectively rate the statements about

the emotions and thoughts from 1 (completely disagree) to 5 (completely agree).

3.3 ARSQ

The Lithuanian version of ARSQ 2.0 was used (Pipinis et al., 2017). The ARSQ is self-report questionnaire that aims to summarize the retrospective subjective experience. It contains thirty statements on thoughts and feelings that participants may experience during resting state period. Each statement is rated on Likert-type scale ranging from 1 (completely disagree) to 5 (completely agree). Thirty statements are divided into ten mind wandering domains that participants might experience during the session: Discontinuity of Mind (DoM), referring to the dynamics of the ongoing thoughts, Theory of Mind (ToM), referring to the other people-related thoughts, Self, referring to the self-related thoughts, Planning, referring to the future directed thoughts, Sleepiness, referring to the level of drowsiness, Comfort, referring to the level of relaxation during the session, Somatic Awareness (SA), referring to the interoceptive awareness of own's body, Health Concern (HC), referring to general well-being, Visual Thought (Vis), referring to the visual imagery during the mind-wandering, Verbal Thought (VT), referring to the spontaneous thoughts formulated in words. The scores of each ARSQ dimension were calculated by taking the mean value of three statements.

3.4 EEG processing

The offline EEG data processing was conducted in MATLAB (The Mathworks, Natick, USA) environment using EEGLAB toolbox (Delorme and Makeig, 2004) and custom written functions. 50 Hz power line noise was removed using multi-tapering and Thomas F-statistics implemented in the CleanLine plugin for EEGLAB (Mullen, 2012). EEG data was submitted to an Independent Component Analysis (ICA) using the Infomax ICA algorithm and components with spatial and temporal characteristics of horizontal and vertical eyes movements and cardiac pulse were used to construct individual spatial filters to suppress these artefacts (Delorme et al., 2007; Jung et al., 2000). Channels with excessive artefacts were manually rejected and reconstructed using three - dimensional spherical spline method (Perrin et al., 1989). EEG recordings were down-sampled to 512 Hz for the microstate analysis and to 1000 Hz for f-PC analysis. Data were segmented into artefact-free, non-overlapping 2 second epochs.

3.5 Frequency Principal Components Analysis

The artefact free epochs were baselined across their duration and decomposed using FFT from DC to 30 Hz, for frequency resolution of 0.5 Hz. Then the values for each frequency were averaged together across the epochs. f-PCA was conducted using EP Toolkit v.2.92 (Dien, 2010). The covariance matrix with unrestricted component extraction and Promax rotation was used, as it was previously showed to be more effective for the temporal approach (Barry and De Blasio, 2018; Dien et al., 2007). Cases to variables ratio was 229.7 (14012 cases: 226 participants X 62 electrodes), (61 variable: 0-30 Hz in 0.5 Hz steps). Factors with more than 3 percent of explained variance were included for further analysis, and the remaining components were excluded. To ensure a sufficient signal-to-noise ratio, electrodes with three maximum values were averaged together for each distinct factor.

3.6 Source Localization

Standardized Low Resolution Electromagnetic Tomography (sLORETA) (Pascual-Marqui et al., 1994, 2002) was used to determine the intracortical distribution of the electrical activity determined as for f-PC significantly associated with ratings scores on ARSQ domains (these were set as external independent variables). The Montreal Neurologic Institute average MRI brain (MNI152) (Mazziotta et al., 2001) was used as a realistic head model where the solution space was restricted to the cortical grey matter, corresponding to 6239 voxels at 5x5x5 mm spatial resolution. The sources for activity were assessed by sLORETA log-transformed current density power. Statistical nonparametric mapping (SnMP) with 5000 permutations was used to determine the significant threshold value for voxels activation (Nichols and Holmes, 2001).

3.7 Global Field Synchronization

For GFS analysis data was recomputed to average reference and filtered between 1 and 30 Hz using Finite Impulse Response filter implemented in EEGLAB (Delorme and Makeig, 2004) with default settings. Each epoch was frequency-transformed using FFT at 1 Hz step yielding a complex value for each frequency and each electrode. The distribution of these values indicates the amount of common phase alignment across the electrodes. Data-points cloud distribution was submitted to two-dimensional principal component

analysis, yielding two eigenvalues per frequency. GFS was defined as a ratio between these two eigenvalues:

$$GFS(f) = \frac{|\lambda_1(f) - \lambda_2(f)|}{\lambda_1(f) + \lambda_2(f)}$$

where λ1 and λ2 are two eigenvalues obtained by using PCA at a particular frequency *f*. GFS values are bounded between 0 and 1. Low values of GFS indicate that there is no predominant phase between the electrodes, thus decreased global functional connectivity, while high GFS values indicates predominant phase (or anti-phase) over electrodes, thus increased global functional connectivity (Achermann et al., 2016; Koenig et al., 2001). GFS values were averaged between the epoch for predefined frequency bands: delta (1–3 Hz), theta (4–7 Hz), alpha (8–13 Hz), and beta (14–30 Hz) (Koenig et al., 2001; Smailovic et al., 2018).

3.8 Microstate analysis

For microstate analysis, data was recomputed to average reference and filtered between 1 and 40 Hz using Butterworth filter of 2nd order. The microstate analysis was performed using microstate plugin for EEGLAB (version v1.2) (http://www.thomaskoenig.ch/index.php/software/microstates-in-eeglab/) and custom written functions. Data was analyzed in two steps: individual and group level. GFP was calculated for every participant:

$$GFP = \sqrt{\frac{\sum_{i=1}^{n}(v_i - \bar{v})^2}{n}}$$

where v_i measured potential of the *i*-th electrode for a given time frame, $\bar{v}$ is average potential for a given time frame and *n* is the number of electrodes. To ensure a sufficient signal-to-noise ratio, only the maps at momentary peaks of the GFP were extracted (Koenig and Brandeis, 2016; Skrandies, 1990; Zanesco, 2020) and submitted to modified k-means clustering algorithm (Pascual-Marqui et al., 1995). To ensure that only spatial distribution of these maps was taken into account, the maps were normalized to a vector of length 1. To identify the optimal number of microstate templates, number of clusters ranged from 2 to 10.

For the second step, individual topographies were averaged across participants using a permutation algorithm that maximizes the common variance between the participant (Koenig et al., 1999). The optimal number of clusters for group level was identified by Silhouettes method (Rousseeuw, 1987). Silhouettes evaluate how similar each data point (individual

topography) is to other data points in its own cluster compared to the data points in other clusters (Bréchet et al., 2019; Dinov and Leech, 2017). Silhouette values are defined as:

$$S = \frac{(b_i - a_i)}{\max(a_i * b_i)}$$

where a_i is the average distance from i-th point to other points in the same cluster, and b_i is the average distance between i-th point and points in different clusters. Silhouettes values ranges from -1 to 1. A high silhouette value indicates that a data-point is well matched to its own cluster, and poorly matched to other clusters. The optimal number of clusters was based on mean value of Silhouettes for each number of clusters - Silhouette coefficient.

As for the measure of distance, Global Map Dissimilarity (GMD) was applied as it is described in the literature (Brunet et al., 2011; Murray et al., 2008; Skrandies, 1990). GMD is defined as an index of topographical differences between two electric fields and is bounded between 0 and 2, where the values closer to 0 indicates topographical similarity. To obtain the temporal parameters of microstates, the fitting procedure consisted in calculating the spatial correlation between every group level topographical map and the individual subject's scalp potential map in every time frame of the individual EEG recording. Each continuous time point of the subject's EEG (not only the GFP peaks) was then assigned to the microstate class of the highest spatial correlation (SC) (winner-takes-all approach), again ignoring polarity. SC is analogous to the Pearson's product-moment correlation coefficient between two topographies (Khanna et al., 2014; Murray et al., 2008):

$$SC = \frac{\sum_{i=1}^{n}(u_i . v_i)}{\sqrt{\sum_{i=1}^{n} {u_i}^2} \cdot \sqrt{\sum_{i=1}^{n} {v_i}^2}}$$

where *u* and *v* are distinct normalized microstate topographies, *i* is measured voltage of electrode and *n* is the number of electrodes. For each subject, three temporal parameters were calculated for each microstate class: mean duration (measured in milliseconds) – referring to the mean temporal duration of consecutive maps assigned to the same microstate class, interpreted to reflect its intracortical generators synchronously activity for each occurrence of a particular microstate configuration (Khanna et al., 2015); occurrence rate (measured in Hertz (Hz)) – defined as the mean number of times a microstate occurred during one second period, interpreted as the tendency of intracortical sources to be synchronously activated and is (Khanna et al., 2015); coverage – defined as the total percent of the time frames for which a microstate is

accounted, it reflects the relative time microstate being activated and is measured in percentages (Khanna et al., 2015; Murray et al., 2008). Additionally, GFP (measured in microvolts (μV)), defined as an average power standard deviation of the time frames for which a microstate is accounted was calculated (Murray et al., 2008; Skrandies, 1990).

3.9 Statistical Analysis

Statistical Analysis was performed using JASP statistical software (Version 0.14.1) (JASP Team, 2020; Love et al., 2019), Statistics and Machine Learning Toolbox implemented in MATLAB (The MathWorks, 2022) and custom written MATLAB functions. A Bayesian Pearson's correlation coefficients, and the corresponding Bayes factors (BF) were computed between scores on ARSQ domains and f-PCs' loading scores, GFS values and microstates temporal characteristics. In Bayesian interference, probability is a measure of the degree of confidence in the occurrence of an event and instead of *p* value it provides a likelihood ratio—Bayes factor. BF is the predictive updating factor which measures the change in relative beliefs about the alternative hypothesis relative to the null hypothesis (Kelter, 2020) and does not require correction for multiple comparisons (Dienes, 2016, 2014, 2011). BF can state evidence for both the alternative and the null hypothesis. Evidence categories for the BF are divided into eleven categories: Decisive evidence for H1 (BF_{10}> 100); Very strong evidence for H1 (100 > BF_{10}> 30); Strong evidence for H1 (30 > BF_{10}> 10); Substantial evidence for H1 (10 > BF_{10}> 3); Anecdotal evidence for H1 (3 > BF_{10}> 1); No evidence (BF_{10} = 1); Anecdotal evidence for H0 (1 > BF_{10}> 1/3); Substantial evidence for H0 (1/3 > BF_{10}> 1/10); Strong evidence for H0 (1/10 > BF_{10}> 1/30); Very strong evidence for H0 (1/30 > BF_{10}> 1/100); Decisive evidence for H0 (BF_{10}< 1/100) (George Assaf and Tsionas, 2018; Wetzels and Wagenmakers, 2012).

3.10 Outliers detection

To determine the possible outliers a custom written MATLAB function for Multidimensional Scaling (MDS) was used. MDS is a method that allows to downscale and visualize similarities among datasets in a low-dimensional space, where the distances between datapoints optimally represents the original similarities (Habermann et al., 2018; Koenig et al., 2011). MDS produced *x* and *y* coordinates for datapoints, which were used to calculate the pairwise Euclidean distances between them. Next, MATLAB built-in function *isoutlier* with default settings was used. MDS was applied separately for f-PCs, GFS values, microstates temporal properties and ARSQ scores.

4. RESULTS

Based on MDS there were no outliers in f-PCs loading scores, GFS values, microstates temporal parameters and ARSQ ratings.

4.1 ARSQ

Mean scores and standard deviations for each ARSQ domain were DoM 3.229 (±0.971), ToM 2.825 (±0.823), Self 3.156 (±0.877), Planning 2.926 (±1.047), Sleepiness 2.681 (±0.923), Comfort 3.700, (±0.829), SA 2.953 (±0.996), HC 1.594 (±0.601), Vis 3.764 (±1.069), VT 2.883 (±1.103). The means and standard deviations are summarized in Figure 7 (A). Intraclass Bayesian Pearson correlation coefficients for ARSQ dimensions are displayed in Figure 7 (B). There were, in total, sixteen positive intraclass correlations between the ARSQ domains, while only HC and Comfort displayed significantly negative relationships ($r = -0.203$, BF10 = 8.772). DoM correlated with all but the Comfort and SA domains, while SA did not display any relationship with other ARSQ domains.

To account for potential age and gender effects, the effect of the fixed factor gender on the ARSQ scores with age as covariate were tested using multivariate ANOVA. Multivariate ANOVA revealed a significant main effect of the covariate age for ARSQ scores [$F(10, 185) = 2.502$, $p = 0.008$], but no effect of gender was observed [$F(10, 185) = 1.348$, $p = 0.208$]. A subsequent correlation analysis showed that only correlations between age and

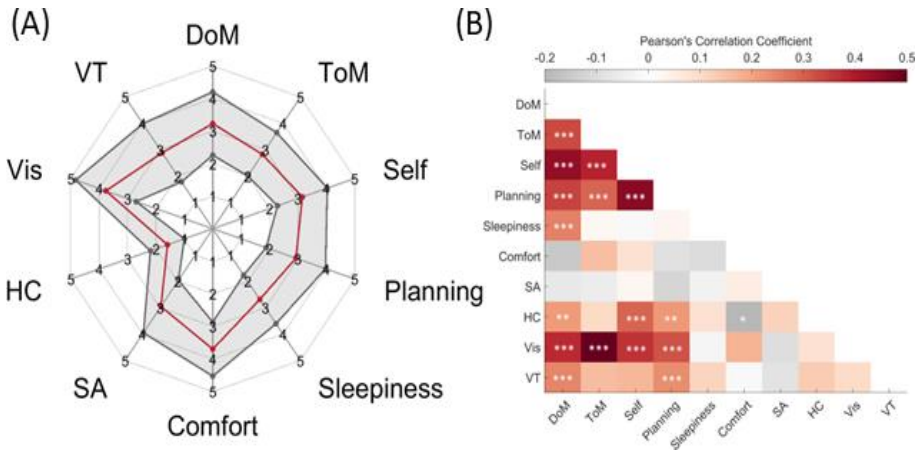

Figure 7. Mean scores (red line) and standard deviations (shaded area) for each of ARSQ ratings (A). Intraclass Bayesian Pearson correlation coefficients between ARSQ dimensions. * 10 > BF10> 3, *** BF10> 100.

ToM and HC domains reached substantial level of evidence (ToM: r = −0.193, BF10 = 3.520, Health: r = −0.198, BF10 = 4.258).

4.2 f-PCA Outcomes

Six factors that explained more than three percentages of variance were used for further analysis Together, these six factors accounted for 82.58% of the variance. The factors were ordered according to explained variance and labeled with the first letter of the corresponding EEG frequency range. There was one factor in the delta frequency range, peaking at 0.5 Hz with fronto-central activity (D1); one at the theta range, peaking at 5.5 Hz with frontal midline activity (T1); three components in the alpha range, peaking at 9 Hz (A1), 10.5 Hz (A2), and 11.5 Hz (A3), respectively, with occipital activity; and one factor in the beta frequency range, peaking at 17 Hz with occipital activity (B1). The f-PCA outcomes are depicted in Figure 8.

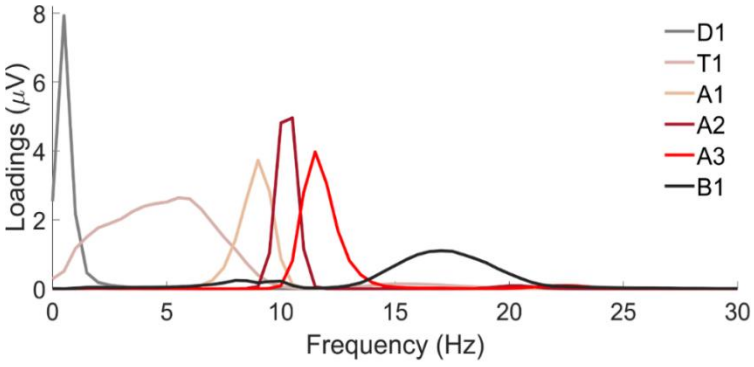

Label	D1	T1	A1	A2	A3	B1
Factor	3	5	1	2	4	6
Peak Hz	0.5	5.5	9	10.5	11.5	17
Var. %	15.15	11.34	19.82	19.56	13.10	3.61

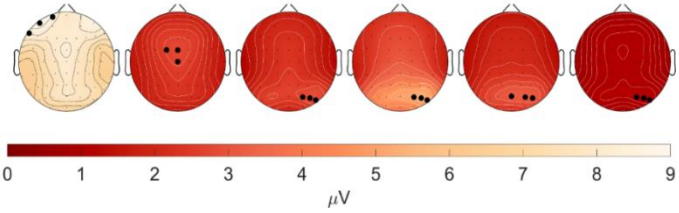

Figure 8. f-PCA outcomes for six factors. Top part: grand average (N=226) loading scores of each factor. Middle part: individual labels, factor numbers, peak frequencies, and variance as percentage. Bottom part: grand average topographies of each component. Three electrodes with maximum values are marked with black dots.

The top part shows the loading scores of each factor, describing how much each variable contributed to a particular principal component; the middle part presents individual labels, factor numbers, peak frequencies and explained variance percentage. The bottom part displays the topographies of each component. Three electrodes with the maximum values, which were averaged together for each component, are marked in black.

4.3 Relationship between f-PC loadings and ARSQ Dimensions

Out of sixty possible correlations (ten ARSQ domains x six factors) only two interactions were statistically significant ($BF_{10} > 3$). T1, peaking at 5.5 Hz, was positively correlated with the ARSQ domain of Sleepiness ($r = 0.200$, $BF_{10} = 7.676$). A1, peaking at 9 Hz, was positively associated with the domain of Comfort ($r = 0.198$, $BF_{10} = 7.115$) (Figure 9A). The Pearson's correlation coefficient and BFs for correlations between f-PC loading scores and ASRQ scores are summarized in Table 5.

Table 5. Bayesian Pearson's correlation coefficient between six data-driven EEG components and ARSQ domains. Significant interactions ($BF_{10} > 3$) are marked in grey squares.

ARSQ \ Factors		A1	A2	D1	A3	T1	B1
DoM	r	-0.081	-0.47	-0.008	0.009	0.059	-0.053
	BF_{10}	0.173	0.107	0.084	0.084	0.122	0.114
ToM	r	0.044	0.045	0.071	0.007	0.086	0.046
	BF_{10}	0.103	0.105	0.145	0.084	0.191	0.105
Self	r	-0.003	-0.062	-0.104	0.010	-0.018	0.062
	BF_{10}	0.083	0.127	0.279	0.084	0.086	0.128
Planning	r	-0.018	-0.018	-0.017	-0.062	-0.048	-0.105
	BF_{10}	0.086	0.086	0.086	0.128	0.107	0.288
Sleepiness	r	-0.040	-0.004	0.031	-0.052	**0.200**	-0.034
	BF_{10}	0.099	0.083	0.093	0.112	**7.676**	0.095
Comfort	r	**0.198**	0.138	0.078	-0.044	0.131	0.082
	BF_{10}	**7.115**	0.713	0.164	0.104	0.573	0.176
SA	r	0.027	-0.012	0.025	0.067	-0.089	-0.009
	BF_{10}	0.090	0.085	0.089	0.137	0.201	0.084
HC	r	-0.008	-0.125	-0.086	-0.069	-0.025	-0.076
	BF_{10}	0.084	0.475	0.189	0.142	0.089	0.158
Vis	r	0.103	0.032	-0.011	-0.116	0.128	0.100
	BF_{10}	0.272	0.093	0.084	0.371	0.521	0.253
VT	r	-0.066	-0.070	-0.090	-0.044	0.020	-0.058
	BF_{10}	0.135	0.145	0.206	0.103	0.087	0.121

4.4 sLORETA outcomes

The loadings of only two f-PCs were significantly correlated with two distinct individual ARSQ ratings. We constrained an sLORETA analysis for the A1 × Comfort and T1 × Sleepiness rating scores only.

The sLORETA analysis resulted in a significant correlation for T1 × Sleepiness ($r = 0.247$, $p < 0.05$), with the main activity evident in the limbic lobe, the anterior cingulate gyrus, and Broadman area 24 and Broadman area 23 (Figure 9B). The A1 × Comfort analysis failed to reach a significant threshold ($r = 0.207$, $p > 0.05$).

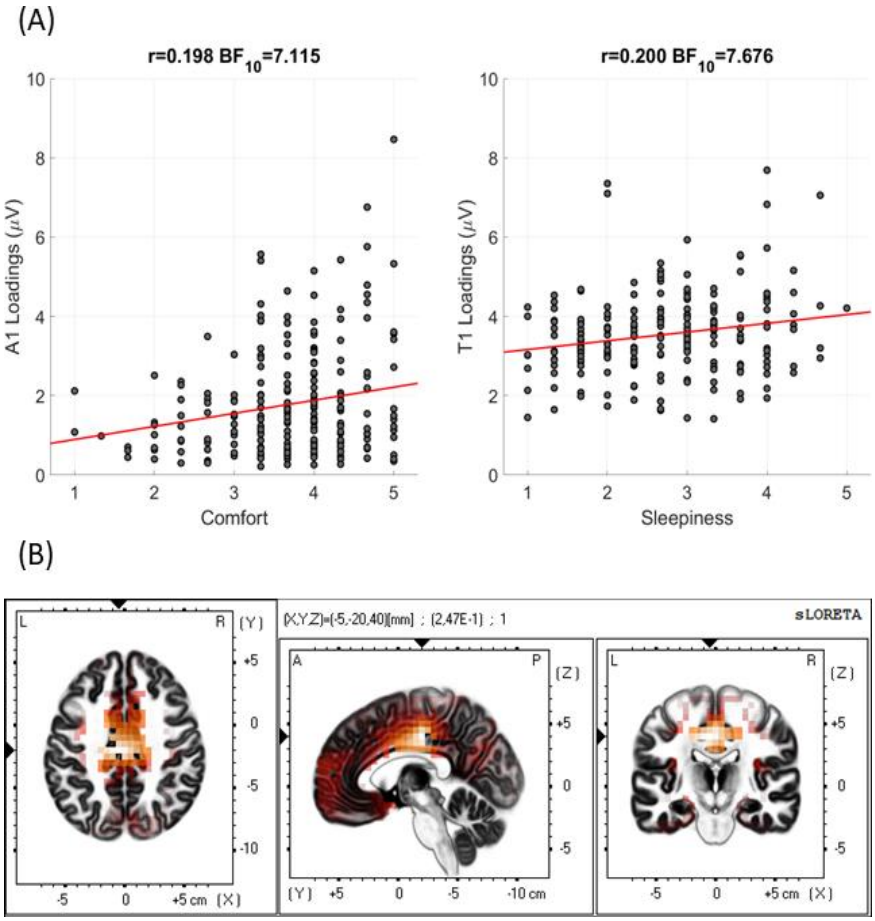

Figure 9. Scatter plots displaying relationship between fPCs' loadings and Amsterdam Resting-State Questionnaire (ARSQ) dimensions (N = 226) (A). Intracortical activity estimated with sLORETA for T1 and ARSQ domain of Sleepiness (B).

GFS mean values for frequency ranges were: Delta: 0.517 (SD. ±0.039), Theta: 0.541 (SD. ±0.026), Alpha: 0.595 (SD. ±0.032), Beta 0.522 (SD. ±0.025) and are in line with those reported in literature with alpha GFS being the highest (Koenig et al., 2001; Park et al., 2008; Smailovic et al., 2018). GFS values and their distributions and the GFS grand-average across participants as a function of frequency is plotted in Figure 10.

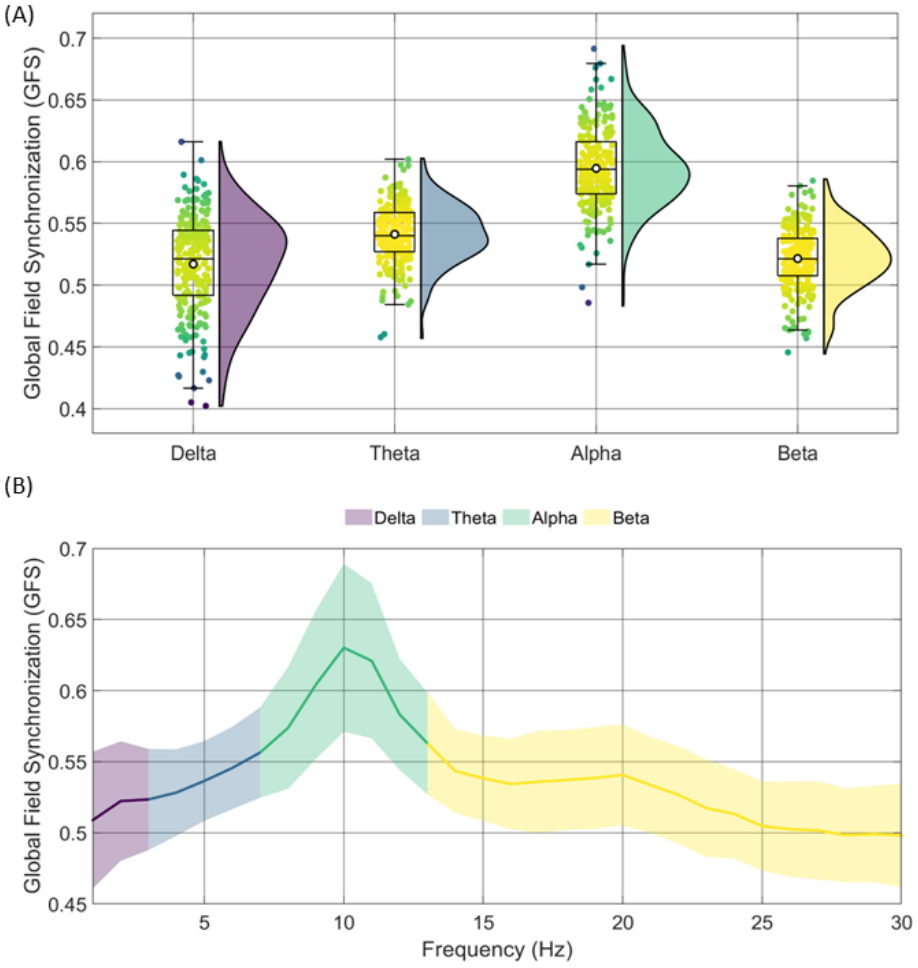

Figure 10. Data distribution of GFS values for each frequency range. The cloud part illustrates GFS values distribution, box plot part shows interquartile range, black horizontal line indicates median, white dot indicates the mean value (A). GFS average between participants (N=226) as a function of frequency. Shaded area indicates standard deviation (B).

4.6 Relationship between GFS and ARSQ Dimensions

Out of forty possible correlations (ten ARSQ domains x four frequency ranges) only two interactions were statistically significant (BF_{10} > 3). GFS value of alpha range was positively correlated with the ARSQ domain of Comfort (r = 0.208, BF_{10} = 11.646). Similarly, the GFS values of beta range, was positively associated with the domain of Comfort (r = 0.197, BF_{10} = 6.664) (Figure 11). The full Pearson's correlation coefficient and BFsfor correlations between the GFS values and ARSQ scores are summarized in Table 5.

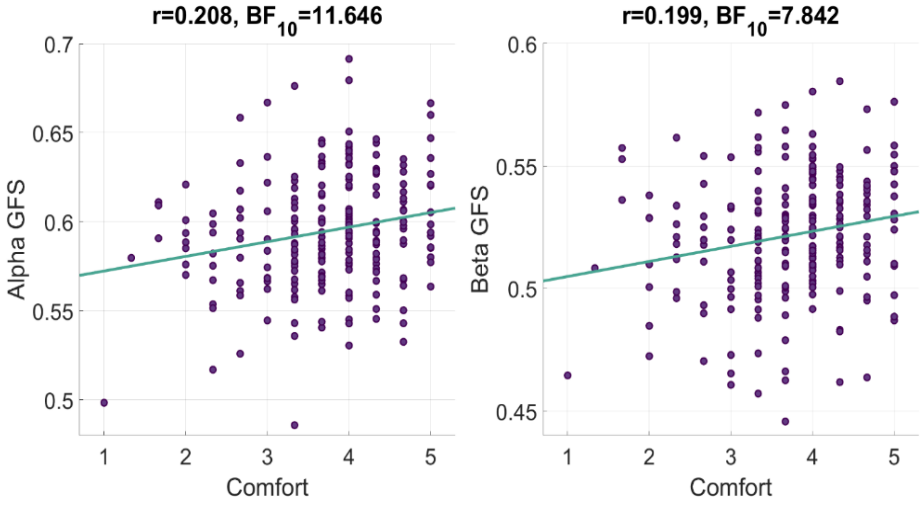

Figure 11. Scatter plots displaying relationship between GFS values and ARSQ domain of Comfort.

Table 6. Bayesian Pearson's correlation coefficient between GFS values and ARSQ domains. Significant correlations are marked in grey squares.

		Delta	**Theta**	**Alpha**	**Beta**
DoM	r	0.010	-0.102	-0.150	0.028
	BF_{10}	0.084	0.270	0.288	0.091
ToM	r	-0.090	-0.082	-0.019	0.071
	BF_{10}	0.206	0.175	0.086	0.145
Self	r	-0.004	0.017	0.107	0.112
	BF_{10}	0.083	0.086	0.304	0.338
Planning	r	-0.112	-0.057	0.031	0.059
	BF_{10}	0.341	0.120	0.092	0.122
Sleepiness	r	0.062	-0.036	-0.072	0.041

		Delta	Theta	Alpha	Beta
	BF_{10}	0.128	0.096	0.149	0.100
Comfort	r	0.091	0.155	**0.208**	**0.199**
	BF_{10}	0.209	1.243	**11.646**	**7.842**
SA	r	0.074	0.062	-0.015	0.011
	BF_{10}	0.152	0.127	0.085	0.084
HC	r	-0.061	0.034	-0.025	-0.021
	BF_{10}	0.126	0.95	0.089	0.087
Vis	r	0.008	0.040	0.043	0.022
	BF_{10}	0.084	0.099	0.102	0.088
VT	r	-0.067	-0.099	0.022	0.073
	BF_{10}	0.137	0.248	0.087	0.150

4.7 Temporal parameters of EEG microstates

Silhouette coefficient (mean value of silhouettes for each number of clusters) yielded an optimal value at k = 7. Four microstate topographies with right frontal to left posterior, left frontal to right posterior, frontal to occipital and fronto-central configurations matched the most frequently reported microstate classes in the literature and were labeled as microstates A, B, C and D, respectively (Koenig et al., 2002). Among three additional topographies, one had left lateralized activity and was similar to microstate E reported in studies by (Bréchet et al., 2019; Custo et al., 2017; Zanesco et al., 2021b) and was labeled accordingly as microstate E. One topography displayed posterior activity and matched microstate F reported in studies by (Bréchet et al., 2019; Custo et al., 2017; D'Croz-Baron et al., 2021), microstate E reported in studies by (Damborská et al., 2019a, 2019b; Murphy et al., 2020) and microstate C′ reported in study (Jabès et al., 2021). and was further labeled as microstate F. The remaining topography had right lateralized activity and was similar to microstate G from study by (Custo et al., 2017) and microstate F reported in studies by (Damborská et al., 2019b; Takarae et al., 2022; Zanesco et al., 2021b), this was further labeled as microstate G (Figure 12). The extracted seven microstates explained 83.3% of the global variance. Mean and standard deviations of the temporal characteristics of each seven microstates are presented in Table 7. The parameters of extracted microstates are in the range

of those reported in the literature (Khanna et al., 2015; Michel and Koenig, 2018; Zanesco et al., 2020b).

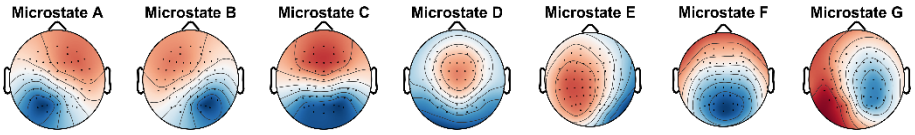

Figure 12. Seven group-level topographies of microstates based on Silhouette method.

Table 7. Temporal parameters of microstates

	Duration (ms)	Occurrence (Hz)	Coverage (%)
MS A	43.36 (±8.26)	3.60 (±0.95)	15.13 (±4.00)
MS B	45.34 (±9.25)	3.80 (±0.89)	16.93 (±4.20)
MS C	52.51 (±14.18)	4.50 (±0.83)	22.91 (±6.50)
MS D	40.91 (±7.16)	3.44 (±1.00)	13.82 (±3.90)
MS E	36.72 (±6.31)	2.62 (±0.73)	9.43 (±2.40)
MS F	39.59 (±7.34)	3.22 (±0.99)	12.56 (±4.00)
MS G	36.06 (±5.81)	2.65 (±0.81)	9.31 (±2.50)

4.8 Association between Temporal Parameters of Microstates and ARSQ Dimensions

Bayesian Pearson correlation showed a negative association between coverage of microstate F and Somatic awareness ($r = -0.210$, $BF_{10} = 6.871$), significant interaction between Self domain and duration of microstate D ($r = -0.203$, $BF_{10} = 5.224$) and occurrence of microstate B ($r = 0.192$, $BF_{10} = 3.305$). Bayesian Pearson correlation also revealed a negative relationship with the occurrence of microstate C ($r = -0.212$, $BF_{10} = 7.638$) and positive relationships with duration of microstate E ($r = 0.220$, $BF_{10} = 10.949$) and duration of microstate G ($r = 0.203$, $BF_{10} = 5.284$). Bayesian Pearson correlation coefficients for temporal characteristics of each microstate class and scores of ARSQ dimensions are summarized in Table 7. Significant associations between microstate characteristics and ARSQ domains are presented in scatter plots in Figure 13.

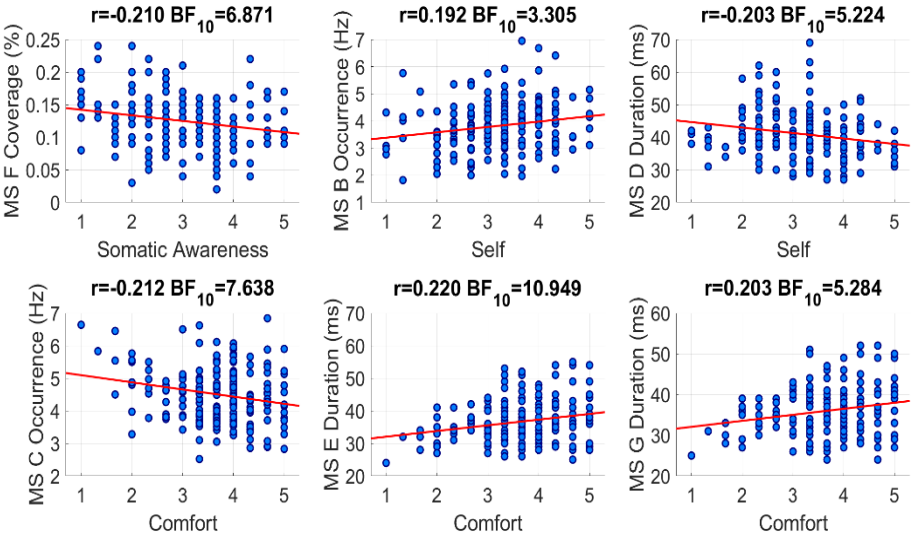

Figure 13. Scatter plots displaying relationship between microstate parameters and Amsterdam Resting-State Questionnaire (ARSQ) dimensions (N = 197).

No correlation was observed between coverage of microstate C and Somatic awareness ($r = -0.007$, $BF_{10} = 0.090$). In addition, we performed spatial correlation analysis between microstate C, when number of clusters is preset to 4 and microstates C and F, when number of clusters is determined to be 7 (Figure 14 A). The results showed that these three topographical maps maintain a high topographical similarity (SC < 0.7). More important, microstate C from *k=4* analysis and microstate F from k=7 analysis yielded a very high spatial correlation value (SC = 0.966), confirming hypothesis, that spatially similar microstates might be merged into a single microstate, when suboptimal number of clusters is used. Bayesian Pearson's correlation coefficient between ARSQ domain scores for Somatic awareness and coverage of microstate C when number of clusters is preset to four, replicated a significant negative association reported by Pipinis et al. (Pipinis et al., 2017) (Figure 14 B).

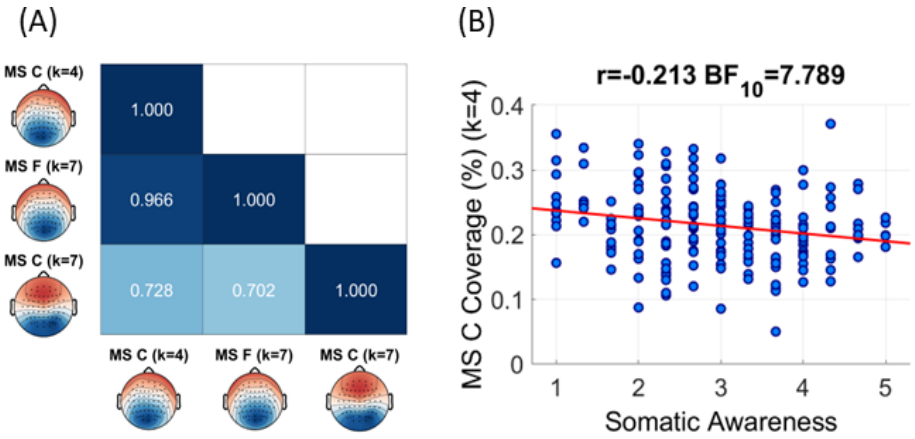

Figure 14. Spatial Correlation between microstate C, when k = 4 (Top), and microstates C and F, when k = 7 (Middle and Bottom) (A). Relationship between microstate C, when k=4, and scores on Somatic awareness (B) (N = 197).

Table 8. Bayesian Pearson's correlation coefficients between microstate characteristics and ARSQ scores. Grey squares indicates significant correlations. Bold squares indicate correlations with substantial-to-strong level of evidence. Strong coefficients at BF_{10}>10 is underlined.

		DoM	ToM	Self	Planning	Sleep	Comfort	SA	Health	Visual	Verbal
Microstate A	Dur	r=-0.020 BF_{10}=0.093	r=0.029 BF_{10}=0.097	r=-0.119 BF_{10}=0.352	r=-0.008 BF_{10}=0.090	r=-0.005 BF_{10}=0.089	r=0.134 BF_{10}=0.512	r=0.034 BF_{10}=0.100	r=-0.018 BF_{10}=0.092	r=0.023 BF_{10}=0.099	r=-0.037 BF_{10}=0.102
	Occ	r=0.012 BF_{10}=0.090	r=0.051 BF_{10}=0.115	r=0.096 BF_{10}=0.220	r=-0.038 BF_{10}=0.103	r=0.111 BF_{10}=0.294	r=-0.082 BF_{10}=0.172	r=-0.019 BF_{10}=0.092	r=0.028 BF_{10}=0.096	r=0.062 BF_{10}=0.129	r=0.035 BF_{10}=0.100
	Cov	r=-0.009 BF_{10}=0.090	r=0.056 BF_{10}=0.121	r=0.010 BF_{10}=0.090	r=-0.055 BF_{10}=0.119	r=0.097 BF_{10}=0.223	r=0.002 BF_{10}=0.089	r=-0.005 BF_{10}=0.089	r=0.050 BF_{10}=0.114	r=0.056 BF_{10}=0.120	r=0.030 BF_{10}=0.097
	GFP	r=-0.016 BF_{10}=0.091	r=0.040 BF_{10}=0.104	r=-0.066 BF_{10}=0.137	r=-0.039 BF_{10}=0.103	r=-0.015 BF_{10}=0.091	r=0.115 BF_{10}=0.324	r=0.001 BF_{10}=0.089	r=-0.027 BF_{10}=0.096	r=0.037 BF_{10}=0.102	r=-0.060 BF_{10}=0.127
Microstate B	Dur	r=-0.028 BF_{10}=0.096	r=0.028 BF_{10}=0.096	r=-0.054 BF_{10}=0.119	r=0.052 BF_{10}=0.116	r=-0.101 BF_{10}=0.242	r=0.182 BF_{10}=2.339	r=-0.004 BF_{10}=0.089	r=-0.063 BF_{10}=0.131	r=0.012 BF_{10}=0.090	r=-0.016 BF_{10}=0.091
	Occ	r=0.068 BF_{10}=0.139	r=-0.017 BF_{10}=0.092	**r=0.192** **BF_{10}=3.305**	r=0.083 BF_{10}=0.173	r=-0.038 BF_{10}=0.103	r=-0.117 BF_{10}=0.337	r=0.024 BF_{10}=0.094	r=0.044 BF_{10}=0.107	r=-0.003 BF_{10}=0.089	r=0.062 BF_{10}=0.130
	Cov	r=0.038 BF_{10}=0.103	r=0.008 BF_{10}=0.090	r=0.130 BF_{10}=0.464	r=0.111 BF_{10}=0.295	r=-0.121 BF_{10}=0.372	r=0.048 BF_{10}=0.111	r=-0.001 BF_{10}=0.089	r=0.004 BF_{10}=0.089	r=0.006 BF_{10}=0.090	r=0.058 BF_{10}=0.123
	GFP	r=-0.019 BF_{10}=0.092	r=0.040 BF_{10}=0.104	r=-0.058 BF_{10}=0.124	r=-0.019 BF_{10}=0.092	r=-0.041 BF_{10}=0.105	r=0.128 BF_{10}=0.442	r=0.008 BF_{10}=0.090	r=-0.034 BF_{10}=0.099	r=0.039 BF_{10}=0.104	r=-0.076 BF_{10}=0.155
Microstate C	Dur	r=-0.070 BF_{10}=0.141	r=-0.028 BF_{10}=0.096	r=-0.124 BF_{10}=0.398	r=-0.063 BF_{10}=0.131	r=-0.003 BF_{10}=0.089	r=0.106 BF_{10}=0.266	r=0.008 BF_{10}=0.090	r=-0.050 BF_{10}=0.113	r=-0.045 BF_{10}=0.109	r=-0.067 BF_{10}=0.138

	Occ	r=0.004 BF_{10}=0.089	r=-0.028 BF_{10}=0.096	r=0.093 BF_{10}=0.205	r=-0.042 BF_{10}=0.106	r=0.074 BF_{10}=0.151	**r=-0.212** **BF_{10}=7.638**	r=-0.021 BF_{10}=0.093	r=0.034 BF_{10}=0.100	r=-0.023 BF_{10}=0.094	r=-0.006 BF_{10}=0.089
	Cov	r=-0.056 BF_{10}=0.120	r=-0.046 BF_{10}=0.109	r=-0.059 BF_{10}=0.125	r=-0.100 BF_{10}=0.237	r=0.027 BF_{10}=0.096	r=-0.037 BF_{10}=0.102	r=-0.007 BF_{10}=0.090	r=-0.011 BF_{10}=0.090	r=-0.047 BF_{10}=0.110	r=--0.063 BF_{10}=0.130
	GFP	r=-0.023 BF_{10}=0.094	r=0.035 BF_{10}=0.101	r=-0.070 BF_{10}=0.144	r=-0.038 BF_{10}=0.103	r=-0.030 BF_{10}=0.097	r=0.112 BF_{10}=0.302	r=0.009 BF_{10}=0.090	r=-0.032 BF_{10}=0.099	r=-0.033 BF_{10}=0.99	r=-0.081 BF_{10}=0.169
Microstate D	**Dur**	r=0.069 BF_{10}=0.141	r=-0.034 BF_{10}=0.100	**r=-0.203** **BF_{10}=5.224**	r=-0.037 BF_{10}=0.102	r=-0.101 BF_{10}=0.239	r=0.177 BF_{10}=1.939	r=0.103 BF_{10}=0.247	r=-0.067 BF_{10}=0.138	r=-0.041 BF_{10}=0.105	r=-0.048 BF_{10}=0.111
	Occ	r=-0.009 BF_{10}=0.090	r=-0.054 BF_{10}=0.119	r=0.008 BF_{10}=0.090	r=-0.088 BF_{10}=0.189	r=0.094 BF_{10}=0.210	r=-0.128 BF_{10}=0.438	r=0.135 BF_{10}=0.531	r=0.054 BF_{10}=0.118	r=0.024 BF_{10}=0.094	r=0.037 BF_{10}=0.102
	Cov	r=-0.057 BF_{10}=0.122	r=-0.078 BF_{10}=0.160	r=-0.115 BF_{10}=0.322	r=-0.100 BF_{10}=0.234	r=0.024 BF_{10}=0.094	r=-0.031 BF_{10}=0.098	r=0.158 BF_{10}=1.034	r=0.026 BF_{10}=0.095	r=-0.053 BF_{10}=0.117	r=0.020 BF_{10}=0.093
	GFP	r=-0.015 BF_{10}=0.091	r=0.026 BF_{10}=0.095	r=-0.093 BF_{10}=0.206	r=-0.043 BF_{10}=0.107	r=-0.024 BF_{10}=0.094	r=0.121 BF_{10}=0.371	r=0.039 BF_{10}=0.103	r=-0.041 BF_{10}=0.105	r=0.033 BF_{10}=0.099	r=-0.076 BF_{10}=0.155
Microstate E	**Dur**	r=-0.040 BF_{10}=0.104	r=0.016 BF_{10}=0.091	r=-0.116 BF_{10}=0.328	r=0.043 BF_{10}=0.107	r=-0.108 BF_{10}=0.279	**r=0.220** **BF_{10}=10.95**	r=0.056 BF_{10}=0.121	r=-0.083 BF_{10}=0.172	r=0.011 BF_{10}=0.090	r=-0.045 BF_{10}=0.108
	Occ	r=0.025 BF_{10}=0.095	r=-0.015 BF_{10}=0.091	r=0.116 BF_{10}=0.329	r= 0.015 BF_{10}=0.091	r=-0.110 BF_{10}=0.090	r=-0.081 BF_{10}=0.167	r=0.034 BF_{10}=0.099	r=0.030 BF_{10}=0.097	r=0.026 BF_{10}=0.095	r=0.008 BF_{10}=0.090
	Cov	r=0.015 BF_{10}=0.091	r=-0.030 BF_{10}=0.097	r=0.030 BF_{10}=0.097	r=0.037 BF_{10}=0.102	r=-0.110 BF_{10}=0.289	r=0.052 BF_{10}=0.116	r=0.067 BF_{10}=0.137	r=-0.027 BF_{10}=0.096	r=0.020 BF_{10}=0.093	r= 0.0007683 BF_{10}=0.089

	GFP	r=-0.015 BF_{10}=0.091	r=0.037 BF_{10}=0.102	r=-0.066 BF_{10}=0.137	r=-0.016 BF_{10}=0.092	r=-0.034 BF_{10}=0.100	r=0.135 BF_{10}=0.530	r=0.021 BF_{10}=0.093	r=-0.040 BF_{10}=0.104	r=0.040 BF_{10}=0.104	r=-0.077 BF_{10}=0.158
Microstate F	**Dur**	r=-0.038 BF_{10}=0.103	r=0.014 BF_{10}=0.091	r=-0.134 BF_{10}=0.507	r=0.088 BF_{10}=0.188	r=-0.030 BF_{10}=0.097	r=0.121 BF_{10}=0.374	r=-0.101 BF_{10}=0.241	r=-0.093 BF_{10}=0.205	r=-0.009 BF_{10}=0.090	r=-0.022 BF_{10}=0.093
	Occ	r=0.051 BF_{10}=0.115	r=0.029 BF_{10}=0.097	r=0.071 BF_{10}=0.145	r=0.119 BF_{10}=0.352	r=0.082 BF_{10}=0.172	r=-0.111 BF_{10}=0.294	r=-0.140 BF_{10}=0.607	r=-0.026 BF_{10}=0.095	r=0.026 BF_{10}=0.092	r=-0.018 BF_{10}=0.092
	Cov	r=0.035 BF_{10}=0.100	r=0.041 BF_{10}=0.105	r=-0.016 BF_{10}=0.092	r=0.146 BF_{10}=0.710	r=0.043 BF_{10}=0.107	r=-0.036 BF_{10}=0.101	**r=-0.210** **BF_{10}=6.871**	r=-0.064 BF_{10}=0.132	r=0.019 BF_{10}=0.092	r=-0.031 BF_{10}=0.098
	GFP	r=-0.006 BF_{10}=0.089	r=0.051 BF_{10}=0.115	r=-0.064 BF_{10}=0.133	r=0.005 BF_{10}=0.089	r=-0.011 BF_{10}=0.090	r=0.103 BF_{10}=0.252	r=-0.034 BF_{10}=0.100	r=-0.044 BF_{10}=0.108	r=0.045 BF_{10}=0.108	r=-0.081 BF_{10}=0.169
Microstate G	**Dur**	r=-0.024 BF_{10}=0.094	r=0.018 BF_{10}=0.092	r=-0.114 BF_{10}=0.315	r=0.025 BF_{10}=0.095	r=-0.090 BF_{10}=0.195	**r=0.203** **BF_{10}=5.284**	r=0.030 BF_{10}=0.097	r=-0.039 BF_{10}=0.104	r<0.001 BF_{10}=0.089	r=-0.029 BF_{10}=0.097
	Occ	r=0.075 BF_{10}=0.153	r=0.023 BF_{10}=0.094	r=0.139 BF_{10}=0.580	r=0.011 BF_{10}=0.090	r=0.046 BF_{10}=0.109	r=-0.068 BF_{10}=0.140	r=0.055 BF_{10}=0.120	r=0.44 BF_{10}=0.108	r=0.024 BF_{10}=0.094	r=0.060 BF_{10}=0.126
	Cov	r=0.083 BF_{10}=0.174	r=0.042 BF_{10}=0.106	r=0.096 BF_{10}=0.217	r=0.041 BF_{10}=0.105	r=-0.023 BF_{10}=0.094	r=0.047 BF_{10}=0.110	r=0.068 BF_{10}=0.140	r=0.042 BF_{10}=0.105	r=0.021 BF_{10}=0.093	r=0.074 BF_{10}=0.151
	GFP	r=-0.010 BF_{10}=0.090	r=0.047 BF_{10}=0.110	r=-0.052 BF_{10}=0.116	r=-0.015 BF_{10}=0.091	r=-0.024 BF_{10}=0.094	r=0.135 BF_{10}=0.523	r=0.017 BF_{10}=0.092	r=-0.030 BF_{10}=0.097	r=0.044 BF_{10}=0.108	r=-0.058 BF_{10}=0.123

5. DISCUSSION

The relationship between subjective experiences at rest and brain functional activity is not well known. An increasing number of studies have aimed at bridging this gap between objectively defined physiological signals and subjective experience during resting-state recording sessions. The ARSQ appeared to be a useful tool to relate biological signals collected over the resting-state session with participants' subjective experiences and emotions. Several studies using different brain-imaging modalities and applying different analysis methods have reported associations with the ARSQ domains: Discontinuity of Mind (Stoffers et al., 2015; Tomescu et al., 2022), Theory of Mind (Marchetti et al., 2015), Self (Tarailis et al., 2021; Tomescu et al., 2022), Planning (Portnova et al., 2019; Zanesco et al., 2021a), Sleepiness (Diaz et al., 2013; Stoffers et al., 2015), Comfort (Stoffers et al., 2015; Tarailis et al., 2021; Zanesco et al., 2021a), Somatic Awareness (Pipinis et al., 2017; Tarailis et al., 2021; Tomescu et al., 2022; Zanesco et al., 2021a), Visual Thoughts (Stoffers et al., 2015), Verbal Thoughts (Tomescu et al., 2022).

In this work the focus was made on the following approaches: spectral EEG characteristics, global synchronization level and topographical aspects.

5.1 f-PCA

Frequency principal components analysis (f-PCA) has been proposed to decompose the EEG frequency spectral structure into meaningful distinct components with the inherent advantage of providing a data-driven approach across the traditional bands.

As an outcome of f-PCA, in the current work, six factors were retained: three components in the alpha range and one each in the delta, theta, and beta ranges. This is comparable with other resting-state f-PCA studies with minor differences regarding topographical display and the variances explained (Barry et al., 2020; Barry and De Blasio, 2018; Tenke and Kayser, 2005). The f-PCA method has an advantage over traditional EEG spectral analysis, as it evaluates naturally occurring frequency components that are not affected or constrained by somewhat arbitrary, chosen EEG frequency band ranges (Barry et al., 2019; Newson and Thiagarajan, 2019), and it is completely data-driven.

Based on the previous observations, we expected several associations involving alpha and theta components to be present. The EEG data were

mainly driven by the alpha activity; the retained three components peaking at 9 (A1), 10.5 (A2), and 11.5 (A3) Hz together explained 41.82% of the total variance. These results are in line with the results reported in other f-PCA studies, where between two (Smith et al., 2020) to five (Tenke and Kayser, 2005) components in the alpha range have been extracted, explaining from 1.4% (A2 component peaking at 9.5 Hz (Barry and De Blasio, 2018)) to 50% (alpha/theta component peaking at 9 Hz (Tenke et al., 2011)) of the variance. Despite differences in the peak frequencies and explained variances, alpha-range components are topographically similar between the studies. In the current study, the A1, A2, and A3 components showed spatial correlation values ranging from 0.92 to 0.98. Functionally, alpha components were linked to the state of the subject's arousal earlier (Barry et al., 2020); thus, the relationship of alpha components to Sleepiness scores could be expected. However, although the retained alpha components explained almost half of the data, we observed a positive association only between A1 and the subjective ratings for the Comfort domain ($r = 0.198$, $BF_{10} = 7.115$) (Figure 9A). The Comfort domain was characterized by questions such as "I felt comfortable", "I felt happy", and "I felt relaxed". Previously, this domain has been associated with the temporal characteristics of broadband EEG microstates C, E, G (Tarailis et al., 2021), and D (Zanesco et al., 2021a). EEG microstates are mainly driven by alpha activity (Milz et al., 2017). Thus, the results, although unexpected, partially supported earlier observations. Nevertheless, the sLORETA analysis attempting to localize the relationship failed to reach a significance level for the A1 x Comfort analysis ($r = 0.207$, $p < 0.05$).

A single component in the theta range of T1 (peaking at 5.5 Hz) had pronounced midline frontal activity and was positively correlated with the subjective ratings for the Sleepiness domain ($r = 0.200$, $BF_{10} = 7.676$), suggesting more theta observed in subjects who reported more sleepiness. This result is in accordance with an initial report by Diaz et al. (Diaz et al., 2013) evaluating the ARSQ's relationship to physiological manifestations. The authors reported a positive correlation between the domain of Sleepiness and sustained midline theta activity. Furthermore, a positive correlation of frontal midline theta power (4–8 Hz) with subjective ratings on the Karolinska sleepiness scale was reported (Strijkstra et al., 2003) and a negative correlation between frontal theta activity and activation of the default mode network (DMN) was shown (Scheeringa et al., 2008). The activity in the DMN is related both to the processing of personally significant information, self-reflection, and self-referential internal mentation (Andrews-Hanna, 2012) and to stimulus-independent thoughts (Mason et al., 2007) that are more likely to

occur during a resting state. Previously, activity in the DMN was shown to positively correlate with Sleepiness (Stoffers et al., 2015). Similarly to Stoffers et al. (Stoffers et al., 2015), we observed decisive evidence for a positive correlation between the ARSQ domains of DoM (referring to 'I had busy thoughts', 'I had rapidly switching thoughts', and 'I had difficulty holding on to my thoughts') and Sleepiness ($r = 0.251$, $BF_{10} = 113.972$), suggesting that the more drowsiness subjects experienced, the more troubles they had in holding on to their thoughts. We attempted to localize the association between the theta component and Sleepiness and performed inverse modeling using sLORETA. The association emerged for activity in the limbic lobe and the anterior cingulate cortex (ACC) (Figure 2D). This result is compatible with reports on the localization of theta activity. Scheeringa et al. (Scheeringa et al., 2008) reported theta activity (2–9 Hz) that originated in the medial prefrontal cortex and ACC. Smith et al. (Smith et al., 2020) localized sources of the theta component, peaking at 5 Hz, in the premotor cortex, including the dorsal ACC. Nishida et al. (Nishida et al., 2004) showed theta (5–7 Hz) activation in the ACC during wakefulness and REM sleep, but not in the slow-wave sleep stage. Thus, the positive correlation between individual ratings for Sleepiness and the activity in the limbic lobe and ACC is in line with results reported in the literature.

No associations were observed with components in the delta and beta frequency ranges, although Portnova et al. (Portnova et al., 2019) previously reported a negative correlation between the power spectrum density from 2–3 Hz and Planning. However, it should be noted that both the extracted D1 (peaking at 0.5 Hz) and B1 (peaking at 17 Hz) components were somewhat different from those reported previously: D1 resembled activity over the left frontal area, peaking at the FP1, AF7, and F7 electrodes, while reports in the literature have observed maximum activities in the central, fronto-central, and right frontal areas (Barry and De Blasio, 2018; Karamacoska et al., 2019a, 2019b). B1 had a right occipital activation with maximum values at the PO4, PO6, and PO8 electrodes that is in line with some reports (Karamacoska et al., 2019a, 2019b) but contradicts others that showed a fronto-central topographical display (Barry and De Blasio, 2018; Tenke and Kayser, 2005). The nature of these discrepancies is not clear. To our knowledge, our study performed an f-PCA analysis for the largest sample of young, healthy adults so far, having enough power to add to the robustness of the results.

5.2 GFS

We utilized GFS as the parameter to estimate global functional connectivity without explicit source models for the interpretation of the results (Koenig et al., 2001; Rusterholz et al., 2017). The GFS method was successfully applied in studies on clinical populations (Koenig et al., 2001; Olamat and Akan, 2017; Smailovic et al., 2022) and different vigilance levels (Achermann et al., 2016; Nicolaou and Georgiou, 2014); no study so far, however, attempted to relate GFS with subjective experience during the resting-state with eyes closed. We showed a strong evidence of relationship between ARSQ domain of Comfort and GFS values in the alpha range ($r=0.208$, $BF_{10}=11.646$) and a substantial evidence for positive relationship between ARSQ domain of Comfort and GFS in the beta frequency range ($r=0.199$, $BF_{10}=7.842$). No other significant associations were demonstrated.

GFS stands as a global measure of functional connectivity that does not require any particular brain region to be involved in the process of interest (Koenig et al., 2001) Thus, higher GFS levels indicate functional connection of large-scale, distributed neural systems, while lower levels – their disconnection. To the best of our knowledge, the GFS assessment in the current study was performed on the largest sample of healthy participants so far. In line with previous reports, activity in the alpha frequency range was the most dominant (Achermann et al., 2016; Koenig et al., 2001; Smailovic et al., 2022) (Figure 10). The activity within the alpha range is frequently related to the general arousal (Barry et al., 2020, 2007) and is considered a sign of cortical idling (Croce et al., 2020; Milz et al., 2016). However, non-arousal functionality of certain aspects of alpha activity was also proposed (Barry et al., 2020), suggesting it may be implemented in some mind-wandering experiences. In line with the above mentioned and in accordance with the results of fPCA analysis where we showed a positive relationship between frequency principal component peaking at 9 Hz and scores of Comfort, we demonstrate a positive association between GFS values in the alpha range and scores on the same ARSQ domain.

The ARSQ domain of Comfort is characterized by questions such as “I felt comfortable”, “I felt happy”, and “I felt relaxed”. Thus, this domain may equally reflect the physical and mental well-being, including the general aspects of vigilance and emotional state. We speculate that the positive relationship between GFS within the alpha range and Comfort scores most likely points to the lowered arousal/vigilance and higher relaxation level-determined influence. Previously, waking GFS in the alpha range (9-11 Hz) in the eyes closed condition was shown to gradually decrease following

prolonged sleep deprivation (Achermann et al., 2016). As the subjective experiences during the sleep deprivation are not comfortable per se (Kaida and Niki, 2014), this observation goes in line with our results. Achermann et al. proposed the thalamus to be responsible for the widespread cortical synchrony as observed for the rhythms with the highest GFS, including waking alpha. Authors also pointed to the results of Schwab et al (Schwab et al., 2015), who found thalamic involvement in the generation of microstates as an indication of thalamus role for the synchrony of oscillations among different cortical regions. This corresponds to the results microstate analysis demonstrating associations between several parameters of resting-state microstates (specific patterns of synchronization (Tait and Zhang, 2022)) to the scores on the Comfort domain. Finally, Ricci et al (Ricci et al., 2022) recently reported that lower comfort in virtual reality settings was associated with a lower alpha power compared to higher comfort experience. Authors proposed that the experience of higher comfort is related to the top-down mechanisms that modulate visual attention, reducing the awareness of external stimuli and restoring a status with greater partial relaxation.

On the contrary, the positive association of GFS values in the beta and scores on Comfort potentially reflects the physical well-being. Earlier, Engel and Fries proposed that beta-band activity might be associated to maintenance of the current motor settings (Engel and Fries, 2010). Participants of our experiment, as described in the methods part, were instructed to relax and spend the entire 5 min. session sitting in the up-right position, i.e. sustained body position that have been experienced as comfortable. The assumption of beta GFS link to Comfort indicating physical aspects also goes in line with the report by Stoffers et al. (Stoffers et al., 2015) on a positive correlation between the fMRI-detected activity in the sensorimotor network and ARSQ domain of Comfort. Noteworthy, there are numerous studies, showing a negative relationship between beta band activity and thermal comfort (Chang et al., 2002; Son and Chun, 2018). We did not assess thermal senses/experiences in our study; nevertheless, experiments were performed in the Laboratory settings with temperature set at 20 ^{o}C that was regarded as comfortable (Oi et al., 2017). Within similar conditions, a positive association between beta power and thermal sensation was demonstrated (Pao et al., 2022), indicating that GFS in the beta range might be also related to the sense of being thermally neutral/comfortable. Finally, the beta activity was previously inversely related to anxiety (Palacios-García et al., 2021), stress (Choi et al., 2015) and mental fatigue (Shigihara et al., 2013); however this goes in opposite with the currently observed association. It should be noted that stress and mental fatigue are regarded extreme variants that are not expected to be experienced

during the resting-state session. In line with this, Diaz et al (2013) demonstrated that Comfort was strongly positively associated to mental health (Diaz et al., 2013) and negatively to Harm avoidance (Diaz et al., 2014). Thus, we speculate that the positive correlation as obtained between GFS in the beta range and Comfort scores of ARSQ reflect the aspects of physical rather than mental comfort.

Based on previous works, we anticipated to observe several other associations. For example, a positive relationship between power characteristics of theta activity and Sleepiness was demonstrated in our fPCA analysis and by Diaz et al (2013) (Diaz et al., 2013; Tarailis et al., 2021), hence we expected that global synchronization in this range would also show links to Sleepiness scores. Similarly, we expected GFS in the alpha range to be positively associated with the ARSQ domain of Planning, as a positive correlation was previously shown with the power spectral density in 12-13 Hz (Portnova et al., 2019). However, none of these links emerged for GFS measure. In line with this, previous studies in clinical samples have also demonstrated distinct effects for power and GFS (Smailovic et al., 2022, 2018). This might reflect the fact that GFS and power measures reflect on different aspects: EEG power is regarded as a representation of the magnitude of activity at certain frequencies (Smit et al., 2012), while GFS (and other phase based outcomes) reflects the degree to which connections are present across the brain (Berger et al., 2014; Ng et al., 2013; Xiao et al., 2018).

5.3 EEG Microstates

The microstate approach allows evaluation of rapidly changing network reorganization that occurs in order to mediate complex mental activities and optimally respond to rapidly changing input.

An initial work by Pipinis et al. (Pipinis et al., 2017) related ARSQ to the parameters of four classical microstates (A, B, C, D), showing a negative association between Somatic Awareness (which is evaluated with statements ‘I was conscious of my body’, ‘I thought about my heartbeat’, ‘I thought about my breathing’) and coverage of microstate C. Lately, Zanesco et al. (Zanesco et al., 2021a), performed a meta analytic correlation combining results by Pipinis et al. and their own results and showed the inverse association between ARSQ domain of Somatic Awareness and a coverage of microstate C. However, Custo et al. demonstrated that when only four microstates are extracted, the functionally different but spatially overlapping microstates—C and F—are merged into a single microstate C (Custo et al., 2017). Thus, we estimated the optimal number of microstates without putting a priori

constraint. The optimal number of microstate configurations was estimated at 7, corresponding to the report by (Custo et al., 2017). Importantly, the spatial correlation between microstates C and F was ~0.7 (Figure 1D), thus supporting the results of Custo et al. (Custo et al., 2017) that the functionally different but spatially overlapping microstates — C and F — might be merged into a single microstate C (Custo et al., 2017). This is further supported by the spatial correlation observed between microstate C from k = 4 with microstates C and F from k = 7.

We suggest that a negative correlation observed between the coverage of microstate F and the dimension of Somatic Awareness in the current work resembles the same associations as observed by Pipinis et al. and Zanesco et al. (Pipinis et al., 2017; Zanesco et al., 2021a). Custo et al. reported the strongest activity for microstate F in the dorsal anterior cingulate cortex, superior frontal gyrus, middle frontal gyrus and insula. These loci overlap with the Salience network and correspond to the sources of the microstate C reported by Britz and colleagues (Britz et al., 2010). Britz et al. (Britz et al., 2010) associated microstate C with integration of interoceptive information with emotional salience. Several studies extracting four canonical microstates reported increased microstate C activity during the resting-state period compared to different tasks (Liu et al., 2020; Seitzman et al., 2017; Zappasodi et al., 2019) and associated it with task-negative Default Mode Network (DMN) (Bréchet et al., 2019; Custo et al., 2017). Likely, part of this involvement is also seen as the negative association between the occurrence of microstate C and the Comfort (measured with questions like 'I felt comfortable', 'I felt relaxed', 'I felt happy') in our study. The ability to relax and feel comfortable is related to interoceptive aspects through the urge to restore balance in physical and emotional context (Forkmann et al., 2019; Wei and Van Someren, 2020). The domain of Comfort was previously related with the ability to switch between tasks (Simpraga et al., 2021), correlated with character traits of self-directedness (associated with individual ability to govern behavior according to situational demand) (Diaz et al., 2014) and mental and physical well-being (Diaz et al., 2013).

To note, the Comfort domain of ARSQ was also positively associated with the duration of microstates E and G. However, due to the fact that we had no a priori expectations regarding microstate classes other than C and F, these correlations should be regarded as exploratory. Nevertheless, we attempt to discuss the observed correlations in the framework of known functional aspects behind certain microstate classes.

Microstate E is a relatively newly described microstate and it was reported only in recent studies. Brechet and colleagues (Bréchet et al., 2019)

found the main sources of microstate E in the right medial prefrontal cortex that is a subsystem of DMN, which participates in the theory of mind and mental simulations (Chen et al., 2020) and Custo et al. (Custo et al., 2017) observed the strongest activity for microstate E in the anterior cingulate cortex, posterior cingulate cortex and precuneus—these areas are parts of DMN. Thus, an opposite relationship between domain of Comfort and microstates C and E probably reflects the different aspects of DMN involvement that is known to play a crucial role in processing of personally significant information, self-reflection and self-referential internal mentation (Andrews-Hanna, 2012).

Microstate G was reported only in six studies so far (Custo et al., 2017; Damborská et al., 2019b; Luo et al., 2020; Takarae et al., 2022; Tarailis et al., 2021; Zanesco et al., 2021b) and the functional role of this microstate remains unclear. Custo et al. (Custo et al., 2017) localized sources for microstate G in the right inferior parietal lobe, superior temporal gyrus and cerebellum and associated microstate G with the sensorimotor network due to the strong activity observed in cerebellum. Stoffers and colleagues (Stoffers et al., 2015) reported a positive correlation between ARSQ domain of Comfort and functional connectivity within Sensorimotor network. Thus, the observed positive association between duration of microstate G and Comfort potentially reflects the physical aspect of well-being stemming from appropriate somatosensory activation.

Finally, the ARSQ domain of Self was positively correlated to the occurrence of microstate B and negatively correlated to the duration of microstate D. Although microstate B was previously associated with verbalization (Antonova et al., 2022; Milz et al., 2016), visual processing (Antonova et al., 2022; D'Croz-Baron et al., 2021; Seitzman et al., 2017), and activity in the visual network (Britz et al., 2010; Custo et al., 2017), Bréchet et al. (Bréchet et al., 2019) related microstate B with conscious experience, autobiographic memory, visualization of the scene and visualization of the self in the scene. Vellante et al. (Vellante et al., 2020) reported a negative association between microstate B and states of dissociation and anxiety in bipolar patients, interpreting results as reflecting autobiographic memory deficits and increased self-focusing. ARSQ dimension of Self is evaluated with statements 'I thought about my feelings', 'I thought about my behavior' and 'I thought about myself'. The last two statements are particularly intriguing in the context of findings by Brechet et al.(Bréchet et al., 2019) and Vellante et al. (Vellante et al., 2020), since they both are directly related to autobiographic memory and self-visualization in the particular scene. It is possible that the observed relationship between microstate B and domain of

Self reflects the aspects of self-visualization. While domain of Self is orientated towards the inner mentation, microstate D is associated to externally orientated processing (Schiller et al., 2019). Several studies reported an increased activity of microstate D during various tasks and states and associated it with attention attributes, working memory, cognitive control, detecting behaviorally relevant stimuli (Bréchet et al., 2019; D'Croz-Baron et al., 2021; Seitzman et al., 2017; Zappasodi et al., 2019) and fronto-parietal network (Britz et al., 2010; Custo et al., 2017). Thus, our observation on the opposite relationship between Self domain and microstates B and D probably reflects the dissociation from external environment during the resting-state with closed eyes.

EEG signal carries information about power, phase and spatio-temporal dynamics. By dividing signal into separate derivates, we can analyze the same signal from different angles. Frequency analysis provides the information about the amount of activity in certain frequency or frequency band and gives the information about which frequency is the most optimal for certain cognitive or sensory information processing. Evaluation of the phase is a way to estimate the global connectivity or connectivity between different areas. It gives information about how well different brain areas communicate at the specific frequency. Topographical analysis reflects momentary broadband neuronal network activity, which is not frequency dependent (Férat et al., 2022).

As it was showed in this work, different aspects of the same signal are related to both - different and the same - domains of ARSQ. For instance, power aspect of EEG signal as evaluated with frequency principal component analysis showed that activity in theta frequency range (5.5 Hz) was related to scores for Sleepiness, but not the phase, as evaluated with global field synchronization. On the other hand, phase synchronization of of beta frequency range, evaluated with global field synchronization, but not the power aspect correlated with domain of Comfort. And both, power and phase parameters of alpha band activity correlated with ARSQ domain of Comfort, indicating that both – magnitude and angle – can be sensitive to this subjective aspect.

Although EEG microstates analysis is applied on broadband activity (1 – 40 Hz), it is driven mostly by alpha band activity (Milz et al., 2017; von Wegner et al., 2021). Here we showed that three different microstates – C, E and G – displayed associations with domain of Comfort. Thus, it appears that subjective ratings for Comfort is the most sensitive to different EEG parameters.

Additionally, we also showed correlation between Somatic Awareness and microstate F (posterior configuration), replicating results reported in studies, which did not used any optimization criteria for optimal number of clusters (Pipinis et al., 2017; Schiller et al., 2021).

It should be noted that the observed correlations were not strong, but in the range of the reported strengths for associations between physiological and psychological variables. It has also been suggested that correlations are highly variable between studies in small sample sizes ($n < 250$) (Schönbrodt and Perugini, 2013). Our sample is the largest up to date, where detailed EEG assessment was performed alongside ARSQ. However, it is important that

future studies on individual differences include larger sample sizes, so they are powered to detect small to moderate correlations between ARSQ ratings and EEG parameters.

CONCLUSIONS

1. Individual loadings of the frontal midline theta component peaking at 5.5 Hz positively correlates with subjectively experienced Sleepiness
2. Individual loadings on the alpha component peaking at 9 Hz positively correlates with the subjective ratings of the Comfort domain during resting-state with closed eyes.
3. Global field synchronization values in the alpha (8-13 Hz) and beta (14-30 Hz) ranges positively correlate with subjective ratings for Comfort during resting-state with closed eyes.
4. Coverage of Microstate F correlated negatively with subjective ratings on Somatic Awareness.
5. Occurrence of microstate B and duration of microstate D correlated positively with subjective ratings on Self.
6. Occurrence of microstate C correlated negatively with subjective ratings on Comfort, and duration of microstate E and microstate G correlated positively with subjective scoring on Comfort during resting-state period with closed eyes.

REFERENCES

1. Achermann, P., Rusterholz, T., Dürr, R., König, T., Tarokh, L., 2016. Global field synchronization reveals rapid eye movement sleep as most synchronized brain state in the human EEG. R. Soc. open Sci. 3, 160201. https://doi.org/10.1098/rsos.160201
2. Andrews-Hanna, J.R., 2012. The brain's default network and its adaptive role in internal mentation. Neuroscientist. https://doi.org/10.1177/1073858411403316
3. Angelini, L., Tamburro, G., Lionetti, F., Spinelli, M., Comani, S., Zappasodi, F., Fasolo, M., Aureli, T., 2023. Alpha and theta brain activity in 9-month-old infants during a live referential gaze paradigm. Psychophysiology 60, e14198. https://doi.org/10.1111/PSYP.14198
4. Antonova, E., Holding, M., Suen, H.C., Sumich, A., Maex, R., Nehaniv, C., 2022. EEG microstates: Functional significance and short-term test-retest reliability. Neuroimage: Reports 2, 100089. https://doi.org/10.1016/J.YNIRP.2022.100089
5. Asai, T., Hamamoto, T., Kashihara, S., Imamizu, H., 2022. Real-Time Detection and Feedback of Canonical Electroencephalogram Microstates: Validating a Neurofeedback System as a Function of Delay. Front. Syst. Neurosci. 16. https://doi.org/10.3389/FNSYS.2022.786200
6. Babiloni, C., Lizio, R., Marzano, N., Capotosto, P., Soricelli, A., Triggiani, A.I., Cordone, S., Gesualdo, L., Del Percio, C., 2016. Brain neural synchronization and functional coupling in Alzheimer's disease as revealed by resting state EEG rhythms. Int. J. Psychophysiol. 103, 88–102. https://doi.org/10.1016/J.IJPSYCHO.2015.02.008
7. Bagdasarov, A., Roberts, K., Bréchet, L., Brunet, D., Michel, C.M., Gaffrey, M.S., 2022. Spatiotemporal dynamics of EEG microstates in four- to eight-year-old children: Age- and sex-related effects. Dev. Cogn. Neurosci. 57, 101134. https://doi.org/10.1016/J.DCN.2022.101134
8. Bai, Y., Xia, X., Li, X., 2017. A Review of Resting-State Electroencephalography Analysis in Disorders of Consciousness. Front. Neurol. 8, 471. https://doi.org/10.3389/FNEUR.2017.00471
9. Barry, R.J., Clarke, A.R., Johnstone, S.J., Magee, C.A., Rushby, J.A., 2007. EEG differences between eyes-closed and eyes-open resting conditions. https://doi.org/10.1016/j.clinph.2007.07.028
10. Barry, R.J., De Blasio, F.M., 2018. EEG frequency PCA in EEG-ERP dynamics. Psychophysiology 55. https://doi.org/10.1111/psyp.13042
11. Barry, R.J., De Blasio, F.M., Fogarty, J.S., Clarke, A.R., 2020. Natural alpha

frequency components in resting EEG and their relation to arousal. Clin. Neurophysiol. 131, 205–212. https://doi.org/10.1016/j.clinph.2019.10.018
12. Barry, R.J., De Blasio, F.M., Karamacoska, D., 2019. Data-driven derivation of natural EEG frequency components: An optimised example assessing resting EEG in healthy ageing. J. Neurosci. Methods 321, 1–11. https://doi.org/10.1016/j.jneumeth.2019.04.001
13. Barry, R.J., Rushby, J.A., Wallace, M.J., Clarke, A.R., Johnstone, S.J., Zlojutro, I., 2005. Caffeine effects on resting-state arousal. Clin. Neurophysiol. 116, 2693–2700. https://doi.org/10.1016/J.CLINPH.2005.08.008
14. Beppi, C., Ribeiro Violante, I., Scott, G., Sandrone, S., 2021. EEG, MEG and neuromodulatory approaches to explore cognition: Current status and future directions. Brain Cogn. 148, 105677. https://doi.org/10.1016/J.BANDC.2020.105677
15. Berger, B., Minarik, T., Liuzzi, G., Hummel, F.C., Sauseng, P., 2014. EEG oscillatory phase-dependent markers of corticospinal excitability in the resting brain. Biomed Res. Int. 2014. https://doi.org/10.1155/2014/936096
16. Binder, M., Górska, U., Pipinis, E., Voicikas, A., Griskova-Bulanova, I., 2020. Auditory steady-state response to chirp-modulated tones: A pilot study in patients with disorders of consciousness. NeuroImage Clin. 27, 102261. https://doi.org/10.1016/J.NICL.2020.102261
17. Biswal, B., Yetkin, F.Z., Haughton, V.M., Hyde, J.S., 1995. Functional Connectivity in the Motor Cortex of Resting Human Brain Using Echo-Planar MRI.
18. Boutros, N.N., Arfken, C., Galderisi, S., Warrick, J., Pratt, G., Iacono, W., 2007. The status of spectral EEG abnormality as a diagnostic test for schizophrenia. https://doi.org/10.1016/j.schres.2007.11.020
19. Bowyer, S.M., 2016. Coherence a measure of the brain networks: past and present. Neuropsychiatr. Electrophysiol. 2016 21 2, 1–12. https://doi.org/10.1186/S40810-015-0015-7
20. Brandeis, D., Naylor, H., Halliday, R., Callaway, E., Yano, L., 1992. Scopolamine Effects on Visual Information Processing, Attention, and Event-Related Potential Map Latencies. Psychophysiology 29, 315–335. https://doi.org/10.1111/J.1469-8986.1992.TB01706.X
21. Bréchet, L., Brunet, D., Birot, G., Gruetter, R., Michel, C.M., Jorge, J., 2019. Capturing the spatiotemporal dynamics of self-generated, task-initiated thoughts with EEG and fMRI. Neuroimage 194, 82–92. https://doi.org/10.1016/j.neuroimage.2019.03.029
22. Bréchet, L., Brunet, D., Perogamvros, L., Tononi, G., Michel, C.M., 2020. EEG microstates of dreams. Sci. Rep. 10, 17069.

https://doi.org/10.1038/s41598-020-74075-z
23. Britz, J., Van De Ville, D., Michel, C.M., 2010. BOLD correlates of EEG topography reveal rapid resting-state network dynamics. Neuroimage. https://doi.org/10.1016/j.neuroimage.2010.02.052
24. Brodbeck, V., Kuhn, A., von Wegner, F., Morzelewski, A., Tagliazucchi, E., Borisov, S., Michel, C.M., Laufs, H., 2012. EEG microstates of wakefulness and NREM sleep. Neuroimage 62, 2129–2139. https://doi.org/10.1016/J.NEUROIMAGE.2012.05.060
25. Brunet, D., Murray, M.M., Michel, C.M., 2011. Spatiotemporal Analysis of Multichannel EEG: CARTOOL. Comput. Intell. Neurosci. 2011, 15. https://doi.org/10.1155/2011/813870
26. Buckner, R.L., Carroll, D.C., 2007. Self-projection and the brain. Trends Cogn. Sci. 11, 49–57. https://doi.org/10.1016/J.TICS.2006.11.004
27. Burle, B., Spieser, L., Roger, C., Casini, L., Hasbroucq, T., Vidal, F., 2015. Spatial and temporal resolutions of EEG: Is it really black and white? A scalp current density view. Int. J. Psychophysiol. 97, 210. https://doi.org/10.1016/J.IJPSYCHO.2015.05.004
28. Chang, P.F., Arendt-Nielsen, L., Chen, A.C.N., 2002. Dynamic changes and spatial correlation of EEG activities during cold pressor test in man. Brain Res. Bull. 57, 667–675. https://doi.org/10.1016/S0361-9230(01)00763-8
29. Chen, X., Chen, N.-X., Shen, Y.-Q., Li, H.-X., Li, L., Lu, B., Zhu, Z.-C., Fan, Z., Yan, C.-G., 2020. The subsystem mechanism of default mode network underlying rumination: A reproducible neuroimaging study. Neuroimage 221, 117185. https://doi.org/10.1016/j.neuroimage.2020.117185
30. Cheyne, J.A., Carriere, J.S.A., Smilek, D., 2006. Absent-mindedness: Lapses of conscious awareness and everyday cognitive failures. Conscious. Cogn. 15, 578–592. https://doi.org/10.1016/J.CONCOG.2005.11.009
31. Choi, Y., Kim, M., Chun, C., 2015. Measurement of occupants' stress based on electroencephalograms (EEG) in twelve combined environments. Build. Environ. 88, 65–72. https://doi.org/10.1016/J.BUILDENV.2014.10.003
32. Cohen, M.X., 2017. Where Does EEG Come From and What Does It Mean? Trends Neurosci. 40, 208–218. https://doi.org/10.1016/J.TINS.2017.02.004
33. Croce, P., Quercia, A., Costa, S., Zappasodi, F., 2020. EEG microstates associated with intra- and inter-subject alpha variability. Sci. Rep. https://doi.org/10.1038/s41598-020-58787-w
34. Custo, A., Van De Ville, D., Wells, W.M., Tomescu, M.I., Brunet, D., Michel, C.M., 2017. Electroencephalographic Resting-State Networks: Source Localization of Microstates. Brain Connect. 7, 671–682. https://doi.org/10.1089/brain.2016.0476

35. Custo, A., Vulliemoz, S., Grouiller, F., Van De Ville, D., Michel, C., 2014. EEG source imaging of brain states using spatiotemporal regression. Neuroimage 96, 106–116. https://doi.org/10.1016/j.neuroimage.2014.04.002
36. D'Croz-Baron, D.F., Bréchet, L., Baker, M., Karp, T., 2021. Auditory and Visual Tasks Influence the Temporal Dynamics of EEG Microstates During Post-encoding Rest. Brain Topogr. 34, 19–28. https://doi.org/10.1007/s10548-020-00802-4
37. Damborská, A., Piguet, C., Aubry, J.M., Dayer, A.G., Michel, C.M., Berchio, C., 2019a. Altered Electroencephalographic Resting-State Large-Scale Brain Network Dynamics in Euthymic Bipolar Disorder Patients. Front. Psychiatry 10. https://doi.org/10.3389/fpsyt.2019.00826
38. Damborská, A., Tomescu, M.I., Honzírková, E., Barteček, R., Hořínková, J., Fedorová, S., Ondruš, Š., Michel, C.M., 2019b. EEG resting-state large-scale brain network dynamics are related to depressive symptoms. Front. Psychiatry 10. https://doi.org/10.3389/fpsyt.2019.00548
39. Delamillieure, P., Doucet, G., Mazoyer, B., Turbelin, M.-R., Delcroix, N., Mellet, E., Zago, L., Crivello, F., Petit, L., Tzourio-Mazoyer, N., Joliot, M., 2010. The resting state questionnaire: An introspective questionnaire for evaluation of inner experience during the conscious resting state. Brain Res. Bull. 81, 565–573. https://doi.org/10.1016/j.brainresbull.2009.11.014
40. Delorme, A., Makeig, S., 2004. EEGLAB: An open source toolbox for analysis of single-trial EEG dynamics including independent component analysis. J. Neurosci. Methods 134, 9–21. https://doi.org/10.1016/j.jneumeth.2003.10.009
41. Delorme, A., Sejnowski, T., Makeig, S., 2007. Enhanced detection of artifacts in EEG data using higher-order statistics and independent component analysis. Neuroimage 34, 1443–1449. https://doi.org/10.1016/J.NEUROIMAGE.2006.11.004
42. Diaz, B.A., Hardstone, R., Mansvelder, H.D., Van Someren, E.J.W., Linkenkaer-Hansen, K., 2016. Resting-State Subjective Experience and EEG Biomarkers Are Associated with Sleep-Onset Latency. Front. Psychol. 7, 492. https://doi.org/10.3389/fpsyg.2016.00492
43. Diaz, B.A., Van Der Sluis, S., Benjamins, J.S., Stoffers, D., Hardstone, R., Mansvelder, H.D., Van Someren, E.J.W., Linkenkaer-Hansen, K., 2014. The ARSQ 2.0 reveals age and personality effects on mind-wandering experiences. Front. Psychol. 5. https://doi.org/10.3389/fpsyg.2014.00271
44. Diaz, B.A., Van Der Sluis, S., Moens, S., Benjamins, J.S., Migliorati, F., Stoffers, D., Den Braber, A., Poil, S.-S., Hardstone, R., Van 't Ent, D., Boomsma, D.I., De Geus, E., Mansvelder, H.D., Van Someren, E.J.W., Linkenkaer-Hansen, K., 2013. The Amsterdam Resting-State Questionnaire

reveals multiple phenotypes of resting-state cognition. Front. Hum. Neurosci. 0, 446. https://doi.org/10.3389/FNHUM.2013.00446
45. Diaz Hernandez, L., Rieger, K., Baenninger, A., Brandeis, D., Koenig, T., 2016. Towards Using Microstate-Neurofeedback for the Treatment of Psychotic Symptoms in Schizophrenia. A Feasibility Study in Healthy Participants. Brain Topogr. 29, 308–321. https://doi.org/10.1007/S10548-015-0460-4/TABLES/3
46. Dien, J., 2012. Applying principal components analysis to event-related potentials: A tutorial. Dev. Neuropsychol. 37, 497–517. https://doi.org/10.1080/87565641.2012.697503
47. Dien, J., 2010. The ERP PCA Toolkit: An open source program for advanced statistical analysis of event-related potential data. J. Neurosci. Methods 187, 138–145. https://doi.org/10.1016/J.JNEUMETH.2009.12.009
48. Dien, J., Khoe, W., Mangun, G.R., 2007. Evaluation of PCA and ICA of simulated ERPs: Promax vs. infomax rotations. Hum. Brain Mapp. 28, 742. https://doi.org/10.1002/HBM.20304
49. Dienes, Z., 2016. How Bayes factors change scientific practice. J. Math. Psychol. 72, 78–89. https://doi.org/10.1016/j.jmp.2015.10.003
50. Dienes, Z., 2014. Using Bayes to get the most out of non-significant results. Front. Psychol. 0, 781. https://doi.org/10.3389/FPSYG.2014.00781
51. Dienes, Z., 2011. Bayesian versus orthodox statistics: Which side are you on? Perspect. Psychol. Sci. 6, 274–290. https://doi.org/10.1177/1745691611406920
52. Dinov, M., Leech, R., 2017. Modeling uncertainties in EEG microstates: Analysis of real and imagined motor movements using probabilistic clustering-driven training of probabilistic neural networks. Front. Hum. Neurosci. 11, 534. https://doi.org/10.3389/FNHUM.2017.00534/BIBTEX
53. Duncan, N.W., Northoff, G., 2013. Overview of potential procedural and participant-related confounds for neuroimaging of the resting state. J. Psychiatry Neurosci. 38, 84. https://doi.org/10.1503/JPN.120059
54. Engel, A.K., Fries, P., 2010. Beta-band oscillations--signalling the status quo? Curr. Opin. Neurobiol. 20, 156–165. https://doi.org/10.1016/J.CONB.2010.02.015
55. Faber, P.L., Travis, F., Milz, P., Parim, N., 2017. EEG microstates during different phases of Transcendental Meditation practice. Cogn. Process. 18, 307–314. https://doi.org/10.1007/s10339-017-0812-y
56. Férat, V., Seeber, | Martin, Michel, C.M., Ros, T., 2022. Beyond broadband: Towards a spectral decomposition of electroencephalography microstates. Hum. Brain Mapp. https://doi.org/10.1002/HBM.25834
57. Ferree, T.C., Clay, M.T., Tucker, D.M., 2001. The spatial resolution of

scalp EEG. Neurocomputing 38–40, 1209–1216. https://doi.org/10.1016/S0925-2312(01)00568-9

58. Forkmann, T., Volz-Sidiropoulou, E., Helbing, T., Drüke, B., Mainz, V., Rath, D., Gauggel, S., Teismann, T., 2019. Sense it and use it: Interoceptive accuracy and sensibility in suicide ideators. BMC Psychiatry 19. https://doi.org/10.1186/s12888-019-2322-1
59. Fox, M.D., Raichle, M.E., 2007. Spontaneous fluctuations in brain activity observed with functional magnetic resonance imaging. Nat. Rev. Neurosci. 2007 89 8, 700–711. https://doi.org/10.1038/nrn2201
60. Fox, M.D., Snyder, A.Z., Vincent, J.L., Corbetta, M., Van Essen, D.C., Raichle, M.E., 2005. The human brain is intrinsically organized into dynamic, anticorrelated functional networks. Proc. Natl. Acad. Sci. U. S. A. 102, 9673–9678. https://doi.org/10.1073/PNAS.0504136102/SUPPL_FILE/04136FIG5.PDF
61. George Assaf, A., Tsionas, M., 2018. Bayes factors vs. P-values. Tour. Manag. 67, 17–31. https://doi.org/10.1016/j.tourman.2017.11.011
62. Gobert, F., Dailler, F., Fischer, C., André-Obadia, N., Luauté, J., 2018. Proving cortical death after vascular coma: Evoked potentials, EEG and neuroimaging. Clin. Neurophysiol. 129, 1105–1116. https://doi.org/10.1016/J.CLINPH.2018.02.133
63. Gonzalez-Castillo, J., Kam, J.W.Y., Hoy, C.W., Bandettini, P.A., 2021. How to Interpret Resting-State fMRI: Ask Your Participants. J. Neurosci. 41, 1130–1141. https://doi.org/10.1523/JNEUROSCI.1786-20.2020
64. Gorgolewski, K.J., Lurie, D., Urchs, S., Kipping, J.A., Craddock, R.C., Milham, M.P., Margulies, D.S., Smallwood, J., 2014. A Correspondence between Individual Differences in the Brain's Intrinsic Functional Architecture and the Content and Form of Self-Generated Thoughts. PLoS One 9. https://doi.org/10.1371/JOURNAL.PONE.0097176
65. Greicius, M.D., Krasnow, B., Reiss, A.L., Menon, V., 2003. Functional connectivity in the resting brain: A network analysis of the default mode hypothesis. Proc. Natl. Acad. Sci. U. S. A. 100, 253–258. https://doi.org/10.1073/PNAS.0135058100/SUPPL_FILE/5058TABLE7.HTML
66. Grin-Yatsenko, V.A., Baas, I., Ponomarev, V.A., Kropotov, J.D., 2009. EEG power spectra at early stages of depressive disorders. J. Clin. Neurophysiol. 26, 401–406. https://doi.org/10.1097/WNP.0B013E3181C298FE
67. Griskova-Bulanova, I., Pipinis, E., Voicikas, A., Koenig, T., 2018. Global field synchronization of 40 Hz auditory steady-state response: Does it change with attentional demands? Neurosci. Lett. 674, 127–131.

https://doi.org/10.1016/J.NEULET.2018.03.033
68. Groppe, D.M., Bickel, S., Keller, C.J., Jain, S.K., Hwang, S.T., Harden, C., Mehta, A.D., 2013. Dominant frequencies of resting human brain activity as measured by the electrocorticogram. https://doi.org/10.1016/j.neuroimage.2013.04.044
69. Grunwald, M., Busse, F., Hensel, A., Riedel-Heller, S., Kruggel, F., Arendt, T., Wolf, H., Gertz, H.J., 2002. Theta-power differences in patients with mild cognitive impairment under rest condition and during haptic tasks. Alzheimer Dis. Assoc. Disord. 16, 40–48. https://doi.org/10.1097/00002093-200201000-00006
70. Gschwind, M., Hardmeier, M., Van De Ville, D., Tomescu, M.I., Penner, I.K., Naegelin, Y., Fuhr, P., Michel, C.M., Seeck, M., 2016. Fluctuations of spontaneous EEG topographies predict disease state in relapsing-remitting multiple sclerosis. NeuroImage Clin. 12, 466–477. https://doi.org/10.1016/j.nicl.2016.08.008
71. Habermann, M., Weusmann, D., Stein, M., Koenig, T., 2018. A student's guide to randomization statistics for multichannel event-related potentials using Ragu. Front. Neurosci. 12. https://doi.org/10.3389/fnins.2018.00355
72. Haveman, M.E., Van Putten, M.J.A.M., Hom, H.W., Eertman-Meyer, C.J., Beishuizen, A., Tjepkema-Cloostermans, M.C., 2019. Predicting outcome in patients with moderate to severe traumatic brain injury using electroencephalography. Crit. Care 23, 1–9. https://doi.org/10.1186/S13054-019-2656-6/FIGURES/3
73. Hedrich, T., Pellegrino, G., Kobayashi, E., Lina, J.M., Grova, C., 2017. Comparison of the spatial resolution of source imaging techniques in high-density EEG and MEG. Neuroimage 157, 531–544. https://doi.org/10.1016/J.NEUROIMAGE.2017.06.022
74. Hurlburt, R.T., Akhter, S.A., 2006. The Descriptive Experience Sampling method. Phenomenol. Cogn. Sci. 2006 53 5, 271–301. https://doi.org/10.1007/S11097-006-9024-0
75. Hurlburt, R.T., Alderson-Day, B., Fernyhough, C., Kühn, S., 2015. What goes on in the resting-state? A qualitative glimpse into resting-state experience in the scanner. Front. Psychol. 6, 1535. https://doi.org/10.3389/fpsyg.2015.01535
76. Jabès, A., Klencklen, G., Ruggeri, P., Michel, C.M., Banta Lavenex, P., Lavenex, P., 2021. Resting-State EEG Microstates Parallel Age-Related Differences in Allocentric Spatial Working Memory Performance. Brain Topogr. https://doi.org/10.1007/s10548-021-00835-3
77. Jackson, A.F., Bolger, D.J., 2014. The neurophysiological bases of EEG

and EEG measurement: A review for the rest of us. Psychophysiology 51, 1061–1071. https://doi.org/10.1111/psyp.12283
78. JASP Team, 2020. JASP (Version 0.14.1).
79. Jollife, I.T., Cadima, J., 2016. Principal component analysis: a review and recent developments. Philos. Trans. A. Math. Phys. Eng. Sci. 374. https://doi.org/10.1098/RSTA.2015.0202
80. Jung, T.-P., Makeig, S., Humphries, C., Lee, T.-W., McKeown, M.J., Iragui, V., Sejnowski, T.J., 2000. Removing electroencephalographic artifacts by blind source separation. Psychophysiology 37, 163–178. https://doi.org/10.1111/1469-8986.3720163
81. Kaida, K., Niki, K., 2014. Total sleep deprivation decreases flow experience and mood status. Neuropsychiatr. Dis. Treat. 10, 19. https://doi.org/10.2147/NDT.S53633
82. Karamacoska, D., Barry, R.J., De Blasio, F.M., Steiner, G.Z., 2019a. EEG-ERP dynamics in a visual Continuous Performance Test. Int. J. Psychophysiol. 146, 249–260. https://doi.org/10.1016/J.IJPSYCHO.2019.08.013
83. Karamacoska, D., Barry, R.J., Steiner, G.Z., 2019b. Using principal components analysis to examine resting state EEG in relation to task performance. Psychophysiology 56. https://doi.org/10.1111/PSYP.13327
84. Kelter, R., 2020. Bayesian alternatives to null hypothesis significance testing in biomedical research: a non-technical introduction to Bayesian inference with JASP. BMC Med. Res. Methodol. 2020 201 20, 1–12. https://doi.org/10.1186/S12874-020-00980-6
85. Khanna, A., Pascual-Leone, A., Farzan, F., 2014. Reliability of resting-state microstate features in electroencephalography. PLoS One 9, e114163. https://doi.org/10.1371/journal.pone.0114163
86. Khanna, A., Pascual-Leone, A., Michel, C.M., Farzan, F., 2015. Microstates in resting-state EEG: Current status and future directions. Neurosci. Biobehav. Rev. 49, 105–113. https://doi.org/10.1016/j.neubiorev.2014.12.010
87. Knott, V., Mahoney, C., Kennedy, S., Evans, K., 2001. EEG power, frequency, asymmetry and coherence in male depression. Psychiatry Res. Neuroimaging 106, 123–140. https://doi.org/10.1016/S0925-4927(00)00080-9
88. Koenig, T., Brandeis, D., 2016. Inappropriate assumptions about EEG state changes and their impact on the quantification of EEG state dynamics. Neuroimage 125, 1104–1106. https://doi.org/10.1016/J.NEUROIMAGE.2015.06.035
89. Koenig, T., Kottlow, M., Stein, M., Melie-García, L., 2011. Ragu: A free tool for the analysis of EEG and MEG event-related scalp field data

using global randomization statistics. Comput. Intell. Neurosci. 2011. https://doi.org/10.1155/2011/938925
90. Koenig, T., Lehmann, D., Merlo, M.C.G., Kochi, K., Hell, D., Koukkou, M., 1999. A deviant EEG brain microstate in acute, neuroleptic-naive schizophrenics at rest. Eur. Arch. Psychiatry Clin. Neurosci. 249, 205–211. https://doi.org/10.1007/s004060050088
91. Koenig, T., Lehmann, D., Saito, N., Kuginuki, T., Kinoshita, T., Koukkou, M., 2001. Decreased functional connectivity of EEG theta-frequency activity in first-episode, neuroleptic-naïve patients with schizophrenia: Preliminary results. Schizophr. Res. 50, 55–60. https://doi.org/10.1016/S0920-9964(00)00154-7
92. Koenig, T., Prichep, L., Dierks, T., Hubl, D., Wahlund, L.O., John, E.R., Jelic, V., 2005. Decreased EEG synchronization in Alzheimer's disease and mild cognitive impairment. Neurobiol. Aging 26, 165–171. https://doi.org/10.1016/j.neurobiolaging.2004.03.008
93. Koenig, T., Prichep, L., Lehmann, D., Sosa, P.V., Braeker, E., Kleinlogel, H., Isenhart, R., John, E.R., 2002. Millisecond by Millisecond, Year by Year: Normative EEG Microstates and Developmental Stages. Neuroimage 16, 41–48. https://doi.org/10.1006/NIMG.2002.1070
94. Koenig, T., van Swam, C., Dierks, T., Hubl, D., 2012a. Is gamma band EEG synchronization reduced during auditory driving in schizophrenia patients with auditory verbal hallucinations? Schizophr. Res. 141, 266–270. https://doi.org/10.1016/J.SCHRES.2012.07.016
95. Koenig, T., Van Swam, C., Dierks, T., Hubl, D., 2012b. Is gamma band EEG synchronization reduced during auditory driving in schizophrenia patients with auditory verbal hallucinations? Schizophr. Res. 141, 266–270. https://doi.org/10.1016/j.schres.2012.07.016
96. Lachaux, J.-P., Rodriguez, E., Martinerie, J., Varela, F.J., 1999. Measuring Phase Synchrony in Brain Signals. Hum Brain Mapp. 8, 194–208. https://doi.org/10.1002/(SICI)1097-0193(1999)8:4
97. LaRocco, J., Le, M.D., Paeng, D.G., 2020. A Systemic Review of Available Low-Cost EEG Headsets Used for Drowsiness Detection. Front. Neuroinform. 14, 42. https://doi.org/10.3389/FNINF.2020.553352/BIBTEX
98. Lehmann, D., 1971. Multichannel topography of human alpha EEG fields. Electroencephalogr. Clin. Neurophysiol. 31, 439–449. https://doi.org/10.1016/0013-4694(71)90165-9
99. Lehmann, D., Faber, P.L., Galderisi, S., Herrmann, W.M., Kinoshita, T., Koukkou, M., Mucci, A., Pascual-Marqui, R.D., Saito, N., Wackermann, J., Winterer, G., Koenig, T., 2005. EEG microstate

duration and syntax in acute, medication-naïve, first-episode schizophrenia: A multi-center study. Psychiatry Res. - Neuroimaging 138, 141–156. https://doi.org/10.1016/j.pscychresns.2004.05.007

100. Lehmann, D., Faber, P.L., Gianotti, L.R.R., Kochi, K., Pascual-Marqui, R.D., 2006. Coherence and phase locking in the scalp EEG and between LORETA model sources, and microstates as putative mechanisms of brain temporo-spatial functional organization. J. Physiol. 99, 29–36. https://doi.org/10.1016/J.JPHYSPARIS.2005.06.005
101. Lehmann, D., Ozaki, H., Pal, I., 1987. EEG alpha map series: brain micro-states by space-oriented adaptive segmentation. Electroencephalogr. Clin. Neurophysiol. 67, 271–288. https://doi.org/10.1016/0013-4694(87)90025-3
102. Lehmann, D., Skrandies, W., 1980. REFERENCE-FREE IDENTIFICATION OF COMPONENTS OF CHECKERBOARD-EVOKED MULTICHANNEL POTENTIAL FIELDS 1, Electroencephalography and Clinical Neurophysiology.
103. Liu, J., Xu, J., Zou, G., He, Y., Zou, Q., Gao, J.H., 2020. Reliability and Individual Specificity of EEG Microstate Characteristics. Brain Topogr. 33, 438–449. https://doi.org/10.1007/s10548-020-00777-2
104. Liu, S., Shen, J., Li, Y., Wang, Jing, Wang, Jianhua, Xu, J., Wang, Q., Chen, R., 2021. EEG Power Spectral Analysis of Abnormal Cortical Activations During REM/NREM Sleep in Obstructive Sleep Apnea. Front. Neurol. 12, 180. https://doi.org/10.3389/FNEUR.2021.643855/BIBTEX
105. Looney, D., Kidmose, P., Park, C., Ungstrup, M., Rank, M., Rosenkranz, K., Mandic, D., 2012. The in-the-ear recording concept: user-centered and wearable brain monitoring. IEEE Pulse 3, 32–42. https://doi.org/10.1109/MPUL.2012.2216717
106. Love, J., Selker, R., Marsman, M., Jamil, T., Dropmann, D., Verhagen, J., Ly, A., Gronau, Q.F., Šmíra, M., Epskamp, S., Matzke, D., Wild, A., Knight, P., Rouder, J.N., Morey, R.D., Wagenmakers, E.J., 2019. JASP: Graphical statistical software for common statistical designs. J. Stat. Softw. 88. https://doi.org/10.18637/jss.v088.i02
107. Luo, Y., Tian, Q., Wang, Changming, Zhang, K., Wang, Chuanyue, Zhang, J., 2020. Biomarkers for Prediction of Schizophrenia: Insights from Resting-State EEG Microstates. IEEE Access 8, 213078–213093. https://doi.org/10.1109/ACCESS.2020.3037658
108. Ma, C.C., Liu, A.J., Liu, A.H., Zhou, X.Y., Zhou, S.N., 2014. Electroencephalogram global field synchronization analysis: A new method for assessing the progress of cognitive decline in Alzheimer's disease. Clin. EEG Neurosci. 45, 98–103.

https://doi.org/10.1177/1550059413489669/ASSET/IMAGES/LARGE/10.1177_1550059413489669-FIG2.JPEG
109. Marchetti, A., Baglio, F., Costantini, I., Dipasquale, O., Savazzi, F., Nemni, R., Sangiuliano Intra, F., Tagliabue, S., Valle, A., Massaro, D., Castelli, I., 2015. Theory of Mind and the Whole Brain Functional Connectivity: Behavioral and Neural Evidences with the Amsterdam Resting State Questionnaire. Front. Psychol. 6. https://doi.org/10.3389/fpsyg.2015.01855
110. Mason, M.F., Norton, M.I., Van Horn, J.D., Wegner, D.M., Grafton, S.T., Macrae, C.N., 2007. Wandering Minds: The Default Network and Stimulus-Independent Thought. Science 315, 393. https://doi.org/10.1126/SCIENCE.1131295
111. Massimini, M., Ferrarelli, F., Huber, R., Esser, S.K., Singh, H., Tononi, G., 2005. Thalamocortical oscillations in the sleeping and aroused brain. Science (80-.). 262, 679–685. https://doi.org/10.1126/science.8235588
112. Mazziotta, J., Toga, A., Evans, A., Fox, P., Lancaster, J., Zilles, K., Woods, R., Paus, T., Simpson, G., Pike, B., Holmes, C., Collins, L., Thompson, P., Macdonald, D., Iacoboni, M., Schormann, T., Amunts, K., Palomero-Gallagher, N., Geyer, S., Parsons, L., Narr, K., Kabani, N., Le Goualher, G., Boomsma, D., Cannon, T., Kawashima, R., Mazoyer, B., 2001. A Probabilistic Atlas and Reference System for the Human Brain: International Consortium for Brain Mapping (ICBM). Philos. Trans. Biol. Sci. 356, 1293–1322. https://doi.org/10.1098/rstb.2001.0915
113. Michel, C.M., Brunet, D., 2019. EEG source imaging: A practical review of the analysis steps. Front. Neurol. 10, 325. https://doi.org/10.3389/fneur.2019.00325
114. Michel, C.M., Koenig, T., 2018. EEG microstates as a tool for studying the temporal dynamics of whole-brain neuronal networks: A review. Neuroimage 180, 577–593. https://doi.org/10.1016/j.neuroimage.2017.11.062
115. Michel, C.M., Koenig, T., Brandeis, D., Gianotti, L.R.R., Wackermann, J., 2009. Electrical neuroimaging, Electrical Neuroimaging. Cambridge University Press. https://doi.org/10.1017/CBO9780511596889
116. Michel, C.M., Murray, M.M., 2012. Towards the utilization of EEG as a brain imaging tool. https://doi.org/10.1016/j.neuroimage.2011.12.039
117. Michel, C.M., Murray, M.M., Lantz, G., Gonzalez, S., Spinelli, L., Grave de Peralta, R., 2004. EEG source imaging. Clin. Neurophysiol. 115, 2195–2222. https://doi.org/10.1016/J.CLINPH.2004.06.001
118. Miladinovic, A., Ajçevic, M., Busan, P., Jarmolowska, J., Deodato, M., Mezzarobba, S., Battaglini, P.P., Accardo, A., 2021. EEG changes and motor deficits in Parkinson's disease patients: Correlation of motor scales and EEG power bands. Procedia Comput. Sci. 192, 2616–2623.

https://doi.org/10.1016/J.PROCS.2021.09.031
119. Milz, P., Faber, P.L., Lehmann, D., Koenig, T., Kochi, K., Pascual-Marqui, R.D., 2016. The functional significance of EEG microstates-Associations with modalities of thinking. Neuroimage 125, 643–656. https://doi.org/10.1016/j.neuroimage.2015.08.023
120. Milz, P., Pascual-Marqui, R.D., Achermann, P., Kochi, K., Faber, P.L., 2017. The EEG microstate topography is predominantly determined by intracortical sources in the alpha band. Neuroimage 162, 353–361. https://doi.org/10.1016/j.neuroimage.2017.08.058
121. Montez, T., Poil, S.S., Jones, B.F., Manshanden, I., Verbunt, J.P.A., Van Dijk, B.W., Brussaard, A.B., Van Ooyen, A., Stam, C.J., Scheltens, P., Linkenkaer-Hansen, K., 2009. Altered temporal correlations in parietal alpha and prefrontal theta oscillations in early-stage Alzheimer disease. Proc. Natl. Acad. Sci. U. S. A. 106, 1614. https://doi.org/10.1073/PNAS.0811699106
122. Mrazek, M.D., Phillips, D.T., Franklin, M.S., Broadway, J.M., Schooler, J.W., 2013. Young and restless: Validation of the Mind-Wandering Questionnaire (MWQ) reveals disruptive impact of mind-wandering for youth. Front. Psychol. 4, 560. https://doi.org/10.3389/FPSYG.2013.00560/BIBTEX
123. Mullen, T., 2012. CleanLine EEGLAB Plugin.
124. Murphy, M., Whitton, A.E., Deccy, S., Ironside, M.L., Rutherford, A., Beltzer, M., Sacchet, M., Pizzagalli, D.A., 2020. Abnormalities in electroencephalographic microstates are state and trait markers of major depressive disorder. Neuropsychopharmacology 45, 2030–2037. https://doi.org/10.1038/s41386-020-0749-1
125. Murray, M.M., Brunet, D., Michel, C.M., 2008. Topographic ERP analyses: A step-by-step tutorial review. Brain Topogr. https://doi.org/10.1007/s10548-008-0054-5
126. Newson, J.J., Thiagarajan, T.C., 2019. EEG Frequency Bands in Psychiatric Disorders: A Review of Resting State Studies. Front. Hum. Neurosci. 12. https://doi.org/10.3389/FNHUM.2018.00521/FULL
127. Ng, B.S.W., Logothetis, N.K., Kayser, C., 2013. EEG Phase Patterns Reflect the Selectivity of Neural Firing. Cereb. Cortex 23, 389–398. https://doi.org/10.1093/CERCOR/BHS031
128. Nichols, T.E., Holmes, A.P., 2001. Nonparametric Permutation Tests For Functional Neuroimaging: A Primer with Examples.
129. Nicolaou, N., Georgiou, J., 2014. Global field synchrony during general anaesthesia. Br. J. Anaesth. 112, 529–539. https://doi.org/10.1093/BJA/AET350
130. Nishida, K., Morishima, Y., Yoshimura, M., Isotani, T., Irisawa, S., Jann, K., Dierks, T., Strik, W., Kinoshita, T., Koenig, T., 2013. EEG

microstates associated with salience and frontoparietal networks in frontotemporal dementia, schizophrenia and Alzheimer's disease. https://doi.org/10.1016/j.clinph.2013.01.005

131. Nishida, M., Hirai, N., Miwakeichi, F., Maehara, T., Kawai, K., Shimizu, H., Uchida, S., 2004. Theta oscillation in the human anterior cingulate cortex during all-night sleep: an electrocorticographic study. Neurosci. Res. 50, 331–341. https://doi.org/10.1016/J.NEURES.2004.08.004
132. Nunez, P.L., Silberstein, R.B., Cadusch, P.J., Wijesinghe, R.S., Westdorp, A.F., Srinivasan, R., 1994. A theoretical and experimental study of high resolution EEG based on surface Laplacians and cortical imaging. Electroencephalogr. Clin. Neurophysiol. 90, 40–57. https://doi.org/10.1016/0013-4694(94)90112-0
133. Oi, H., Hashimoto, T., Nozawa, T., Kanno, A., Kawata, N., Hirano, K., Yamamoto, Y., Sugiura, M., Kawashima, R., 2017. Neural correlates of ambient thermal sensation: An fMRI study. Sci. Reports 2017 71 7, 1–11. https://doi.org/10.1038/s41598-017-11802-z
134. Olamat, A.E., Akan, A., 2017. Synchronization analysis of epilepsy data using global field synchronization. 2017 25th Signal Process. Commun. Appl. Conf. SIU 2017. https://doi.org/10.1109/SIU.2017.7960194
135. Özçoban, M.A., Tan, O., Aydin, S., Akan, A., 2018. Decreased global field synchronization of multichannel frontal EEG measurements in obsessive-compulsive disorders. Med. Biol. Eng. Comput. 56, 331–338. https://doi.org/10.1007/S11517-017-1689-8/TABLES/3
136. Palacios-García, I., Silva, J., Villena-González, M., Campos-Arteaga, G., Artigas-Vergara, C., Luarte, N., Rodríguez, E., Bosman, C.A., 2021. Increase in Beta Power Reflects Attentional Top-Down Modulation After Psychosocial Stress Induction. Front. Hum. Neurosci. 15, 142. https://doi.org/10.3389/FNHUM.2021.630813/BIBTEX
137. Palagini, L., Cellini, N., Mauri, M., Mazzei, I., Simpraga, S., Dell'osso, L., Linkenkaer-Hansen, K., Riemann, D., 2016. Multiple phenotypes of resting-state cognition are altered in insomnia disorder. Sleep Heal. 2, 239–245. https://doi.org/10.1016/j.sleh.2016.05.003
138. Pao, S.L., Wu, S.Y., Liang, J.M., Huang, I.J., Guo, L.Y., Wu, W.L., Liu, Y.G., Nian, S.H., 2022. A Physiological-Signal-Based Thermal Sensation Model for Indoor Environment Thermal Comfort Evaluation. Int. J. Environ. Res. Public Health 19. https://doi.org/10.3390/IJERPH19127292
139. Park, Y.M., Che, H.J., Im, C.H., Jung, H.T., Bae, S.M., Lee, S.H., 2008. Decreased EEG synchronization and its correlation with symptom severity in Alzheimer's disease. Neurosci. Res. 62, 112–117. https://doi.org/10.1016/J.NEURES.2008.06.009

140. Pascual-Marqui, R.D., Michel, C.M., Lehmann, D., 1995. Segmentation of Brain Electrical Activity into Microstates; Model Estimation and Validation. IEEE Trans. Biomed. Eng. 42, 658–665. https://doi.org/10.1109/10.391164
141. Pascual-Marqui, R.D., Michel, C.M., Lehmann, D., 1994. Low resolution electromagnetic tomography: a new method for localizing electrical activity in the brain. Int. J. Psychophysiol. 18, 49–65. https://doi.org/10.1016/0167-8760(84)90014-X
142. Pascual-Marqui, R D, Esslen, M., Kochi, K., Lehmann, D., Pascual-Marqui, Roberto D, 2002. Functional imaging with low resolution brainelectromagnetic tomography (LORETA): review, newcomparisons, and new validation, Japanese Journal of Clinical Neurophysiology.
143. Perrin, F., Pernier, J., Bertrand, O., Echallier, J.F., 1989. Spherical splines for scalp potential and current density mapping. Electroencephalogr. Clin. Neurophysiol. 72, 184–187. https://doi.org/10.1016/0013-4694(89)90180-6
144. Pipinis, E., Melynyte, S., Koenig, T., Jarutyte, L., Linkenkaer-Hansen, K., Ruksenas, O., Griskova-Bulanova, I., 2017. Association Between Resting-State Microstates and Ratings on the Amsterdam Resting-State Questionnaire. Brain Topogr. 30, 245–248. https://doi.org/10.1007/s10548-016-0522-2
145. Portnova, G. V., Ukraintseva, Y. V., Liaukovich, K.M., Martynova, O. V., 2019. Association of the retrospective self-report ratings with the dynamics of EEG. Heliyon 5, e02533. https://doi.org/10.1016/j.heliyon.2019.e02533
146. Prashad, S., Dedrick, E.S., Filbey, F.M., 2018. Cannabis users exhibit increased cortical activation during resting state compared to non-users. Neuroimage 179, 176. https://doi.org/10.1016/J.NEUROIMAGE.2018.06.031
147. Raichle, M.E., Macleod, A.M., Snyder, A.Z., Powers, W.J., Gusnard, D.A., Shulman, G.L., 1996. A default mode of brain function. Natl. Acad. Sci.
148. Reichle, E.D., Reineberg, A.E., Schooler, J.W., 2010. Eye movements during mindless reading. Psychol. Sci. 21, 1300–1310. https://doi.org/10.1177/0956797610378686
149. Ricci, G., De Crescenzio, F., Santhosh, S., Magosso, E., Ursino, M., 2022. Relationship between electroencephalographic data and comfort perception captured in a Virtual Reality design environment of an aircraft cabin. Sci. Rep. 12. https://doi.org/10.1038/S41598-022-14747-0
150. Rodríguez Martinez, E.I., Barriga-Paulino, C.I., Zapata, M.I., Chinchilla, C., López-Jiménez, A.M., Gómez, C.M., 2012. Narrow band

quantitative and multivariate electroencephalogram analysis of peri-adolescent period. BMC Neurosci. 13, 1–23. https://doi.org/10.1186/1471-2202-13-104/FIGURES/12
151. Roehri, N., Bréchet, L., Seeber, M., Pascual-Leone, A., Michel, C.M., 2022. Phase-Amplitude Coupling and Phase Synchronization Between Medial Temporal, Frontal and Posterior Brain Regions Support Episodic Autobiographical Memory Recall. Brain Topogr. 35, 191–206. https://doi.org/10.1007/S10548-022-00890-4/FIGURES/5
152. Rosazza, C., Minati, L., 2011. Resting-state brain networks: literature review and clinical applications. Neurol. Sci. 2011 325 32, 773–785. https://doi.org/10.1007/S10072-011-0636-Y
153. Rousseeuw, P.J., 1987. Silhouettes: A graphical aid to the interpretation and validation of cluster analysis. J. Comput. Appl. Math. 20, 53–65. https://doi.org/10.1016/0377-0427(87)90125-7
154. Rusterholz, T., Achermann, P., Dürr, R., Koenig, T., Tarokh, L., 2017. Global field synchronization in gamma range of the sleep EEG tracks sleep depth: Artifact introduced by a rectangular analysis window. J. Neurosci. Methods 284, 21–26. https://doi.org/10.1016/J.JNEUMETH.2017.04.002
155. Scheeringa, R., Bastiaansen, M.C.M., Petersson, K.M., Oostenveld, R., Norris, D.G., Hagoort, P., 2008. Frontal theta EEG activity correlates negatively with the default mode network in resting state. Int. J. Psychophysiol. 67, 242–251. https://doi.org/10.1016/J.IJPSYCHO.2007.05.017
156. Schiller, B., Heinrichs, M., Beste, C., Stock, A., 2021. Acute alcohol intoxication modulates the temporal dynamics of resting electroencephalography networks. Addict. Biol. https://doi.org/10.1111/adb.13034
157. Schiller, B., Koenig, T., Heinrichs, M., 2019. Oxytocin modulates the temporal dynamics of resting EEG networks. Sci. Rep. 9. https://doi.org/10.1038/s41598-019-49636-6
158. Schönbrodt, F.D., Perugini, M., 2013. At what sample size do correlations stabilize? J. Res. Pers. 47, 609–612. https://doi.org/10.1016/j.jrp.2013.05.009
159. Schwab, S., Koenig, T., Morishima, Y., Dierks, T., Federspiel, A., Jann, K., 2015. Discovering frequency sensitive thalamic nuclei from EEG microstate informed resting state fMRI. Neuroimage 118, 368–375. https://doi.org/10.1016/J.NEUROIMAGE.2015.06.001
160. Seeber, M., Michel, C.M., 2021. Synchronous Brain Dynamics Establish Brief States of Communality in Distant Neuronal Populations. eNeuro 8. https://doi.org/10.1523/ENEURO.0005-21.2021
161. Seitzman, B.A., Abell, M., Bartley, S.C., Erickson, M.A., Bolbecker,

A.R., Hetrick, W.P., 2017. Cognitive manipulation of brain electric microstates. Neuroimage 146, 533–543. https://doi.org/10.1016/j.neuroimage.2016.10.002

162. Shigihara, Y., Tanaka, M., Ishii, A., Kanai, E., Funakura, M., Watanabe, Y., 2013. Two types of mental fatigue affect spontaneous oscillatory brain activities in different ways. Behav. Brain Funct. 9, 2. https://doi.org/10.1186/1744-9081-9-2
163. Simpraga, S., Alvarez-Jimenez, R., Mansvelder, H.D., Van Gerven, J.M.A., Groeneveld, G.J., Poil, S.S., Linkenkaer-Hansen, K., 2017. EEG machine learning for accurate detection of cholinergic intervention and Alzheimer's disease. Sci. Rep. 7. https://doi.org/10.1038/S41598-017-06165-4
164. Simpraga, S., Weiland, R.F., Mansvelder, H.D., Polderman, T.J., Begeer, S., Smit, D.J., Linkenkaer-Hansen, K., 2021. Adults with autism spectrum disorder show atypical patterns of thoughts and feelings during rest. Autism 136236132199092. https://doi.org/10.1177/1362361321990928
165. Skrandies, W., 1990. Global Field Power and Topographic Similarity, Brain Topography.
166. Smailovic, U., Ferreira, D., Ausén, B., Ashton, N.J., Koenig, T., Zetterberg, H., Blennow, K., Jelic, V., 2022. Decreased Electroencephalography Global Field Synchronization in Slow-Frequency Bands Characterizes Synaptic Dysfunction in Amnestic Subtypes of Mild Cognitive Impairment. Front. Aging Neurosci. 14, 72. https://doi.org/10.3389/FNAGI.2022.755454/BIBTEX
167. Smailovic, U., Koenig, T., Kåreholt, I., Andersson, T., Kramberger, M.G., Winblad, B., Jelic, V., 2018. Quantitative EEG power and synchronization correlate with Alzheimer's disease CSF biomarkers. Neurobiol. Aging 63, 88–95. https://doi.org/10.1016/J.NEUROBIOLAGING.2017.11.005
168. Smailovic, U., Koenig, T., Laukka, E.J., Kalpouzos, G., Andersson, T., Winblad, B., Jelic, V., 2019. EEG time signature in Alzheimer´s disease: Functional brain networks falling apart. NeuroImage Clin. 24. https://doi.org/10.1016/j.nicl.2019.102046
169. Smallwood, J., Schooler, J.W., 2015. The Science of Mind Wandering: Empirically Navigating the Stream of Consciousness. Annu. Rev. Psychol 66, 487–518. https://doi.org/10.1146/annurev-psych-010814-015331
170. Smallwood, J., Schooler, J.W., 2006. The restless mind. Psychol. Bull. 132, 946–958. https://doi.org/10.1037/0033-2909.132.6.946
171. Smit, D.J.A., Boomsma, D.I., Schnack, H.G., Pol, H.E.H., De Geus, E.J.C., 2012. Individual Differences in EEG Spectral Power Reflect

Genetic Variance in Gray and White Matter Volumes. Twin Res. Hum. Genet. 15, 384–392. https://doi.org/10.1017/THG.2012.6

172. Smith, E.E., Tenke, C.E., Deldin, P.J., Trivedi, M.H., Weissman, M.M., Auerbach, R.P., Bruder, G.E., Pizzagalli, D.A., Kayser, J., 2020. Frontal theta and posterior alpha in resting EEG: A critical examination of convergent and discriminant validity. Psychophysiology 57, e13483. https://doi.org/10.1111/PSYP.13483
173. Son, Y.J., Chun, C., 2018. Research on electroencephalogram to measure thermal pleasure in thermal alliesthesia in temperature step-change environment. Indoor Air 28, 916–923. https://doi.org/10.1111/INA.12491
174. Stam, C.J., Nolte, G., Daffertshofer, A., 2007. Phase lag index: Assessment of functional connectivity from multi channel EEG and MEG with diminished bias from common sources. Hum. Brain Mapp. 28, 1178–1193. https://doi.org/10.1002/HBM.20346
175. Stoffers, D., Diaz, B.A., Chen, G., Braber, A. den, Ent, D. van 't, Boomsma, D.I., Mansvelder, H.D., Geus, E. de, Someren, E.J.W. Van, Linkenkaer-Hansen, K., 2015. Resting-State fMRI Functional Connectivity Is Associated with Sleepiness, Imagery, and Discontinuity of Mind. PLoS One 10. https://doi.org/10.1371/JOURNAL.PONE.0142014
176. Strijkstra, A.M., Beersma, D.G.M., Drayer, B., Halbesma, N., Daan, S., 2003. Subjective sleepiness correlates negatively with global alpha (8–12 Hz) and positively with central frontal theta (4–8 Hz) frequencies in the human resting awake electroencephalogram. Neurosci. Lett. 340, 17–20. https://doi.org/10.1016/S0304-3940(03)00033-8
177. Tait, L., Tamagnini, F., Stothart, G., Barvas, E., Monaldini, C., Frusciante, R., Volpini, M., Guttmann, S., Coulthard, E., Brown, J.T., Kazanina, N., Goodfellow, M., 2020. EEG microstate complexity for aiding early diagnosis of Alzheimer's disease. Sci. Reports 2020 101 10, 1–10. https://doi.org/10.1038/s41598-020-74790-7
178. Tait, L., Zhang, J., 2022. MEG cortical microstates: Spatiotemporal characteristics, dynamic functional connectivity and stimulus-evoked responses. Neuroimage 251. https://doi.org/10.1016/J.NEUROIMAGE.2022.119006
179. Takarae, Y., Zanesco, A., Keehn, B., Chukoskie, L., Müller, R.A., Townsend, J., 2022. EEG microstates suggest atypical resting-state network activity in high-functioning children and adolescents with autism spectrum development. Dev. Sci. https://doi.org/10.1111/desc.13231
180. Tan, D.E.B., Tung, R.S., Leong, W.Y., Than, J.C.M., 2012. Sleep Disorder Detection and Identification. Procedia Eng. 41, 289–295. https://doi.org/10.1016/J.PROENG.2012.07.175

181. Tarailis, P., De Blasio, F.M., Simkute, D., Griskova-Bulanova, I., 2022. Data-Driven EEG Theta and Alpha Components Are Associated with Subjective Experience during Resting State. J. Pers. Med. 12, 896. https://doi.org/10.3390/jpm12060896
182. Tarailis, P., Šimkutė, D., Koenig, T., Griškova-Bulanova, I., 2021. Relationship between Spatiotemporal Dynamics of the Brain at Rest and Self-Reported Spontaneous Thoughts: An EEG Microstate Approach. J. Pers. Med. 11, 1216. https://doi.org/10.3390/jpm11111216
183. Tenke, C.E., Kayser, J., 2005. Reference-free quantification of EEG spectra: Combining current source density (CSD) and frequency principal components analysis (fPCA). Clin. Neurophysiol. 116, 2826–2846. https://doi.org/10.1016/J.CLINPH.2005.08.007
184. Tenke, C.E., Kayser, J., Manna, C.G., Fekri, S., Kroppmann, C.J., Schaller, J.D., Alschuler, D.M., Stewart, J.W., McGrath, P.J., Bruder, G.E., 2011. Current Source Density Measures of EEG Alpha Predict Antidepressant Treatment Response. Biol. Psychiatry 70, 388. https://doi.org/10.1016/J.BIOPSYCH.2011.02.016
185. Tenke, C.E., Kayser, J., Pechtel, P., Webb, C.A., Dillon, D.G., Goer, F., Murray, L., Deldin, P., Kurian, B.T., McGrath, P.J., Parsey, R., Trivedi, M., Fava, M., Weissman, M.M., McInnis, M., Abraham, K., E. Alvarenga, J., Alschuler, D.M., Cooper, C., Pizzagalli, D.A., Bruder, G.E., 2017. Demonstrating Test-Retest Reliability of Electrophysiological Measures for Healthy Adults in a Multisite Study of Biomarkers of Antidepressant Treatment Response. Psychophysiology 54, 34. https://doi.org/10.1111/PSYP.12758
186. The MathWorks, I., 2022. Statistics and Machine Learning Toolbox - MATLAB.
187. Tomescu, M.I., Papasteri, C.C., Sofonea, A., Boldasu, R., Kebets, V., Pistol, C.A.D., Poalelungi, C., Benescu, V., Podina, I.R., Nedelcea, C.I., Berceanu, A.I., Carcea, I., 2022. Spontaneous thought and microstate activity modulation by social imitation. Neuroimage 118878. https://doi.org/10.1016/J.NEUROIMAGE.2022.118878
188. Van De Ville, D., Britz, J., Michel, C.M., 2010. EEG microstate sequences in healthy humans at rest reveal scale-free dynamics. Proc. Natl. Acad. Sci. U. S. A. 107, 18179–18184. https://doi.org/10.1073/PNAS.1007841107/-/DCSUPPLEMENTAL
189. Van Diessen, E., Numan, T., Van Dellen, E., Van Der Kooi, A.W., Boersma, M., Hofman, D., Van Lutterveld, R., Van Dijk, B.W., Van Straaten, E.C.W., Hillebrand, A., Stam, C.J., 2015. Opportunities and methodological challenges in EEG and MEG resting state functional

brain network research. Clin. Neurophysiol. 126, 1468–1481. https://doi.org/10.1016/j.clinph.2014.11.018
190. Vaughan, H.G., 1982. THE NEURAL ORIGINS OF HUMAN EVENT-RELATED POTENTIALS. Ann. N. Y. Acad. Sci. 388, 125–138. https://doi.org/10.1111/J.1749-6632.1982.TB50788.X/FORMAT/PDF
191. Vecchio, F., Pappalettera, C., Miraglia, F., Alù, F., Orticoni, A., Judica, E., Cotelli, M., Pistoia, F., Rossini, P.M., 2021. Graph Theory on Brain Cortical Sources in Parkinson's Disease: The Analysis of 'Small World' Organization from EEG. Sensors (Basel). 21. https://doi.org/10.3390/S21217266
192. Vejmola, Č., Tylš, F., Piorecká, V., Koudelka, V., Kadeřábek, L., Novák, T., Páleníček, T., 2021. Psilocin, LSD, mescaline, and DOB all induce broadband desynchronization of EEG and disconnection in rats with robust translational validity. Transl. Psychiatry 2021 111 11, 1–8. https://doi.org/10.1038/s41398-021-01603-4
193. Vellante, F., Ferri, F., Baroni, G., Croce, P., Migliorati, D., Pettoruso, M., De Berardis, D., Martinotti, G., Zappasodi, F., Giannantonio, M. Di, 2020. Euthymic bipolar disorder patients and EEG microstates: a neural signature of their abnormal self experience? J. Affect. Disord. 272, 326–334. https://doi.org/10.1016/j.jad.2020.03.175
194. von Wegner, F., Bauer, S., Rosenow, F., Triesch, J., Laufs, H., 2021. EEG microstate periodicity explained by rotating phase patterns of resting-state alpha oscillations. Neuroimage 224, 117372. https://doi.org/10.1016/J.NEUROIMAGE.2020.117372
195. von Wegner, F., Knaut, P., Laufs, H., 2018. EEG microstate sequences from different clustering algorithms are information-theoretically invariant. Front. Comput. Neurosci. 12. https://doi.org/10.3389/fncom.2018.00070
196. Wei, Y., Van Someren, E.J., 2020. Interoception relates to sleep and sleep disorders. Curr. Opin. Behav. Sci. https://doi.org/10.1016/j.cobeha.2019.11.008
197. Weinstein, Y., 2018. Mind-wandering, how do I measure thee with probes? Let me count the ways. Behav. Res. Methods 50, 642–661. https://doi.org/10.3758/S13428-017-0891-9/TABLES/9
198. Wetzels, R., Wagenmakers, E.J., 2012. A default Bayesian hypothesis test for correlations and partial correlations. Psychon. Bull. Rev. 19, 1057–1064. https://doi.org/10.3758/s13423-012-0295-x
199. Xiao, R., Shida-Tokeshi, J., Vanderbilt, D.L., Smith, B.A., 2018. Electroencephalography power and coherence changes with age and motor skill development across the first half year of life. PLoS One 13.

https://doi.org/10.1371/JOURNAL.PONE.0190276
200. Yoshimura, M., Koenig, T., Irisawa, S., Isotani, T., Yamada, K., Kikuchi, M., Okugawa, G., Yagyu, T., Kinoshita, T., Strik, W., Dierks, T., 2007. A pharmaco-EEG study on antipsychotic drugs in healthy volunteers. Psychopharmacology (Berl). 191, 995–1004. https://doi.org/10.1007/s00213-007-0737-8
201. Zanesco, A.P., 2020. EEG Electric Field Topography is Stable During Moments of High Field Strength. Brain Topogr. 33, 450–460. https://doi.org/10.1007/s10548-020-00780-7
202. Zanesco, A.P., Denkova, E., Jha, A.P., 2021a. Associations between self-reported spontaneous thought and temporal sequences of EEG microstates. Brain Cogn. 150, 105696. https://doi.org/10.1016/j.bandc.2021.105696
203. Zanesco, A.P., Denkova, E., Jha, A.P., 2020a. Self-reported mind wandering and response time variability differentiate prestimulus electroencephalogram microstate dynamics during a sustained attention task. J. Cogn. Neurosci. 33, 28–45. https://doi.org/10.1162/jocn_a_01636
204. Zanesco, A.P., King, B.G., Skwara, A.C., Saron, C.D., 2020b. Within and between-person correlates of the temporal dynamics of resting EEG microstates. Neuroimage 211. https://doi.org/10.1016/j.neuroimage.2020.116631
205. Zanesco, A.P., Skwara, A.C., King, B.G., Powers, C., Wineberg, K., Saron, C.D., 2021b. Meditation training modulates brain electric microstates and felt states of awareness. Hum. Brain Mapp. hbm.25430. https://doi.org/10.1002/hbm.25430
206. Zappasodi, F., Croce, P., Giordani, A., Assenza, G., Giannantoni, N.M., Profice, P., Granata, G., Rossini, P.M., Tecchio, F., 2017. Prognostic Value of EEG Microstates in Acute Stroke. Brain Topogr. 30, 698–710. https://doi.org/10.1007/S10548-017-0572-0/FIGURES/5
207. Zappasodi, F., Perrucci, M.G., Saggino, A., Croce, P., Mercuri, P., Romanelli, R., Colom, R., Ebisch, S.J.H., 2019. EEG microstates distinguish between cognitive components of fluid reasoning. Neuroimage 189, 560–573. https://doi.org/10.1016/j.neuroimage.2019.01.067
208. Zhang, K., Shi, W., Wang, C., Li, Y., Liu, Z., Liu, T., Li, J., Yan, X., Wang, Q., Cao, Z., Wang, G., 2021. Reliability of EEG microstate analysis at different electrode densities during propofol-induced transitions of brain states. Neuroimage 231, 117861. https://doi.org/10.1016/J.NEUROIMAGE.2021.117861

PUBLICATIONS

Publications included in the thesis

- **Tarailis P**, Šimkutė D, Griškova-Bulanova I. (Submitted). Global functional connectivity is associated with mind wandering domain of Comfort. Brain Topography
- **Tarailis P**, De Blasio FM, Šimkutė D, Griškova-Bulanova I (2022). Data-Driven EEG Theta and Alpha Components Are Associated with Subjective Experience during Resting State. Journal of Personalized Medicine Journal of Personalized Medicine 12(6),896. https://doi.org/10.3390/jpm12060896
- **Tarailis P**, Simkute D, Koenig T, Griskova-Bulanova I. (2021) Relationship between Spatiotemporal Dynamics of the Brain at Rest and Self-Reported Spontaneous Thoughts: An EEG Microstate Approach. Journal of Personalized Medicine 11(11), 1216. https://doi.org/10.3390/jpm11111216

Conferences on the thesis topic

- (Poster) **P.Tarailis,** F.M.De Blasio, I.Griskova-Bulanova "EEG Theta Component Correlates with Sleepiness Scores". the 13th International conference of Lithuanian Neuroscience Association, 26th November 2021, Kaunas, Lithuania
- (Poster) **P.Tarailis**, F.M.De Blasio, I.Griskova-Bulanova "Relationship between data-driven EEG components and subjective experience during resting state". IPEG Online Meeting, 27-29th, 2021
- (Poster) **P. Tarailis,** T. Koenig, I.Griskova-Bulanova "The relationship between EEG microstates and subjective experience", the 11th International scientific conference "NEURONUS 2020 IBRO Neuroscience Forum, 8-11th December 2020, Krakow, Poland
- (Poster) **P. Tarailis**, T. Koenig, I.Griskova-Bulanova "Neuroelectric microstates and subjective experience: A pilot study on five microstates classes", the 12th International conference of Lithuanian Neuroscience Association, 6th November 2020, Vilnius, Lithuania

Other publications

- **Tarailis P**, Koenig T, Michel C.M, Griškova-Bulanova I. (2023). *The functional aspects of resting EEG microstates: a systematic review*. Brain Topography; https://doi.org/10.1007/S10548-023-00958-9
- Mockevičius A, Yokota Y, **Tarailis P**, Hasegawa H, Naruse Y, Griškova-Bulanova I (2023). *Extraction of Individual EEG Gamma Frequencies from the Responses to Click-Based Chirp-Modulated Sounds*. Sensors 2023, 23(5), 2826; https://doi.org/10.3390/s23052826
- Ghodousi M, Pousson JE, Voicikas A, Bernhofs V, Pipinis E, **Tarailis P**, Burmistrova L, Lin YP, Griškova-Bulanova I (2022) *EEG connectivity during emotional musical performance*. Sensors 22(11):4064
- Simkute D, Nagula I, **Tarailis P**, Burkauskas J, Griskova-Bulanova I.(2021) *Internet usage habits and experienced levels of psychopathology: a pilot study on association with spontaneous eye blinking rate*. Journal of Personalized Medicine 11(4), 288
- Parciauskaite V, Voicikas A, Jurkuvenas A, **Tarailis P**, Kraulaidis M, Pipinis E, Griskova- Bulanova, I. (2019) *40-Hz Auditory Steady-State Responses and the Complex Information Processing: Exploratory Study in Healthy Young Males*. PLOS One v.14 (10)

Other conferences

- (Oral presentation) **P.Tarailis,** I. Griškova-Bulanova, M, Živanovič, S.R. FIlipovič, J. Bjekič " *The effects of tACS on EEG microstates*".50 years of Microstates, 31st August – 3rd September, Bern, Switzerland
- (Poster) **P.Tarailis,** A. Voicikas, E.Pipinis, I. Griškova-Bulanova „*Individual gamma frequency based neurofeedback: a pilot study*". FENS Regional meeting, 25-27 August, 2021, Krakow, Poland

ABOUT THE AUTHOR

Povilas Tarailis **Curriculum vitae**

Contact information:

Junior researcher,
PhD student
Life Sciences Center
Saulėtekio ave. 7,
LT-10257
Vilnius, Lithuania
Vilnius University

Phone:
+37068390211

Email:
povilas.tarailis@gmc.vu.lt
tarailispovilas@gmail.com

Education:

- PhD student in Biophysics since 2018 to present.
- Master's degree in Neurobiology 2018.
- Bachelor's degree. in Philosophy 2016.

Research experience:

- 2022.10 Visiting researcher at University of Geneva, Department of Basic Neuroscience, Functional Brain Mapping Laboratory. Supervisor: Dr. Lucie Brechet
- 2022.05 Visiting researcher at National Institute of Mental Health, Czechia
- 2021.08-09 Full time visiting researcher at University Hospital of Psychiatry, University of Bern, Switzerland. IBRO grant-based. Supervisor: prof. Thomas Koenig
- 2021- Researcher at project "Individual gamma frequency-based neurofeedback". Supervisor: dr. Inga Griškova – Bulanova
- 2020.11-12 Researcher at University Hospital of Psychiatry, University of Bern, Switzerland. IBRO grant-based. Supervisor: prof. Thomas Koenig
- 2019.11 - 2020.03 Researcher at Aarhus University Hospital. COST action "The neural architecture of consciousness" (CA18106). Supervisor: prof. Kristian Sandberg
- 2019-2021 Researcher at project "Brain-Computer Music Interfacing

for Embodied Musical Interaction“. Supervisor: dr. Inga Griškova – Bulanova
- Since 2018 Researcher for PhD thesis “Evaluation of electrical brain activity of the resting state: relation with subjective experiences”. Supervisor: dr. Inga Griškova – Bulanova
- 2016 - 2018.06 researcher for master thesis “Evaluation of EEG Responses to Somatosensory Periodic Stimulation”. Supervisor: dr. Inga Griškova – Bulanova.

Funding obtained:

- 2022 COST (CA18607) Short Term Scientific Mission
- 2022 Lithuanian Neuroscience Association traveling grant
- 2022 COST (CA18607) Traveling Grant
- 2022 Lithuanian Neuroscience Association Traveling Grant
- 2021 Vilnius University Science Promotion Funding ‘Electrophysiological manifestations of subjective perception of resting state’ (MSFJM8/2021), (Project leader)
- 2021 International Brain Research Organization (IBRO) Pan European Regional Committee In Europe Short Stay Grant
- 2020 International Brain Research Organization (IBRO) Pan European Regional Committee In Europe Short Stay Grant
- 2020 ERASMUS+ Grant
- 2019-2020 COST (CA18607) Short Term Scientific Mission
- 2019 COST (CA18607) Traveling Grant

Courses Attended:

- MathWorks “Image processing with MATLAB”
- MathWorks “MATLAB for Data Processing and Visualization”
- MathWorks “Introduction to Linear Algebra with MATLAB”
- MathWorks “Introduction to Statistical Methods with MATLAB”
- Online workshop “Psychophysiological data quantification using Principal Components Analysis (PCA)”, 2021.04.07
- Online course “Scientific Writing Pro”, 2020.12-2021.01
- MRI safety training course, 2019 November 29th, Aarhus University hospital
- Introduction to R statistics. 2018.11.12-13. Vilnius, Lithuania
- Workshop „Stepping into the Future – a Multi-Disciplinary Approach

to Brain-Machine Interaction “; 2018 May 4th - 5th Vilnius, Lithuania

- "Laboratory (experimental) animal science" course, 2017.09 – 2018.01, Vilnius, Lithuania

Professional memberships:

- International Pharmaco-EEG Society (IPEG), since 2021.10
- The International Society for Brain Electromagnetic Topography (ISBET), since 2020.05
- Lithuanian Neuroscience Association (LNA), since 2016.12
- Federation of European Neuroscience Societies (FENS), since 2016.12

SANTRAUKA

1. ĮVADAS

Ramybės būsenos metodas yra naudojamas siekiant įvertinti smegenų aktyvumą, kai tiriamajam nėra pateikiama jokia užduotis (Rosazza and Minati, 2011). Per pastaruosius tris dešimtmečius smegenų ramybės būsenos vaizdavimo metodas sulaukė didelio dėmesio ir populiarumo kognityvinio ir klinikinio neuromokslų srityse, dėl savo paprastumo, lengvo standartizavimo ir jautrumo smegenų sutrikimams. Tyrimai, atlikti taikant šį metodą, parodė, kad smegenys, užuot buvusios neaktyvios, pasižymi dideliu aktyvumu. Šiam aktyvumui tirti taikomi įvairūs smegenų vaizdinimo ir analizės metodai, leidžiantys įvairiai interpretuoti smegenų erdvinę ir laikinę savi-organizaciją. Ankstyvieji funkcinio magnetinio rezonanso (fMRI) tyrimai parodė, kad ramybės būsenos sesijų metu smegenys demonstruoja sinchroninį aktyvumą, panašų į stebimą dalyviams atliekant užduotį (Biswal et al., 1995; Raichle et al., 1996).

Nepaisant lengvo pritaikymo, ramybės būsenos metodas gali būti jautrus galimam subjektyvių pojūčių heterogeniškumui, kuris gali skirtis tarp žmonių (Hurlburt et al., 2015; Smallwood and Schooler, 2015, 2006; Weinstein, 2018). Skirtingai nuo tiriamųjų patirties sukeltinių potencialų tyrimuose, kada visi dalyviai atlieka tą pačią užduotį, ramybės būsenos metu, tiriamųjų pojūčiai ir mintys yra nevaržomi ir gali būti vedami tiek vidinių tiek išorinių šaltinių (Gorgolewski et al., 2014; Smallwood and Schooler, 2015). Šis spontaniškas aktyvumas svyruoja nuo vienos akimirkos iki kitos, o dalyviai pasineria į mintis apie praeitį, ateities planus ar į save ir kitus nukreiptus apmąstymus (Smallwood and Schooler, 2006; Zanesco et al., 2021a).

Skirtingi analizės metodai yra taikomi vertinant smegenų ramybės būsenos aktyvumą, gautą naudojant skirtingus smegenų vaizdinimo metodus. Vienas iš plačiai naudojamų metodų yra elektroencefalografija (EEG). EEG yra pigus ir plačiai naudojamas metodas vertinti elektrinį smegenų aktyvumą. EEG signalas savyje turi informaciją apie galią, fazę, kompleksiškumą, globalius laikinius ir erdvinius paternus, todėl galima visapusiškai vertinti įvairius smegenų veiklos aspektus.

Populiariausias būdas vertinti ramybės būseną yra galios analizė, kai EEG signalas yra suskirstomas yra numatytus dažnių diapazonus (delta, teta, alfa, beta, gama). Deja, dažnių diapazonų ribos dažnai varijuoja (Newson and Thiagarajan, 2019), o tai gali turėti įtakos rezultatų interpretavimui ir tyrimų palyginimui. Taigi, siekiant įveikti šią problemą, buvo pasiūlyta dažnių

pagrindinių komponenčių analizė kaip būdas išskaidyti EEG signalą į reikšmingus atskirus komponentus (Barry et al., 2019; Dien, 2012). Šis metodas buvo naudotas keliuose tyrimuose su įvairaus amžiaus dalyviais (Barry et al., 2019; Rodríguez Martinez et al., 2012) ir buvo pasiūlytas kaip jautrus biologinis žymuo antidepresantų gydime (Tenke et al., 2017, 2011). Tačiau šio metodo rezultatų ryšys su subjektyviais pojūčiais ramybės būsenos metu nebuvo vertintas.

Kitas populiarus metodas vertinti ramybės būsenos EEG yra mikrobūsenų analizė (Khanna et al., 2015). EEG mikrobūsenų analizėje kiekvienas laiko taškas yra apibrėžiamas kaip individuali, nepersidengianti topografija (Khanna et al., 2015; Koenig et al., 2002). Šis metodas leidžia vertinti smegenų tinklų globalų aktyvumą. EEG mikrobūsenų metodas buvo sėkmingai naudotas vertinant smegenų aktyvumą įvairių būsenų metu, pavyzdžiui, atmerktų / užmerktų akių (Seitzman et al., 2017; Zanesco et al., 2020), kognityvinių užduočių atlikimo metu (Bréchet et al., 2019; D'Croz-Baron et al., 2021; Liu et al., 2020; Poskanzer et al., 2021), ar esant neuropsichologiniams sutrikimams (Kikuchi et al., 2011; Murphy et al., 2020; Nishida et al., 2013; Rieger et al., 2016). Tačiau šis metodas buvo minimaliai naudotas siekiant įvertinti ryšį tarp smegenų aktyvumo ir subjektyvių potyrių ramybės būsenoje.

Gerai žinoma, jog funkciniai ryšiai tarp EEG aktyvumo šaltinių yra svarbus rodiklis nurodantis smegenų funkcionavimą. Siekiant įvertinti ryšius tarp skirtingų smegenų sričių, yra taikomi fazės vertinimo metodai (Van Diessen et al., 2015). Deja, šie metodai susiduria su tam tikrais metodologiniais sunkumais, kurie dažnai yra ignoruojami. Lehmann ir kt. (Lehmann et al., 2006) parodė, kad reikšmingi ryšiai tarp elektrodų porų keičiasi pakeičiant referentinį elektrodą. Todėl svarbu vertinti fazių sinchronizaciją, kuri nėra priklausoma nuo referentinio elektrodo. Koenig ir kt. (Koenig et al., 2001) pristatė nuo referentinio elektrodo nepriklausomą parametrą vertinti globalų funkcinį ryšį – globalios fazės sinchronizaciją. Šis metodas buvo sėkmingai panaudotas tiek klinikinėje, tiek sveikoje populiacijoje, tačiau iki šiol nebuvo taikomas vertinant ryšį tarp smegenų aktyvumo ir subjektyvių potyrių ramybės būsenoje.

Dėl nuolat kintančios mąstysenos sunku susieti subjektyvią psichologinę veiklą su stebimais biologiniais signalais. Egzistuoja keli skirtingi metodai, kaip pamatuoti ir kiekybiškai įvertinti subjektyvius pojūčius ir mintis tiek ramybės būsenoje tiek sukeltinių potencialų sesijos metu (Weinstein, 2018). Objektyvus / netiesioginis būdas yra matuojant elgsenos aspektai: reakcijos laikas (Cheyne et al., 2006) arba akių judesiai (Reichle et al., 2010). Subjektyvus / netiesioginis būdas daugiausia dėmesio skiria

dalyvių vidinių būsenų savianalizei. Subjektyvųjį / tiesioginį požiūrį dar galima skirstyti į savęs fiksavimo, kai dalyviai bet kuriuo metu gali pranešti apie savo subjektyvius pojūčius arba kai jų dėmesys nukrypsta nuo užduoties, ir išorinio fiksavimo, kai dalyviai sustabdomi arba jiems nurodoma prisiminti subjektyvią patirtį ir pojūčius duotuoju momentu.

Nepaisant to, kad šie būdai yra populiarūs, surinkti ir įvertinti subjektyvius pojūčius ir emocijas naudojant specifinius klausimynus yra paprastesnis ir greitesnis būdas. Egzistuoja keletas skirtingų ramybės būsenos klausimynų, kurie yra naudojami smegenų vaizdinimo ir elgesniniuose tyrimuose (Delamillieure et al., 2010; Diaz et al., 2014, 2013; Gorgolewski et al., 2014). Šie klausimynai apima keletą ramybės būsenos kognityvinių domenų ir suteikia standartizuotą būdą kiekybiškai įvertinti subjektyvias tiriamųjų būsenas. Subalansavus grupes pagal jų kognityvines būsenas, būtų galima nustatyti didesnius grupių skirtumus, o tai padėtų geriau interpretuoti rezultatus ir padidinti smegenų vaizdinimo biologinių žymenų jautrumą ir specifiškumą klinikiniuose ir farmakologiniuose tyrimuose (Diaz et al., 2013).

1.1. Tikslas ir uždaviniai

Šis darbas buvo skirtas įvertinti ryšį tarp subjektyvių tiriamųjų pojūčių ir smegenų fiziologinių rodiklių surinktų naudojant EEG, skiriant dėmesį į galios, fazės sinchronizacijos ir topografinius aspektus. Darbo uždaviniai:

1. Susieti subjektyvius dalyvių pojūčius su EEG pagrindinių komponenčių galios įverčiais.
2. Susieti subjektyvius dalyvių pojūčius su EEG globalios fazės sinchronizacijos įverčiais.
3. Susieti subjektyvius dalyvių pojūčius su EEG mikrobūsenų laikiniais parametrais.

1.2 Mokslinis Naujumas

1. Pirmą kartą subjektyvūs pojūčiai buvo susieti su duomenimis grįstu metodu dažnių srityje, naudojant dažnių pagrindinių komponenčių analizę.
2. Pirmą kartą subjektyvūs pojūčiai buvo susieti su globalios fazės sinchronizacijos įverčiais.
3. Antrą kartą subjektyvūs pojūčiai buvo susieti su duomenimis grįstais EEG mikrobūsenų laikiniais parametrais.

1.3 Praktinis pritaikymas

1. Globalios fazės sinchronizacija alfa (8 – 13 Hz) ir beta (13 – 30 Hz) dažnių diapazonuose gali būti naudojama įvertinti subjektyvius Komforto pojūčius įvertinant Amsterdamo Ramybės Būsenos Klausimynu.
2. Smegenų aktyvumas alfa (9 Hz) ir teta (5.5 Hz) diapazonuose gali būti naudojamas vertinant subjektyvius Komforto ir Mieguistumo pojūčius įvertinus Amsterdamo Ramybės Būsenos Klausimynu.
3. Mikrobūsenos F indėlis gali būti naudojamas įvertinti subjektyvius Somatinio sąmoningumo pojūčius. Mikorbūsenos B pasirodymo dažnis ir mikrobūsenos D vidutinė trukmė gali būti naudojama vertinti su savimi susijusių minčių vertinimą. Mikrobūsenos C pasirodymo dažnis gali būti naudojamas vertinti subjektyvų Komforto vertinimą. Mikrobūsenų E ir F vidutinė trukmė gali būti naudojama vertinti subjektyvų Komforto įvertinimus Amsterdamo Ramybės Būsenos Klausimynu.

1.3 Ginamieji teiginiai

1. Globalios fazės sinchronizacijos vertės alfa (8 -13 Hz) ir beta (13 -30 Hz) dažnių diapazonuose koreliuoja su subjektyviais Komforto vertinimais.
2. Pagrindinių komponenčių įverčiai teta ir alfa dažniuose koreliuoja su subjektyviais Mieguistumo ir Komforto vertinimais.
3. EEG mikrobūsenų parametrai koreliuoja su skirtingais Amsterdamo Ramybės Būsenos Klausimyno domenais.

2. METODIKA

Tyrimui patvirtintas Vilniaus regioninis biomedicininių tyrimų etikos komitetas (Nr. 2019/10-1159-649, patvirtinimo data: 2019 m. spalio 8 d.), visi tiriamieji davė raštišką informuotą sutikimą dalyvauti tyrime.

2.1. Dalyviai

Tyrime dalyvavo du šimtai dvidešimt šeši dalyviai (Moterys = 131, Vyrai = 95, amžiaus vidurkis 23.41, ± standartinis nuokrypis 3,87). Dalyvių amžius buvo nuo 19 iki 35 metų. Visi dalyviai turėjo normalią arba koreguotą iki normalios regą. Visos tyrime dalyvavusios moterys buvo sveikos, ne nėščios, nenaudojo hormoninės kontracepcijos ir nurodė, kad jų menstruacijų ciklas reguliarus. 107 moterys tyrime dalyvavo ankstyvosios folikulinės fazės (mėnesinių) metu, 20 - liuteininės fazės metu ir 4 - ovuliacijos fazės metu. Aštuoniolika dalyvių buvo kairiarankiai, o likusieji - dešiniarankiai. Dalyvių buvo paprašyta 2 val. prieš tyrimą nevartoti nikotino ir kofeino. Kiekvienam analizės metodui naudotų dalyvių grupių aprašymas pateiktas pirmoje lentelėje.

Lentelė 1. Aprašomoji dalyvių statistika kiekviename tyrime.

	d-PKA ir GFS	**EEG mikrobūsenos**
N	226	197
Vyrai	95	94
Moterys	131	103
Amžiaus vidurkis ir standartinis nuokrypis	23.41 (±3.87)	23.97 (±3.81)

2.2 Duomenų rinkimas

Siekiant išvengti, kad tiriamieji neužmigtų ir būtų užtikrintas pakankamas duomenų kiekis ir kokybė (Jobert et al., 2012; Liu et al., 2020; Tagliazucchi and Laufs, 2014), penkios minutes ramybės būsenos EEG buvo įrašoma pritemdytoje, garsą slopinančioje ir nuo tinklo triukšmo izoliuotoje patalpoje, kol dalyviai patogiai sėdėjo vertikalioje padėtyje. Prieš pradedant duomenų rinkimą, dalyviams buvo pateiktos instrukcijos sėdėti ramiai užmerktomis akimis ir apie nieką konkrečiai negalvoti, neužmigti.

EEG duomenys buvo surinkti naudojant EEG įrangą (ANT Neuro, Nyderlandai) ir 64 sidabro/sidabro chlorido elektrodus, išdėstytus pagal tarptautinę 10 – 10 sistemą ant WaveGuard kepurės (Pav. 1). Referentiniai elektrodai buvo M1/M2, įžeminimo elektrodas buvo šalia Fz elektrodo. Visų elektrodų impendancas buvo mažesnis nei 20 kΩ.

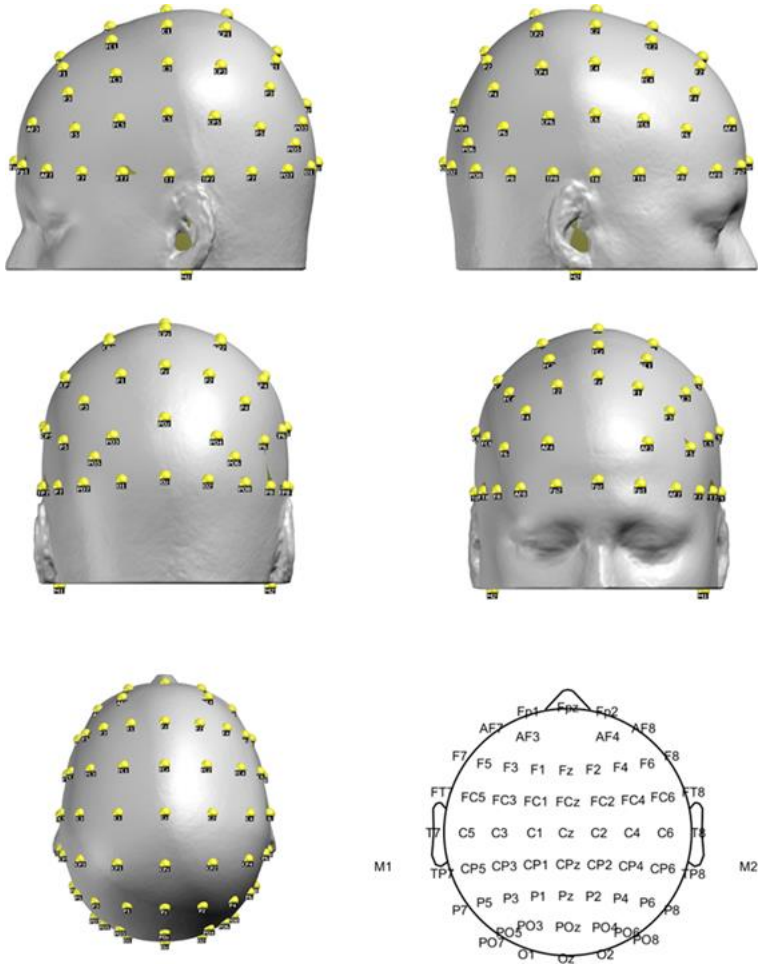

Pav. 1. 64 elektrodų išdėstymas pagal tarptautinę 10-10 sistemą, naudotas duomenų rinkime

Papildomai dvi poros elektrodų (VEOG ir HEOG) buvo naudotos užregistruoti vertikalius ir horizontalius akių judesius. VEOG elektrodai buvo pritvirtinti virš ir po dešine akimi. HEOG elektrodų pora buvo pritvirtinta apie 2 cm nuo akių kraštų. Duomenys buvo skaitmenizuoti 2048 Hz dažniu.

Iškart po EEG sesijos dalyviai užpildė lietuvišką ARSQ versiją, kurioje turėjo retrospektyviai įvertinti teiginius apie galimas emocijas ir pojūčius ramybės būsenos metu, nuo 1 (visiškai nesutinku) iki 5 (visiškai sutinku).

2.3 Amsterdamo ramybės būsenos klausimynas

Įvertinti subjektyvius pojūčius Lietuviška ARBK 2.0 versija (Pipinis et al., 2017) buvo naudota. ARBK yra savarankiškai pildomas klausimynas, kuriuo siekiama įvertinti retrospektyvią subjektyvią patirtį. Klausimyną sudaro 30 teiginių apie galimus pojūčius ir emocijas, kuriuos dalyviai gali patirti sesijos metu (Lentelė 2). Kiekvienas teiginys yra vertinamas pagal Likerto skalę nuo 1 (visiškai nesutinku) iki 5 (visiškai sutinku). Šie teiginiai yra suskirstyti į dešimt atskirų domenų: Minčių nutrūkstamumas (MN) (ang. *Discontinuity of Mind*), nurodantis vykstančių minčių dinaminius pokyčius, Minčių teorija (MT) (ang. *Theory of Mind*), nurodantis mintis susijusias su kitais žmonėmis, Pats (ang. *Self*), nurodantis mintis susijusias su savimi, Planavimas, susijęs su į ateitį nukreiptomis mintimis, Mieguistumas, susijęs su mieguistumo lygiu, Komfortas, nurodantis atsipalaidavimo lygis sesijos metu, Somatinis sąmoningumas (SS), nurodantis interocepcinį savo kūno suvokimą, Sveikata, nurodantis bendra savijautą, Vizualinės mintys (Viz), nurodantys vizualinias mintis sesijos metu, Verbalinės mintys (VM), nurodantis mintis suformuotas žodžiais, Kiekvieno ARBK domeno balai buvo apskaičiuoti imant trijų teiginių vidurkį.

Lentelė 2. Dešimties domenų ARBK naudotas tyrime

Minčių nutrūkstamumas	„Galvoje sukosi daug minčių.“ „Mano mintys greitai keitėsi.“ „Man buvo sunku išlaikyti savo mintis.“
Minčių teorija	„Aš galvojau apie kitus.“ „Aš galvojau apie žmones, kurie man patinka.“ „Įsivaizdavau save kitų vietoje.“
Pats	„Aš galvojau apie savo veiksmus.“ „Aš galvojau apie savo elgesį.“ „Aš galvojau apie save.“
Planavimas	„Aš galvojau apie dalykus, kuriuos turiu padaryti.“ „Aš galvojau apie problemų sprendimą.“ „Aš galvojau apie savo ateitį.“
Mieguistumas	„Jaučiausi pavargęs.“

	„Jaučiausi mieguistas.“ „Man buvo sunku išlikti budriam.“
Komfortas	„Jaučiausi jaukiai.“ „Jaučiausi atsipalaidavęs.“ „Jaučiausi laimingas.“
Somatinis sąmoningumas	„Aš suvokiau savo kūną.“ „Aš galvojau apie savo širdies plakimą.“ „Aš galvojau apie savo kvėpavimą.“
Sveikata	„Jaučiausi liguistas.“ „Aš galvojau apie savo sveikatą.“ „Jaučiau skausmą.“
Vizualinės mintys	„Aš galvojau vaizdais.“ „Įsivaizdavau įvykius.“ „Įsivaizdavau vietas.“
Verbalinės mintys	„Aš galvojau žodžiais.“ „Kalbėjausi mintyse.“ „Įsivaizdavau, kad kalbu su savimi.“

2.4 EEG duomenų apdorojimas

EEG duomenų apdorojimas buvo atliktas MATLAB (The Mathworks, Natick, USA) programoje naudojant EEGLAB plėtinį (Delorme and Makeig, 2004) ir rankiniu būdu parašytas funkcijas. 50 Hz tinklo triukšmas buvo pašalintas naudojant *CleanLine* įskiepį (Mullen, 2012). EEG duomenys buvo pateikti Nepriklausomų komponentų analizei, naudojant *Infomax ICA* algoritmą su numatytaisiais parametrais, ir komponentai, turintys erdvines ir laikines charakteristikas horizontalių ir vertikalių akių judesių bei širdies pulso, buvo naudojamos sukurti individualius erdvinius filtrus šiems artefaktams pašalinti (Delorme et al., 2007; Jung et al., 2000). Triukšmingi kanalai buvo pašalinti rankiniu būdu ir rekonstruoti (Perrin et al., 1989). EEG duomenų skaitmenizavimo dažnis buvo sumažintas iki 1000 Hz d-PKA ir 512 Hz GFS ir EEG mikrobūsenų analizėms. Duomenys buvo susugmentuota į nepersidengiančias 2 sekundžių epochas.

2.5 Dažnių Pagrindinių komponenčių analizė

Išvalytos epochos buvo koreguotos pagal epochos bazinę liniją ir transformuota į dažnių domeną naudojant greitąją Fourier transformaciją nuo 0 iki 30 Hz 0.5 Hz žingsniu ir kiekvieno dažnio vertės buvo suvidurkintos per epochas. D-PKA buvo atlikta naudojant *EP Toolkit* pletinį (Dien, 2010) (versija 2.92). Kovariacijų matrica su neribotu komponentų išskyrimu ir

Promax tiesine transformacija (pasukimu) buvo naudota komponentų išskyrimui. Atvejų ir kintamųjų santykis buvo 229,7 (14012 atvejų: 226 dalyviai X 62 elektrodai), (61 kintamasis: 0-30 Hz 0,5 Hz žingsniu). Į tolesnę analizę buvo įtraukti komponentai, paaiškinantys daugiau kaip 3 proc. duomenų, o likusieji komponentai buvo pašalinti. Siekiant užtikrinti pakankamą signalo ir triukšmo santykį, elektrodai su trimis didžiausiomis vertėmis kiekvienam atskiram komponentui buvo suvidurkinti.

2.6 Šaltinių lokalizavimas

Standartizuota žemos rezoliucijos elektromagnetinė tomografija (sLORETA) (Pascual-Marqui et al., 1994, 2002) buvo naudota nustatyti smegenų sritis susijusias su d-PK generavimo šaltiniais ir ARBK domenais. Monrealio neurologijos instituto smegenų modelis (MNII52) (Mazziotta et al., 2001) buvo naudotas kaip realus galvos modelis, kurio erdvė buvo apribota žievės pilkojoje medžiagoje, šią padalinant į 6239 vokselius, kurių skiriamoji geba yra 5x5x5 mm. Statistinis neparametrinis smegenų žemėlapių sudarymas (ang. *Statistical nonparametric mapping* (SnMP)) su 5000 permutacijų buvo naudojamas nustatyti reikšmingiems vokselių aktyvumams (Nichols and Holmes, 2001).

2.7 Globalios Fazės Sinchronizacija

GFS analizei duomenys buvo perskaičiuoti palyginamuosius elektrodus pakeičiant į visų elektrodų vidurkį. Duomenys buvo nufiltruoti tarp 1 ir 30 Hz naudojant baigtinio impulso atsak o(angl. *Finite Impulse Response*) filtrą implementuotą į EEGLAB plėtinį (Delorme and Makeig, 2004) su numatytaisiais parametrais. Kiekviena epocha buvo transformuota į dažnių domeną naudojant greitąją Fourier trensformaciją 1 Hz žingsniu taip gaunant kompleksinę vertę kiekvienam dažniui ir kiekvienam elektrodui. Šių verčių pasiskirstymas nurodo kiek bendra fazė tarp visų elektrodų. Kompleksinės vertės buvo pateiktos dvimatei pagrindinių komponenčių analizei, ir gautos dvi tikrinės vertės kiekvienam dažniui. GFS yra šių dviejų tikrinių verčių santykis:

$$GFS(f) = \frac{|\lambda_1(f) - \lambda_2(f)|}{\lambda_1(f) + \lambda_2(f)}$$

kur λ_1 ir λ_2 yra tikrinės vertės gautos po pagrindinių komponenčių analizės duotajame dažnyje *f*. GFS vertės yra tarp 0 ir 1. Žemos vertės nurodo, kad nėra

bendros fazės tarp elektrodų. Aukštos vertės GFS vertės nurodo bendrą fazę (arba anti – fazę) tarp elektrodų ir padidejusius globalius funkcinius ryšius (Achermann et al., 2016; Koenig et al., 2001). GFS vertės buvo suvidurkintos per epochas pasirinktuose dažnių diapozonuose: delta (1 – 3 Hz), teta (4 – 7 Hz), alfa (8 – 13 Hz), beta (14 -30 Hz) (Koenig et al., 2001; Smailovic et al., 2018).

2.8 Mikrobūsenų analizė

Mikrobūsenų analizei duomenys buvo perskaičiuoti palyginamuosius elektrodus pakeičiant į visų elektrodų vidurkį ir nufiltruoti tarp 1 ir 40 Hz naudojant *Butterworth* filtrą. Mikrobūsenų analizė buvo atlikta naudojant EEGLAB įskiepį (http://www.thomaskoenig.ch/index.php/software/microstates-in-eeglab/) (versija 1.2) ir rankiniu būdu parašytas funkcijas. Duomenys buvo analizuoti dvejuose žingsniuose: individualiame ir grupės lygiuose. Pirmiausia individualiame lygyje, buvo suskaičiuota Globalaus Lauko Galia:

$$GLG = \sqrt{\frac{\sum_{i=1}^{n}(v_i - \bar{v})^2}{n}}$$

kur v_i yra užregistruota potencialas i-ajme elektrode duotajame laiko momente, $\bar{v}$ yra vidutinis visų elektrodų potencialas užregistruotas duotajame laiko momente, n yra elektrodų skaičius. Užtikrinti pakankamą signalo ir triukšmo santykį tik topografijos ties GLG pikais buvo išskirtos (Koenig and Brandeis, 2016; Skrandies, 1990; Zanesco, 2020) ir pateiktos į modifikuotą *k-means* klasterizavimo algoritmą (Pascual-Marqui et al., 1995). Topografijos buvo normalizuotos vienetui, taip užtikrinant, kad tik elektrinis topografijos pasiskirstymas būtų vertinamas. Siekiant nustatyti optimalų klasterių skaičių, klasterizavimas buvo pakartotas nuo 2 iki 10 klasterių. Antrajame žingsnyje, individualios visų tiriamųjų topografijos buvo suvidurkintos naudojant permutacinį algoritmą (Koenig et al., 1999). Nustatyti optimalus klasterių skaičių grupės lygyje buvo naudotas Siluetų metodas (Rousseeuw, 1987). Siluetai vertina kiek kiekvienas individualus duomenų taškas (individuali topografija) yra panašus į kitus duomenų taškus tame pačiame klasteryje, lyginant su taškai esančiais kituose klasteriuose (Bréchet et al., 2019; Dinov and Leech, 2017). Siluetų vertės yra apskaičiuojamos pagal formulę:

$$S = \frac{(b_i - a_i)}{\max(a_i * b_i)}$$

ur a_i yra vidutinis atstumas tarp i-tojo duomenų taško ir kitų duomenų taškų tame pačiame klasteryje, ir b_i yra vidutinis atstumas tarp i-tojo duomenų taško ir duomenų taškų esančių kituose klasteriuose. Siluetų vertės svyruoja nuo -1 iki 1. Aukšta Siluetų vertė nurodo, kad duomenų taškas gerai atitinka kitus duomenų taškus tame pačiame klasteryje ir prastai atitinka taškus esančius kituose klasteriuose. Optimalus klasterių skaičius buvo nustatytas suvidurkinant Siluetų vertes per klasterių skaičių. Atstumo nustatymui buvo naudotas Globalus Topografijų Skirtumas (GTS) (Brunet et al., 2011). GTS yra indeksas nurodantis skirtumus tarp dviejų topografijų ir svyruoja nuo 0 iki 2, kur vertės arti 0 nurodo topografinį panašumą.

Siekiant gauti laikinius mikrobūsenų parametrus, erdvinė koreliacija buvo suskaičiuota tarp kiekvienos grupės lygio topografijos ir individualaus tiriamojo topografijų kiekviename EEG įrašo laiko taške. Tada kiekvienas laiko taškas (ne tik GLG pikas) buvo priskirtas mikrobūsenai, su kuria turi didžiausią erdvinę koreliaciją. Erdvinė koreliacija yra Pirsono koreliacijos koeficiento atitikmuo tarp dviejų topografijų (Khanna et al., 2014; Murray et al., 2008).

Kiekvienam tiriamajam buvo apskaičiuoti trys laikiniai parametrai kiekvienai mikrobūsenai: vidutinė trukmė (matuojama milisekundėmis (ms)), kuri nurodo mikrobūsenos generavimo šaltinių sinchroninį aktyvumą (Khanna et al., 2015); pasirodymo dažnis (matuojamas hercais (Hz)), nurodantis tendenciją generavimo šaltiniams būti aktyvuotiems (Khanna et al., 2015); indėlis (matuojamas procentais), nurodantis reliatyvią laiko dalį, kurią mikrobūsena buvo aktyvi (Khanna et al., 2015; Murray et al., 2008). Papildomai buvo apskaičiuota GLG (matuojama mikrovoltais (μV)) (Murray et al., 2008; Skrandies, 1990).

2.9 Statistinė analizė

Statistinė analizė buvo atlikta naudojant JASP statistinę programą (versija 0.14.1) (JASP Team, 2020; Love et al., 2019), Statistikos ir Mašininio mokymosi plėtinį implementuotą į MATLAB ir rankiniu būdu parašytas funkcijas. Apskaičiuota Bajeso Pirsono koreliacijos koeficientai ir Bajeso faktoriai (BF) tarp ARBK domenų, d-PK įverčių, GFS verčių ir mikrobūsenų laikinių parametrų. Bajesinėje statistikoje tikimybė yra apibrėžiama įvykio pasireiškimo patikimumo laipsnis ir vietoje p reikšmes yra raportuojama tikimybės santykis – Bajeso faktorius. BF yra santykis vertinantis kitimą tarp alternatyvios ir nulinės hipotezės (Kelter, 2020), kuris nereikalauja

daugybinių testų korekcijos (Dienes, 2016, 2014, 2011). BF gali nurodyti tikimybę tiek alternatyvios, tiek nulinės hipotezės atžvilgiu. BF įrodymų kategorijos skirstomos į vienuolika kategorijų: Lemiami H1 įrodymai (BF10> 100); Labai stiprūs H1 įrodymai (100 > BF10> 30); Stiprūs H1 įrodymai (30 > BF10> 10); Esminiai H1 įrodymai (10 > BF10> 3); Nepatvirtinti H1 įrodymai (3 > BF10> 1); Nėra įrodymų (BF10 = 1); Nepatvirtinti H0 įrodymai (1 > BF10> 1/3); Reikšmingi įrodymai H0 (1/3 > BF10> 1/10); Stiprūs įrodymai H0 (1/10 > BF10> 1/30); Labai stiprūs įrodymai H0 (1/30 > BF10> 1/100); Lemiami įrodymai H0 (BF10< 1/100) (George Assaf and Tsionas, 2018; Wetzels and Wagenmakers, 2012).

2.10 Nuokrypio taškų aptikimas

Siekiant nustatyti galimus nuokrypio taškus, buvo naudota Pagrindinių Koordinačių Analizė (PKoA). PKoA yra dimensijų redukavimo metodas, leidžiantis vizualiai pavaizduoti panašumus tarp duomenų dvimatėje koordinačių plokštumoje (Habermann et al., 2018; Koenig et al., 2011). Po PKoA duomenys buvo atvaizduoti dvimatėje koordinačių plokštumoje ir duomenų taškų *x* ir *y* buvo panaudotos apskaičiuoti Euklidinį atstumą tarp visų duomenų taškų. Tada, MATLAB funkcija *isoutlier* su numatytaisiais parametrais buvo panaudota rasti galimus nuokrypio taškus. PKoA buvo panaudota ARBK, d-PK, GFS verčių ir mikrobūsenų parametrams atskirai.

3. REZULTATAI

Remiantis PKoA nuokrypio taškų nebuvo nustatyta nei tarp ARBK, nei, d-PK nei GFS įverčių, nei tarp mikrobūsenų parametrų.

3.1 Amsterdamo ramybės būsenos klausimynas

ARBK domenų įverčių vidurkiai ir standartiniai nuokrypiai buvo: MN 3.229 (±0.971), MT 2.825 (±0.823), Pats 3.156 (±0.877), Planavimas 2.926 (±1.047), Mieguistumas 2.681 (±0.923), Komfortas 3.700, (±0.829), SS 2.953 (±0.996), Sveikata 1.594 (±0.601), Viz 3.764 (±1.069), VM 2.883 (±1.103). Vidurkiai ir standartiniai nuokrypiai yra pavaizduoti Pav. 2A. Bajeso Pirsono koreliacijos koeficientai tarp ARBK domenų pavaizduoti Pav. 2B. Iš viso rasta 16 reikšmingų teigiamų koreliacijų tarp ARBK domenų, ir tik viena neigiama tarp Sveikatos ir Komforto domenų ($r = -0.203$, $BF_{10} = 8.772$). MN koraliavo su beveik visais domenais išskyrus Komfortą ir SS. SS nekoreliavo nei su vienu ARBK domenu.

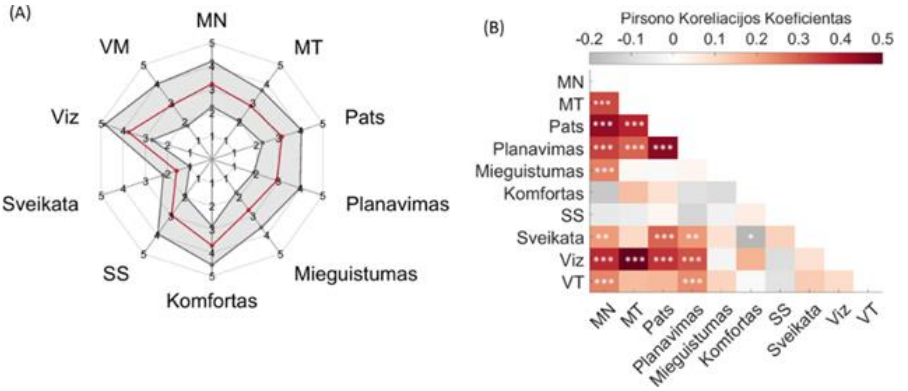

Pav. 2. ARBK domenų vidurkiai (raudona linija) ir standartiniai nuokrypiai (pilkas plotas (A). Bajeso Pirsono koreliacijos koeficientai tarp ARBK domenų. **** BF10 > 100, *** 100 > BF10 > 30, ** 30 > BF10 > 10, and * 10 > BF10 > 3.

Įvertinti galimą amžiaus ir lyties poveikį ARBK rezultatams, buvo panaudota daugiamatė ANOVA. Daugiamatė ANOVA parodė reikšmingą amžiaus poveikį ARBK rezultatams [F(10, 185) = 2,502, p = 0,008], bet ne lyties [F(10, 185) = 1,348, p = 0,208]. Tolimesnė koreliacinė analizė parodė, kad tik koreliacijos tarp amžiaus ir MT bei Sveikatos domenų buvo reikšmingos (MT: r = -0,193, BF_{10} = 3,520, Sveikata: r = -0,198, BF_{10} = 4,258).

Šeši faktoriai paaiškinantys daugiau nei tris procentus duomenų buvo naudoti tolimesnėje analizėje. Kartu šie šeši faktoriai paaiškino 82.58% duomenų variabilumo. Faktoriai buvo sunumeruoti pagal tai, kiek duomenų jie paaiškina ir pažymėti pagal EEG dažnių diapazonų pirmąją raidę. Delta dažnių diapazone buvo vienas faktorius, kurio maksimali vertė buvo ties 0,5 Hz ir kuris turėjo frontalinį aktyvymą (D1); vienas - teta dažnių diapazone, kurio maksimumas buvo ties 5,5 Hz ir kuris buvo turėjo front-centrinį aktyvumą (T1); trys alfa dažnių diapazone, kurių maksimumas buvo ties 9 Hz (A1), 10,5 Hz (A2) ir 11,5 Hz (A3) ir kurie turėjo pakaušinies sritys aktyvumą, ir vienas beta dažnių diapazono faktorius,, kurio maksimali vertė buvo ties 17 Hz ir kuris turėjo pakaušiies srities aktyvumą. (B1). d-PKA rezultatai

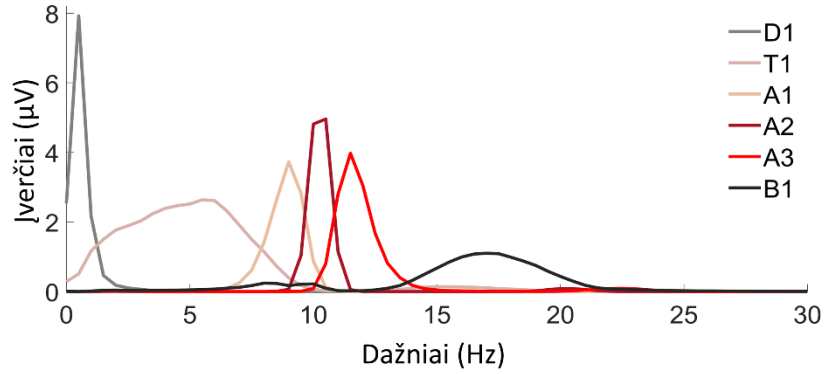

Komp.	D1	T1	A1	A2	A3	B1
Fakt.	3	5	1	2	4	6
Pikas Hz	0.5	5.5	9	10.5	11.5	17
Var. %	15.15	11.34	19.82	19.56	13.10	3.61

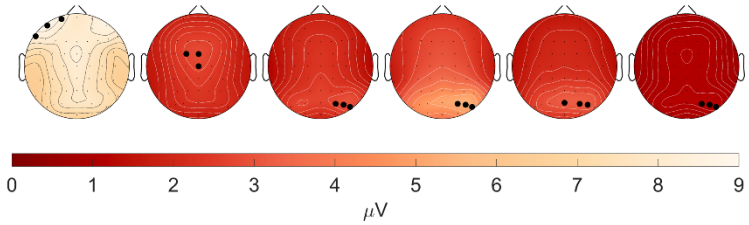

Pav. 3. D-PKA rezultatai šešiems faktoriams. Viršutinė dalis: Vidutinis (N=226) kiekvienos komponentės įvertis. Vidurinė dalis: Komponentės pavadinimas (Komp.), komponentės numeris (Fakt.) dažnis kuriame komponentė pasiekia maksimumą ir paaiškintas variabilumas. Apatinė dalis: kiekvienos komponentės topografija. Trys elektrodai su didžiausiomis vertėmis, kurių reikšmės buvo suvidurkintos pažymėtos juodais apskritimais.

pavaizduoti Pav. 3. Viršutinėje dalyje pateikiami kiekvieno faktoriaus įverčiai, nurodantys, kiek kiekvienas kintamasis prisidėjo prie konkretaus komponento; vidurinėje dalyje pateikiami faktorių numeriai, maksimalios vertės ir paaiškinta variabilumo procentinė dalis. Apatinėje dalyje pateikiamos kiekvieno komponento topografijos. Trys elektrodai su didžiausiomis reikšmėmis, kurios buvo naudotos kiekvieno komponento vidurkiams apskaičiuoti, pažymėti juodais apskritimais.

3.3 Ryšys tarp d-PK įverčių ir ARBK domenų

Iš 60 galimų koreliacijų (10 ARBK domenų, 6 faktoriai) tik dvi interakcijos buvo statistiškai reikšmingos ($BF_{10} > 3$). T1 faktorius teigiamai koreliavo su ARBK domeno Mieguistumas įverčiais (r = 0.200, BF10 = 7.676). A1 faktorius teigiamai koreliavo su ARBK domeno Komfortas įverčiais (r = 0.198, BF_{10} = 7.115) (Pav. 4A). Bajeso Pirsono koreliacijos koeficientai ir BF tarp d-PK įverčių ir ARBK pateikti lentelėje.

Lentelė 3. Bajeso Pirsono koreliacijos koeficientai tarp 6 komponentų ir ARBK domenų. Reikšmingos koreliacijos ($BF_{10} > 3$) paryškintos pilkame fone

		A1	**A2**	**D1**	**A3**	**T1**	**B1**
MN	r	-0.081	-0.47	-0.008	0.009	0.059	-0.053
	$BF1_0$	0.173	0.107	0.084	0.084	0.122	0.114
MT	r	0.044	0.045	0.071	0.007	0.086	0.046
	$BF1_0$	0.103	0.105	0.145	0.084	0.191	0.105
Pats	r	-0.003	-0.062	-0.104	0.010	-0.018	0.062
	$BF1_0$	0.083	0.127	0.279	0.084	0.086	0.128
Plan.	r	-0.018	-0.018	-0.017	-0.062	-0.048	-0.105
	$BF1_0$	0.086	0.086	0.086	0.128	0.107	0.288
Mieg.	r	-0.040	-0.004	0.031	-0.052	**0.200**	-0.034
	$BF1_0$	0.099	0.083	0.093	0.112	**7.676**	0.095
Komf.	r	**0.198**	0.138	0.078	-0.044	0.131	0.082
	$BF1_0$	**7.115**	0.713	0.164	0.104	0.573	0.176
SS	r	0.027	-0.012	0.025	0.067	-0.089	-0.009
	$BF1_0$	0.090	0.085	0.089	0.137	0.201	0.084
Sveik.	r	-0.008	-0.125	-0.086	-0.069	-0.025	-0.076
	$BF1_0$	0.084	0.475	0.189	0.142	0.089	0.158
Viz	r	0.103	0.032	-0.011	-0.116	0.128	0.100
	$BF1_0$	0.272	0.093	0.084	0.371	0.521	0.253
VM	r	-0.066	-0.070	-0.090	-0.044	0.020	-0.058
	$BF1_0$	0.135	0.145	0.206	0.103	0.087	0.121

3.4 sLORETA rezultatai

Tik dviejų d-PK įverčiai buvo reikšmingai susiję su dviem skitingais ARBK domenais, tad sLORETA analizė buvo atlikta tik tarp A1 ir Komforto įverčių, bei tarp T1 ir Mieguistumo įverčių.

sLORETA analizė parodė statistiškai reikšmingą koreliaciją tarp T1 ir mieguistumo ($r = 0.247$, $p < 0.05$), kur pagrindinis aktyvumas buvo nustatytas limbinėje srityje, priekinėje juostinėje žievėje ir Broadmano zonos 24 ir 23. Koreliacija tarp A1 ir Komforto nebuvo statistiškai reikšminga ($r = 0.207$, $p > 0.05$).

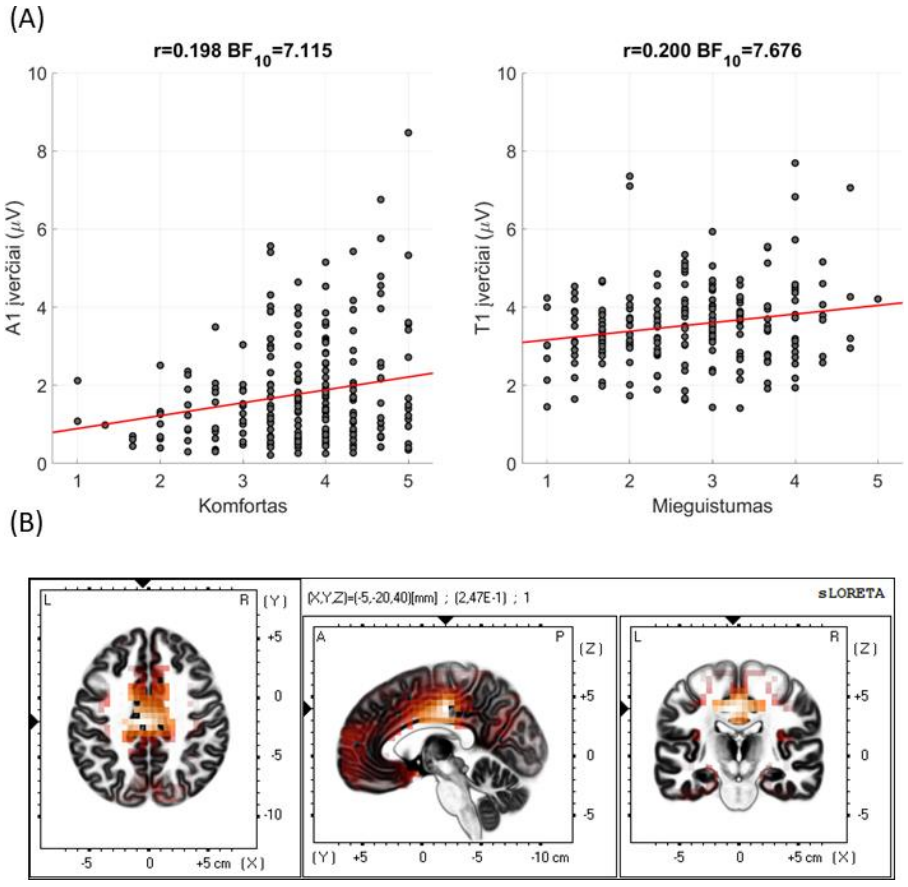

Pav. 4. Sklaidos grafikai, kuriose vaizduotas ryšy tarp d-PK įverčių ir ARBK domenų (N=226) (A). sLORETA rezultatai tarp T1 įverčių ir ARBK Mieguistumo domeno (B).

3.5 GFS įverčiai

GFS vidutinės vertės dažnių diapazonams buvo: delta: 0.517 (SN. ±0.039), teta: 0.541 (SN. ±0.026), alfa: 0.595 (SN. ±0.032), beta 0.522 (SN. ±0.025) ir sutampa su rezultatais, raportuotais literatūroje (Koenig et al., 2001; Park et al., 2008; Smailovic et al., 2018). GFS vertės ir pasiskirstymas, bei GFS vidutinė reikšmė per dažnius pavaizduoti Pav. 5.

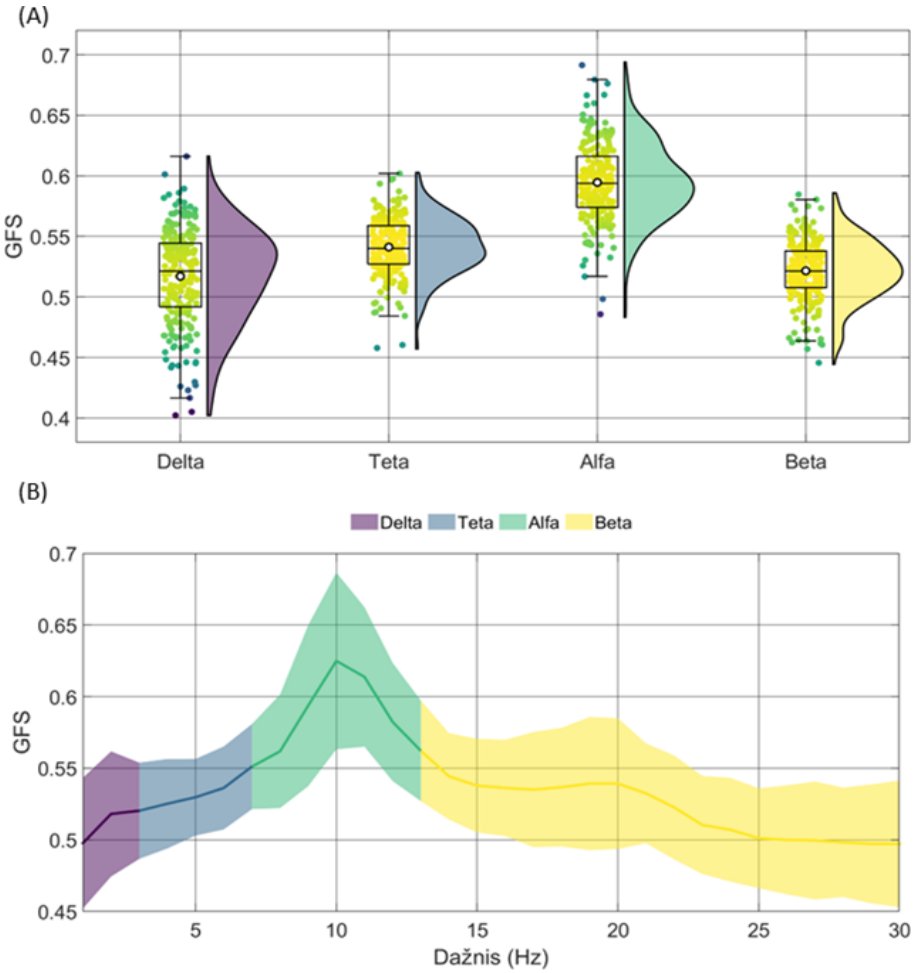

Pav. 5. GFS verčių pasiskirstymas kiekviename diapazone (N=226) (A). GFS vidutinė vertė kiekviename dažnyje ir standartinis nuokrypis (B)

3.6 Ryšys tarp GFS verčių ir ARBK domenų

Iš keturiasdešimties galimų koreliacijų (dešimt ARBK domenai, keturi dažnių diapazonai) tik dvi sąveikos buvo statistiškai reikšmingos (BF10 > 3). GFS

alfa diapazono vertės teigiamai koreliavo su ARBK Komforto domenu (r = 0,208, BF_{10} = 11,646). Beta diapazono GFS vertės teigiamai koreliavo su ARBK Komforto domenu (r = 0,197, BF10 = 6,664). Pilna koreliacijų lentelė pateikta lentelėje 4.

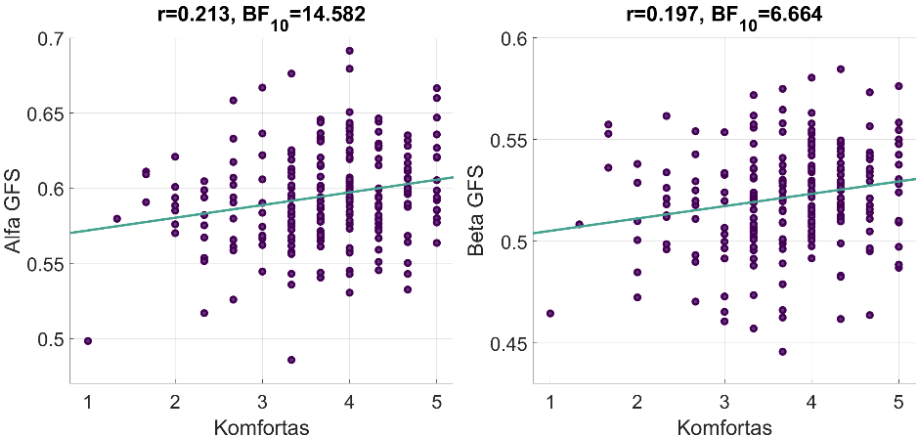

Pav. 6. Sklaidos grafikai tarp Alfa ir Beta GFS verčių ir ARBK Komforto domeno (N=226).

Lentelė 4. . Bajeso Pirsono koreliacijos koeficientai tarp GFS verčių ir ARBK domenų. Reikšmingos koreliacijos (BF_{10} > 3) paryškintos pilkame fone.

		Delta	Teta	Alfa	Beta
MN	r	0.010	-0.102	-0.150	0.028
	$BF1_0$	0.084	0.270	0.288	0.091
MT	r	-0.090	-0.082	-0.019	0.071
	$BF1_0$	0.206	0.175	0.086	0.145
Pats	r	-0.004	0.017	0.107	0.112
	$BF1_0$	0.083	0.086	0.304	0.338
Plan.	r	-0.112	-0.057	0.031	0.059
	$BF1_0$	0.341	0.120	0.092	0.122
Mieg.	r	0.062	-0.036	-0.072	0.041
	$BF1_0$	0.128	0.096	0.149	0.100
Komf.	r	0.091	0.155	**0.208**	**0.199**
	$BF1_0$	0.209	1.243	**11.646**	**7.842**
SS	r	0.074	0.062	-0.015	0.011
	$BF1_0$	0.152	0.127	0.085	0.084
Sveik.	r	-0.061	0.034	-0.025	-0.021

		Delta	Teta	Alfa	Beta
	$BF1_0$	0.126	0.95	0.089	0.087
Viz	r	0.008	0.040	0.043	0.022
	$BF1_0$	0.084	0.099	0.102	0.088
VM	r	-0.067	-0.099	0.022	0.073
	$BF1_0$	0.137	0.248	0.087	0.150

3.7 Laikiniai EEG mikrobūsenų parametrai

Remenitis Siluetų koeficientu (vidutinė Siluetų vertė per klasterių skaičių), optimalus klasterių skaičius buvo 7. Keturios mikrobūsenų topografijos atitiko su keturiomis dažniausiai literatūroje raportuojamomis mikrobūsenų topografijomis ir buvo atitinkamai pavadintos A, B, C ir D EEG mikrobūsenomis (Koenig et al., 2002).

Iš trijų likusių topografijų, viena sutapo su mikrobūsena E pranešta literatūroje (Bréchet et al., 2019; Custo et al., 2017; Zanesco et al., 2021b) ir atitinkamai buvo pažymėta kaip mikrobūsena E. Viena topografija sutapo su mikrobūsena F, raportuota tyrimuose (Bréchet et al., 2019; Custo et al., 2017; D'croz-Baron et al., 2021), mikrobūsena E (Damborská et al., 2019a, 2019b; Murphy et al., 2020), ir mikrobūsena C′, raportuota (Jabès et al., 2021), tad buvo pavadinta mikrobūsena F. Paskutinė topografija sutapo su mikrobūsena G, raportuota tyrime (Custo et al., 2017) ir mikrobūsena F, raportuota (Damborská et al., 2019b; Takarae et al., 2022; Zanesco et al., 2021b), tad buvo pavadinti mikrobūsena G (Pav. 7). Šios septynios topografijos paaiškino 83.3% duomenų. Laikinių parametrų vidurkiai ir standartiniai nuokrypiai pateikti lentelėje 5. Parametrai atitinka raportuotus parametrus literatūroje (Khanna et al., 2015; Michel and Koenig, 2018; Zanesco et al., 2020)

Pav. 7. 7 mikrobūsenų topografijos (N=197).

Lentelė 5. Laikiniai mikrobūsenų parametrų vidurkiai ir standartiniai nuokrypiai.

	Trukmė (ms)	Dažnis (Hz)	Indėlis (%)
MS A	43.36 (±8.26)	3.60 (±0.95)	15.13 (±4.00)
MS B	45.34 (±9.25)	3.80 (±0.89)	16.93 (±4.20)
MS C	52.51 (±14.18)	4.50 (±0.83)	22.91 (±6.50)
MS D	40.91 (±7.16)	3.44 (±1.00)	13.82 (±3.90)
MS E	36.72 (±6.31)	2.62 (±0.73)	9.43 (±2.40)
MS F	39.59 (±7.34)	3.22 (±0.99)	12.56 (±4.00)
MS G	36.06 (±5.81)	2.65 (±0.81)	9.31 (±2.50)

3.8 Ryšys tarp mikrobūsenų laikinių parametrų ir ARBK domenų

Bajeso Pirsono koreliacija parodė neigiamą ryšį tarp mikrobūsenos F indėlio ir SS ($r = -0.210$, $BF10 = 6.871$), reikšmingą ryšį tarp domeno Pats ir mikrobūsenos D trukmės ($r = -0.203$, $BF10 = 5.224$) ir mikrobūsenos B dažnio ($r = 0.192$, $BF10 = 3.305$). Bajeso Pirsono koreliacija parodė jog ARBK domenas Komfortas neigiamai koreliavo su mikrobūsenos C dažniu ($r = -0.212$, $BF10 = 7.638$), teigiamai koreliavo su mikrobūsenos E trukme ($r = 0.220$, $BF10 = 10.949$) ir mikrobūsenos G trukme ($r = 0.203$, $BF10 = 5.284$). Bajeso Pirsono koreliacijos koeficientai tarp mikrobūsenų parametrų ir ARBK domenų pateikti lentelėje . Reikšmingos koreliacijos pateiktos Pav. 8). Tarp mikrobūsenos C ir SS domenų statistiškai reikšmingos koreliacijos nebuvo ($r = -0.007$, $BF_{10} = 0.090$). Papildomai buvo atlikta erdvinės koreliacijos (EK) analizė tarp mikrobūsenų C, kai klasterių skaičius yra lygus 4, ir mikrobūsenų topografijų C ir F, kai klasterių skaičius lygus 7. Rezultatai parodė kad visos topografijos yra erdviškai panašios ($EK > 0.7$). Taip pat, erdvinė koreliacija tarp mikrobūsenos C, kai klasterių skaičius yra lygus 4 ir mikrobūsenos F, kai klasterių skaičius lygus7 buvo 0.966, kas patvirtino hipotezė, jog erdviškai panašios topografijos gali būti sujungtos į vieną topografiją, jei pasirenkamas neoptimalus klasterių skaičius (Pav. 9). Bajeso Pirsono koreliacijos koeficientas tarp ARBK SS domeno ir mikrobūsenos C indelio, kai klasterių

skaičius yra 4, atkartojo neigiamą koreliaciją raportuotą literatūroje (Pipinis et al., 2017).

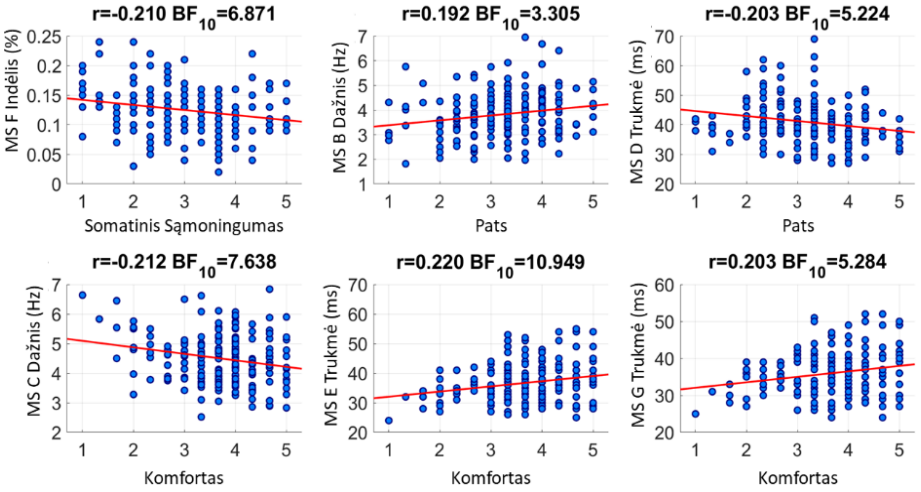

Pav. 8. Sklaidos grafikai tarp statistiškai reikšmingų mikrobūsenų parametrų ir ARBK domenų (N=197).

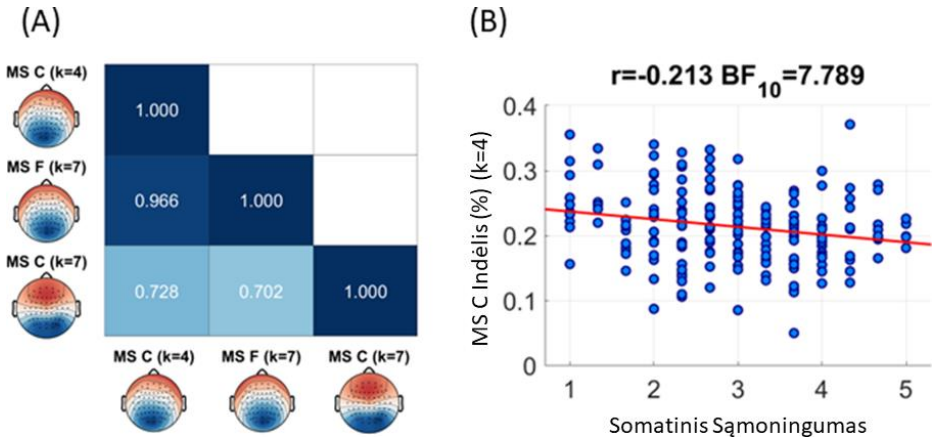

Pav. 9. Erdvinė koreliacija tarp mikrobūsenos C (k=4), ir mikrobūsenų F ir C (k=7) (A). Sklaidos grafikas tarp mikrobūsenos C indėlio (kai k=4), ir ARBK SS domeno (N=197).

Lentelė 6. Bajeso Pirsono koreliacijos koeficientai tarp EEG mikrobūsenų parametrų ir ARBK domenų. Statistiškai reikšmingos koreliacijos paryškintos pilkame fone.

		MN	MT	Pats	Plan.	Mieg.	Komfortas	SS	Sveik.	Viz.	VT
Mikrobūsena A	**Trukmė**	r=-0.020 BF_{10}=0.093	r=0.029 BF_{10}=0.097	r=-0.119 BF_{10}=0.352	r=-0.008 BF_{10}=0.090	r=-0.005 BF_{10}=0.089	r=0.134 BF_{10}=0.512	r=0.034 BF_{10}=0.100	r=-0.018 BF_{10}=0.092	r=0.023 BF_{10}=0.099	r=-0.037 BF_{10}=0.102
	Dažnis	r=0.012 BF_{10}=0.090	r=0.051 BF_{10}=0.115	r=0.096 BF_{10}=0.220	r=-0.038 BF_{10}=0.103	r=0.111 BF_{10}=0.294	r=-0.082 BF_{10}=0.172	r=-0.019 BF_{10}=0.092	r=0.028 BF_{10}=0.096	r=0.062 BF_{10}=0.129	r=0.035 BF_{10}=0.100
	Indėlis	r=-0.009 BF_{10}=0.090	r=0.056 BF_{10}=0.121	r=0.010 BF_{10}=0.090	r=-0.055 BF_{10}=0.119	r=0.097 BF_{10}=0.223	r=0.002 BF_{10}=0.089	r=-0.005 BF_{10}=0.089	r=0.050 BF_{10}=0.114	r=0.056 BF_{10}=0.120	r=0.030 BF_{10}=0.097
	GLG	r=-0.016 BF_{10}=0.091	r=0.040 BF_{10}=0.104	r=-0.066 BF_{10}=0.137	r=-0.039 BF_{10}=0.103	r=-0.015 BF_{10}=0.091	r=0.115 BF_{10}=0.324	r=0.001 BF_{10}=0.089	r=-0.027 BF_{10}=0.096	r=0.037 BF_{10}=0.102	r=-0.060 BF_{10}=0.127
Mikrobūsena B	**Trukmė**	r=-0.028 BF_{10}=0.096	r=0.028 BF_{10}=0.096	r=-0.054 BF_{10}=0.119	r=0.052 BF_{10}=0.116	r=-0.101 BF_{10}=0.242	r=0.182 BF_{10}=2.339	r=-0.004 BF_{10}=0.089	r=-0.063 BF_{10}=0.131	r=0.012 BF_{10}=0.090	r=-0.016 BF_{10}=0.091
	Dažnis	r=0.068 BF_{10}=0.139	r=-0.017 BF_{10}=0.092	**r=0.192** **BF_{10}=3.305**	r=0.083 BF_{10}=0.173	r=-0.038 BF_{10}=0.103	r=-0.117 BF_{10}=0.337	r=0.024 BF_{10}=0.094	r=0.044 BF_{10}=0.107	r=-0.003 BF_{10}=0.089	r=0.062 BF_{10}=0.130
	Indėlis	r=0.038 BF_{10}=0.103	r=0.008 BF_{10}=0.090	r=0.130 BF_{10}=0.464	r=0.111 BF_{10}=0.295	r=-0.121 BF_{10}=0.372	r=0.048 BF_{10}=0.111	r=-0.001 BF_{10}=0.089	r=0.004 BF_{10}=0.089	r=0.006 BF_{10}=0.090	r=0.058 BF_{10}=0.123
	GLG	r=-0.019 BF_{10}=0.092	r=0.040 BF_{10}=0.104	r=-0.058 BF_{10}=0.124	r=-0.019 BF_{10}=0.092	r=-0.041 BF_{10}=0.105	r=0.128 BF_{10}=0.442	r=0.008 BF_{10}=0.090	r=-0.034 BF_{10}=0.099	r=0.039 BF_{10}=0.104	r=-0.076 BF_{10}=0.155
Mikrobūsena C	**Trukmė**	r=-0.070 BF_{10}=0.141	r=-0.028 BF_{10}=0.096	r=-0.124 BF_{10}=0.398	r=-0.063 BF_{10}=0.131	r=-0.003 BF_{10}=0.089	r=0.106 BF_{10}=0.266	r=0.008 BF_{10}=0.090	r=-0.050 BF_{10}=0.113	r=-0.045 BF_{10}=0.109	r=-0.067 BF_{10}=0.138
	Dažnis	r=0.004 BF_{10}=0.089	r=-0.028 BF_{10}=0.096	r=0.093 BF_{10}=0.205	r=-0.042 BF_{10}=0.106	r=0.074 BF_{10}=0.151	**r=-0.212** **BF_{10}=7.638**	r=-0.021 BF_{10}=0.093	r=0.034 BF_{10}=0.100	r=-0.023 BF_{10}=0.094	r=-0.006 BF_{10}=0.089
	Indėlis	r=-0.056 BF_{10}=0.120	r=-0.046 BF_{10}=0.109	r=-0.059 BF_{10}=0.125	r=-0.100 BF_{10}=0.237	r=0.027 BF_{10}=0.096	r=-0.037 BF_{10}=0.102	r=-0.007 BF_{10}=0.090	r=-0.011 BF_{10}=0.090	r=-0.047 BF_{10}=0.110	r=--0.063 BF_{10}=0.130
	GLG	r=-0.023 BF_{10}=0.094	r=0.035 BF_{10}=0.101	r=-0.070 BF_{10}=0.144	r=-0.038 BF_{10}=0.103	r=-0.030 BF_{10}=0.097	r=0.112 BF_{10}=0.302	r=0.009 BF_{10}=0.090	r=-0.032 BF_{10}=0.099	r=-0.033 BF_{10}=0.99	r=-0.081 BF_{10}=0.169
Mikrobūsena D	**Trukmė**	r=0.069 BF_{10}=0.141	r=-0.034 BF_{10}=0.100	**r=-0.203** **BF_{10}=5.224**	r=-0.037 BF_{10}=0.102	r=-0.101 BF_{10}=0.239	r=0.177 BF_{10}=1.939	r=0.103 BF_{10}=0.247	r=-0.067 BF_{10}=0.138	r=-0.041 BF_{10}=0.105	r=-0.048 BF_{10}=0.111

	Dažnis	r=-0.009 BF_{10}=0.090	r=-0.054 BF_{10}=0.119	r=0.008 BF_{10}=0.090	r=-0.088 BF_{10}=0.189	r=0.094 BF_{10}=0.210	r=-0.128 BF_{10}=0.438	r=0.135 BF_{10}=0.531	r=0.054 BF_{10}=0.118	r=0.024 BF_{10}=0.094	r=0.037 BF_{10}=0.102
	Indėlis	r=-0.057 BF_{10}=0.122	r=-0.078 BF_{10}=0.160	r=-0.115 BF_{10}=0.322	r=-0.100 BF_{10}=0.234	r=0.024 BF_{10}=0.094	r=-0.031 BF_{10}=0.098	r=0.158 BF_{10}=1.034	r=0.026 BF_{10}=0.095	r=-0.053 BF_{10}=0.117	r=0.020 BF_{10}=0.093
	GLG	r=-0.015 BF_{10}=0.091	r=0.026 BF_{10}=0.095	r=-0.093 BF_{10}=0.206	r=-0.043 BF_{10}=0.107	r=-0.024 BF_{10}=0.094	r=0.121 BF_{10}=0.371	r=0.039 BF_{10}=0.103	r=-0.041 BF_{10}=0.105	r=0.033 BF_{10}=0.099	r=-0.076 BF_{10}=0.155
Mikrobūsena E	**Trukmė**	r=-0.040 BF_{10}=0.104	r=0.016 BF_{10}=0.091	r=-0.116 BF_{10}=0.328	r=0.043 BF_{10}=0.107	r=-0.108 BF_{10}=0.279	**r=0.220 BF_{10}=10.95**	r=0.056 BF_{10}=0.121	r=-0.083 BF_{10}=0.172	r=0.011 BF_{10}=0.090	r=-0.045 BF_{10}=0.108
	Dažnis	r=0.025 BF_{10}=0.095	r=-0.015 BF_{10}=0.091	r=0.116 BF_{10}=0.329	r= 0.015 BF_{10}=0.091	r=-0.110 BF_{10}=0.090	r=-0.081 BF_{10}=0.167	r=0.034 BF_{10}=0.099	r=0.030 BF_{10}=0.097	r=0.026 BF_{10}=0.095	r=0.008 BF_{10}=0.090
	Indėlis	r=0.015 BF_{10}=0.091	r=-0.030 BF_{10}=0.097	r=0.030 BF_{10}=0.097	r=0.037 BF_{10}=0.102	r=-0.110 BF_{10}=0.289	r=0.052 BF_{10}=0.116	r=0.067 BF_{10}=0.137	r=-0.027 BF_{10}=0.096	r=0.020 BF_{10}=0.093	r= 0.0007683 BF_{10}=0.089
	GLG	r=-0.015 BF_{10}=0.091	r=0.037 BF_{10}=0.102	r=-0.066 BF_{10}=0.137	r=-0.016 BF_{10}=0.092	r=-0.034 BF_{10}=0.100	r=0.135 BF_{10}=0.530	r=0.021 BF_{10}=0.093	r=-0.040 BF_{10}=0.104	r=0.040 BF_{10}=0.104	r=-0.077 BF_{10}=0.158
Mikrobūsena F	**Trukmė**	r=-0.038 BF_{10}=0.103	r=0.014 BF_{10}=0.091	r=-0.134 BF_{10}=0.507	r=0.088 BF_{10}=0.188	r=-0.030 BF_{10}=0.097	r=0.121 BF_{10}=0.374	r=-0.101 BF_{10}=0.241	r=-0.093 BF_{10}=0.205	r=-0.009 BF_{10}=0.090	r=-0.022 BF_{10}=0.093
	Dažnis	r=0.051 BF_{10}=0.115	r=0.029 BF_{10}=0.097	r=0.071 BF_{10}=0.145	r=0.119 BF_{10}=0.352	r=0.082 BF_{10}=0.172	r=-0.111 BF_{10}=0.294	r=-0.140 BF_{10}=0.607	r=-0.026 BF_{10}=0.095	r=0.026 BF_{10}=0.092	r=-0.018 BF_{10}=0.092
	Indėlis	r=0.035 BF_{10}=0.100	r=0.041 BF_{10}=0.105	r=-0.016 BF_{10}=0.092	r=0.146 BF_{10}=0.710	r=0.043 BF_{10}=0.107	r=-0.036 BF_{10}=0.101	**r=-0.210 BF_{10}=6.871**	r=-0.064 BF_{10}=0.132	r=0.019 BF_{10}=0.092	r=-0.031 BF_{10}=0.098
	GLG	r=-0.006 BF_{10}=0.089	r=0.051 BF_{10}=0.115	r=-0.064 BF_{10}=0.133	r=0.005 BF_{10}=0.089	r=-0.011 BF_{10}=0.090	r=0.103 BF_{10}=0.252	r=-0.034 BF_{10}=0.100	r=-0.044 BF_{10}=0.108	r=0.045 BF_{10}=0.108	r=-0.081 BF_{10}=0.169
Mikrobūsena G	**Trukmė**	r=-0.024 BF_{10}=0.094	r=0.018 BF_{10}=0.092	r=-0.114 BF_{10}=0.315	r=0.025 BF_{10}=0.095	r=-0.090 BF_{10}=0.195	**r=0.203 BF_{10}=5.284**	r=0.030 BF_{10}=0.097	r=-0.039 BF_{10}=0.104	r<0.001 BF_{10}=0.089	r=-0.029 BF_{10}=0.097
	Dažnis	r=0.075 BF_{10}=0.153	r=0.023 BF_{10}=0.094	r=0.139 BF_{10}=0.580	r=0.011 BF_{10}=0.090	r=0.046 BF_{10}=0.109	r=-0.068 BF_{10}=0.140	r=0.055 BF_{10}=0.120	r=0.44 BF_{10}=0.108	r=0.024 BF_{10}=0.094	r=0.060 BF_{10}=0.126
	Indėlis	r=0.083 BF_{10}=0.174	r=0.042 BF_{10}=0.106	r=0.096 BF_{10}=0.217	r=0.041 BF_{10}=0.105	r=-0.023 BF_{10}=0.094	r=0.047 BF_{10}=0.110	r=0.068 BF_{10}=0.140	r=0.042 BF_{10}=0.105	r=0.021 BF_{10}=0.093	r=0.074 BF_{10}=0.151
	GLG	r=-0.010 BF_{10}=0.090	r=0.047 BF_{10}=0.110	r=-0.052 BF_{10}=0.116	r=-0.015 BF_{10}=0.091	r=-0.024 BF_{10}=0.094	r=0.135 BF_{10}=0.523	r=0.017 BF_{10}=0.092	r=-0.030 BF_{10}=0.097	r=0.044 BF_{10}=0.108	r=-0.058 BF_{10}=0.123

4. DISKUSIJA

Ryšys tarp subjektyvių potyrių ir smegenų aktyvumo nėra gerai žinomas. Vis daugiau tyrimų bando išsiaiškinti ryšį tarp objektyviai matomų fiziologinių signalų ir subjektyvių potyrių ramybės būsenos sesijos metu. ARBK yra naudingas įrankis leidžiantis susieti biologinius signalus su subjektyviais potyriais ir emocijomis. Skirtingų modalumų smegenų vaizdavimo tyrimuose buvo parodytas ryšys tarp smegenų aktyvumo ir ARBK domenų: Minčių nutrūkstamumo (Stoffers et al., 2015; Tomescu et al., 2022), minčių teorija (Marchetti et al., 2015), Pats (Tarailis et al., 2021; Tomescu et al., 2022), Planavimo (Portnova et al., 2019; Zanesco et al., 2021a), Mieguistumo (Diaz et al., 2013; Stoffers et al., 2015), Komforto (Stoffers et al., 2015; Tarailis et al., 2021; Zanesco et al., 2021a), Somatinio Sąmoningumo (Pipinis et al., 2017; Tarailis et al., 2021; Tomescu et al., 2022; Zanesco et al., 2021a), Vizualinių Minčių (Stoffers et al., 2015), Verbalinių Minčių (Tomescu et al., 2022).

Šiame darbe buvo fokusuojamasi šiems EEG analizės būdams: EEG spektrinei analizei, globalios sinchronizacijos analizei ir topografiniai analizei.

4.1 d-PKA

Dažnių pagrindinių komponenčių analizė buvo pasiūlyta kaip metodas galintis išskaidyti EEG dažnių spektrinę struktūrą į reikšmingus atskirus duomenimis grįstus komponentus.

Atlikus d-PKA, šeši faktoriai buvo išskirti: trys alfa dažnių diapazone ir po vieną delta, teta ir beta dažnių diapazonuose. Šie rezultatai sutampa su rezultatais raportuotais literatūroje, su tam tikrais topografijų skirtumais ir duomenų variabilumo paaiškinimo dalimi (Barry et al., 2020; Barry and De Blasio, 2018; Tenke and Kayser, 2005). d-PKA yra pranašesnė už tradicinę EEG spektrinę analizę, kadangi šis metodas vertina natūraliai atsirandažius dažnių komponentus, kuriems įtakos neturi nustatyti EEG dažnių diapazonai (Barry et al., 2019; Newson and Thiagarajan, 2019), ir šis metodas yra grįstas duomenimis.

Remiantis ankstesniais tyrimais, buvo tikėtasi, kad bus keletas asociacijų su alfa ir teta komponentais. Didžioji EEG dalis buvo lemta alfa aktyvyumo, trys komponentai, kurių pikai buvo ties 9 (A1), 10.5 (A2) ir 11.5 (A3) Hz kartu paaiškino 41.82% duomenų variabilumo. Šie rezultatai sutampa su kitais d-PKA tyrimų rezultatais, kur buvo išskirti nuo dviejų (Smith et al., 2020) iki penkių (Tenke and Kayser, 2005) alfa diapazono komponentų,

paaiškinančių nuo 1.4 % (A2 komponentas, kurio maksimumas buvo ties 9.5 Hz (Barry and De Blasio, 2018), iki 50% (alfa/teta komponentas, kurio maksimumas buvo ties 9 Hz (Tenke et al., 2011). Nepaisant skirtumų ties maksimaliais dažniais ir duomenų variabilumo paaiškinime, alfa komponentų topografijos tarp tyrimų yra panašios. Šiame tyrime A1, A2 ir A3 komponentų erdvinė koreliacija svyravo tarp 0.92 ir 0.98. Ankstesniame tyrime alfa komponentai buvo susiję su tiriamojo sužadinimu (Barry et al., 2020), tad šiame tyrime buvo tikimasi alfa komponentų ryšio su ARBK Mieguistumo domenu. Tačiau, nors trys alfa komponentai paaiškino beveik pusę duomenų variabilumo, tačiau teigiamas ryšys buvo tik tarp A1 įverčių ir subjektyvių Komforto įverčių (r = 0,198, BF10 = 7,115). Komforto domenas apibendrina tris teiginius: „Jaučiausi jaukiai“, „Jaučiausi atsipalaidavęs.“, „Jaučiausi laimingas“. Ankstesniuose tyrimuose šis domenas buvo siejama su plataus dažnio EEG mikrobūsenų C, E, G (Tarailis et al., 2021) ir mikrobūsenos D (Zanesco et al., 2021a) laikinėmis charakteristikomis. EEG mikrobūsenas daugiausia lemia alfa aktyvumas (Milz et al., 2017). Taigi šis rezultatas, nors ir netikėtas, iš dalies patvirtino ankstesnius pastebėjimus. Nepaisant to, sLORETA analizė, kuria bandyta lokalizuoti A1 komponentės aktyvumą, reikšmingumo lygio ($r = 0,207$, $p < 0,05$).

T1 komponentė, kurios maksimali vertė buvo ties 5.5 Hz, turėjo frontalinį vidurio linijos aktyvumą, teigimai koreliavo su ARBK Mieguistumo domeno įverčiais (r = 0,200, BF10 = 7,676), kas reiškia, jog teta aktyvumas buvo didesnis pas žmones, kurie įvertino savo mieguistumą sesijos metu didesniais balais. Šis rezultatas sutampa su Diaz ir kt. raportuotu rezultatu (Diaz et al., 2013). Taip pat, yra buvo pranešta, jog frontalinės srities teta aktyvumas (4 – 8 Hz) koreliuoja su subjektyviais Karolinksos miego skalės balais (Strijkstra et al., 2003), bei neigiamai koreliuoja su numatytojo rėžimo tinklo (NRT) aktyvumu (Scheeringa et al., 2008). NRT susijęs su asmeniškais reikšmingos informacijos apdorojimu, savirefleksija, vidiniu mąstymu (Andrews-Hanna, 2012), tiek su nuo stimulo nepriklausomomis mintimis (Mason et al., 2007), kurios pasireiškia esant ramybės būsenoje. Ankstesni tyrimai parodė jog, NRT aktyvumas teigimai koreliuoja su ARBK Mieguistumo domenu (Stoffers et al., 2015). Kaip ir Stoffers ir kt. tyrime, šiame tyrime buvo parodytas stiprus ryšys tarp ARBK Minčių nutrūkstamumo ir Mieguistumo domenų (r = 0,251, BF10 = 113,972), kas rodo, kad didesnį mieguistumą patyrusiems tiriamiesiems buvo sunkiau išlaikyti mintis. sLORETA rezultatai parodė, teigiamą koreliaciją tarp T1 komponentės ir Mieguistumo skalės limbinėje sistemoje ir priekinėje juostinėje žievėje ir tai atitinka rezultatus raportuotus literatūroje. Scheeringa ir kt (Scheeringa et al., 2008)) raportavo teta aktyvumą (2-9 Hz) medialinėje prefrontalinėje žievėje

ir priekinėje juostinėje žievėje. Smith ir kt. (Smith et al., 2020) raportavo teta komponentės (maksimali vertė ties 5 Hz) aktyvumą premotorinėje žievėje, bei galinėje priekinėje juostinėje žievėje. Nishida ir kt. (Nishida et al., 2004) parodė teat (5-7 Hz) aktyvumą priekinėje juostinėje žievėje esant budrumo būsenoje ir REM miego stadijose, bet ne lėtų bangų miego stadijoje. Teigiama koreliacija tarp individualių Mieguistumo domenų vertinimų ir limbinės srities bei priekinės juostinės žievės aktyvumo atitinka literatūroje pateikiamus rezultatus.

Tarp ARBK domenų ir delta ir beta komponentų sąsajų nebuvo pastebėta, nors Portnova ir kt. (Portnova et al., 2019) raportavo neigiamą koreliaciją tarp 2-3 Hz aktyvumo ir ARBK Planavimo domeno. Reikiaa pažymėti, kad tiek išskirtos D1 (maksimumas 0,5 Hz), tiek B1 (maksimumas 17 Hz) komponentės šiek tiek skyrėsi nuo literatūroje raportuotų komponenčių: D1 komponentė turėjo frontalinį kairės pusės aktyvumą, kurio maksimumai buvo ties FP1, AF7 ir F7 elektrodais, tuo tarpu literatūros raportuojamos D1 kompionentės aktyvumai yra pastebimi centrinėje, frontalinėje ir dešinėje frontalinėje srityse (Barry and De Blasio, 2018; Karamacoska et al., 2019b, 2019a). B1 komponentės didžiausias aktyvumas buvo pakaušinėje srityje, ties PO4, PO6 ir PO8 elektrodais, kas iš dalies atitinka rezultatus praneštus literatūroje (Karamacoska et al., 2019b, 2019a), tačiau nesutampa su kitais, kuriuose buvo stebimas frontocentrinis topografinis aktyvumas (Barry and De Blasio, 2018; Tenke and Kayser, 2005). Šių nesutapimų pobūdis nėra aiškus.

4.2 Globalios fazės sinchronizacija

Įvertinti globalų funkcinį ryšį, šiame tyrime buvo naudotas GFS metodas (Koenig et al., 2001; Rusterholz et al., 2017). GFS metodas buvo sėkmingai taikytas atliekant tyrimus tiek su klinikiniais pacientais (Koenig et al., 2001; Olamat and Akan, 2017; Smailovic et al., 2022), skirtinguose budrumo lygiuose (Achermann et al., 2016; Nicolaou and Georgiou, 2014), tačiau iki šiol nebuvo bandyta susieti GFS aktyvumą su subjektyviais potyriais. Šiame tyrime parodėme stiprų ryšį tarp ARBK Komforto domeno ir GFS reikšmių alfa (r=0,208, BF10=11,646) ir beta dažnių diapazone (r=0,199, BF10=7,842). Kitų reikšmingų sąsajų nenustatyta nebuvo.

GFS yra globalaus funkcinio ryšio matas, nereikalaujantis konkrečios smegenų srities aktyvumo dominuojančiame procese (Koenig et al., 2001). Didesnės GFS vertės nurodo globalų funkcinį ryšį tarp smegenų, kai mažos vertės nurodo funkcinio ryšio sumažėjimą ar nebuvimą.Mūsų turimomis žiniomis, šiame tyrime GFS analizė buvo atlikta su iki šiol didžiausia sveikų

dalyvių imtimi. Kaip ir ankstesniuose tyrimuose, didžiausios vertės buvo alfa dažnių diapazone (Achermann et al., 2016; Koenig et al., 2001; Smailovic et al., 2022). Aktyvumas alfa dažnių diapazone siejamas su sužadinamumu (Barry et al., 2020, 2007) ir laikomas smegenų žievės neveiklumo požymiu (Croce et al., 2020; Milz et al., 2016). Tačiau taip pat buvo pasiūlyta, kad tam tikri alfa aktyvumo aspektai, kurie nėra susiję su susijaudinimu (Barry et al., 2020). d-PKA parodėme teigiamą ryšį tarp A1 komponentės, kurios maksimali reikšmė buvo ties 9 Hz, ir ARBK Komforto domeno, taip ir GFS analizėje parodėme teigiamą ryšį tarp GFS raikšmių alfa diapazone ir to paties ARBK domeno.

ARBK Komforto domenas apibendrina tris teiginius: „Jaučiausi jaukiai“, „Jaučiausi atsipalaidavęs.“, „Jaučiausi laimingas“. Tad šis domenas gali atspindėti tiek fizinę, tiek psichinę būseną, įskaitant bendrus budrumo ir emocinės būsenos aspektus. Teigiamas ryšys tarp GFS alfa dažnio diapazono ir Komforto įverčių rodo mažesnį sužadinamumo/budrumo lygį ir didesnį atsipalaidavimą. Ankstesnis tyrimas parodė, GFS alfa (9 – 11 Hz) verčių laipsninį mažėjimą po ilgalaikės miego deprivacijos. Subjektyvūs pojūčiai esant miego trūkumui savaime nėra malonūs (Kaida and Niki, 2014), mūsų rezultatai sutampa su rezultatais, raportuotais literatūroje. Achermann ir kt. (Achermann et al., 2016) teigė, kad už globalius funkcinius ryšius atsakingas yra gumburas. Autoriai taip pat atkreipė dėmesį į Schwab ir kt. (Schwab et al., 2015) rezultatus, kur buvo parodytas gumburo aktyvumas generuojant EEG mikrobūsenos, kaip indikatorius, jog gumburas dalyvauja skirtingų smegenų žievės sričių sinchronizacijoje. Tai atitinka EEG mikrobūsenų rezultatus, rodančius sąsajas tarp kelių ramybės būsenos mikrobūsenų laikinių parametrų ir ARBK Komforto domeno. Galiausiai Ricci ir kt. (Ricci et al., 2022) parodė kad žemesnis komforto lygis virtualios realybės aplinkoje siejamas su žemesne alfa galia. Autoriai pasiūlė, kad didesnio komforto pojūtis susijęs su *top-down* mechanizmais, kurie moduliuoja regimąjį dėmesį, bei mažina išorinių dirgiklių suvokimą.

Teigiamas ryšys tarp GFS beta diapazono verčių ir Komforto domeno gali atspindėti fizinį gerbūvį. Ankstesniame tyrime Engel ir Fries (Engel and Fries, 2010) pasiūlė, jog beta dažnių diapazono aktyvumas gali būti susijęs su esama motorine būsena. Dalyviams mūsų tyrime buvo pateiktos instrukcijos sesijos metu sėdėti ramiai. Prielaida, kad beta GFS ir Komforto vertės nurodo fizinius aspektus, taip pat atitinka Stoffers ir kt. praneštus rezultatus (Stoffers et al., 2015). Autoriai raportavo teigiamą koreliaciją tarp aktyvumo sensomotoriniame tinkle ir ARBK Komforto domeno. Pažymėtina, kad yra nemažai tyrimų, rodančių neigiamą ryšį tarp beta dažnių diapazono aktyvumo

ir terminio komforto (Chang et al., 2002; Son and Chun, 2018). Mūsų atliktame tyrime nevertinome dalyvių šiluminių pojūčių ir; vis dėlto eksperimentai buvo atliekami laboratorijos sąlygomis, kur buvo palaikoma 20^{o} C temperatūra, kuri laikoma malonia/komfortiška (Oi et al., 2017). Panašiomis sąlygomis buvo parodytas teigiamas ryšys tarp beta dažnio galios ir šilumos pojūčio (Pao et al., 2022), kas rodo, kad GFS beta diapazono vertės taip pat gali būti susiję su šiluminio neutralumo/komforto pojūčiu. Galiausiai beta aktyvumas anksčiau buvo neigiamai susijęs su nerimu (Palacios-García et al., 2021), stresu (Choi et al., 2015) ir protiniu nuovargiu (Shigihara et al., 2013). Reikėtų pažymėti, kad stresas ir protinis nuovargis laikomi kraštutiniais variantais, kurių nesitikima patirti ramybės būsenos sesijos metu. Remdamiesi tuo, Diaz ir kiti (2013) parodė, kad Komfortas stipriai teigiamai susijęs su psichine sveikata (Diaz ir kt., 2013) ir neigiamai su Žalos vengimu (Diaz ir kt., 2014). Taigi manome, kad teigiama koreliacija tarp beta GFS verčių ir Komforto balų, atspindi fizinio, bet ne psichinio komforto aspektus.

Remiantis ankstesniais tyrimais, tikėjomės pastebėti keletą kitų asociacijų. Pavyzdžiui, teigiamas ryšys tarp teta aktyvumo galios charakteristikų ir Mieguistumo domeno buvo įrodytas mūsų d-PKA ir Diaz ir kt tyrimuose (Diaz et al., 2013; Tarailis et al., 2021), todėl tikėjomės, kad globalios fazės sinchronizacija šiame dažnių diapazone taip pat rodys sąsajas su Mieguistumo domeno įverčiais. Taip pat, tikėjomės, kad alfa dažnių diapazono GFS vertės bus teigiamai susijusi su Planavimo domenu, nes anksčiau buvo įrodyta teigiama koreliacija su galios spektru 12-13 Hz diapazone (Portnova et al., 2019). Tačiau nė viena iš šių sąsajų GFS matui nepasirodė. Ankstesni tyrimai taip pat parodė skirtingą poveikį GFS vertėms ir spektriniai galiai (Smailovic et al., 2022, 2018). Tai gali būti susiję su tuo, jog GFS ir spektrinė galia atspindi skirtingus smegenų aktyvumo aspektus: spektrinė galia nurodo EEG aktyvumo dydį tam tikruose dažniuose (Smit et al., 2012), o GFS (ir kiti sinchronizacijos parametrai) atspindi funkcinių ryšių buvimą smegenyse (Berger et al., 2014; Ng et al., 2013; Xiao et al., 2018).

4.3 EEG mikrobūsenos

Mikrobūsenų metodas leidžia įvertinti greitai besikeičiančius neuroninių tinklų aktyvumus, kurie dalyvauja protinėje veikloje ir apdorojant išorinę informaciją.

Pipinis ir kt (Pipinis et al., 2017) susiejo ARBK domenų įverčius su keturių klasikinių mikrobūsenų laikiniais parametrais ir parodė neigiamą koreliaciją tarp Somatinio Sąmoningumo (kuris vertinamas trimis teiginiais

„Aš suvokiau savo kūną“, „Aš galvojau apie savo širdies plakimą“, „Aš galvojau apie savo kvėpavimą“) ir mikrobūsenos C indėlio. Zanesco ir kt. (Zanesco et al., 2021a)atliko metaanalitinę koreliaciją tarp rezultatų gautų savo imtyje ir raportuotų Pipinio ir kt. tyrime (Pipinis et al., 2017) ir parodė neigiamą ryšį tarp ARBK SS domeno ir mikrobūsenos C indėlio. Tačiau Custo ir kt. (Custo et al., 2017) parodė, kad kai pasirenkama suklazterizuoti duomenis į 4 mikrobūsenas, funkciškai skirtingos, tačiau erdviškai panašios mikrobūsenos C ir F yra suklasterizuojamos į vieną mikrobūseną C. Mūsų tyrime optimalus mikrobūsenų skaičius buvo nustatytas k=7, sutampantis su rezultatais raportuotais Custo ir kt. tyrime (Custo et al., 2017). Svarbu tai, kad erdvinė koreliacija tarp mikrobūsenos C ir F buvo apie 0.7, kas patvirtina Custo ir kt (2017) tyrimo rezultatus, kad funkciškai skirtingos, bet erdviškai panašios mikrobūsenos C ir F gali būti sujungtos į vieną mikrobūseną. Tai patvirtina ir erdvinės koreliacijos analizė tarp mikrobūsenos C, kada klasterių skaičius lygus 4, ir mikrobūsenos F, kada klasterių skaičius lygus 7.

Manome, kad šiame darbe gauta neigiama koreliacija tarp mikrobūsenos F indėlio ir SS domeno atkartoja tą patį ryšį pastebėtą Pipinio ir kt. bei Zanesco ir kt. (Pipinis et al., 2017; Zanesco et al., 2021a) tyrimuose. Custo ir kt. (2017) parodė, jog mikrobūsenos F generavimo šaltiniai yra priekinėje juostinėje žievėje, viršutiniame priekiniame vingyje, viduriniame priekiniame vingyje ir saloje. Šie regionai persidengia su Dirgiklių Svarbumo Įvertinimo Tinklu (SDSĮT) ir mikrobūsenos C generavimo šaltiniais, raportuotais Britz ir kt. (Britz et al., 2010) .Britz ir kt (2010) susiejo mikrobūseną C su interocepcinės informacijos integracija ir emociniu jautrumu. Keletas tyrimų, kur duomenys buvo pasirinkta suklasterizuoti į 4 mikrobūsenas, raportavo padidėjusį mikrobūsenos C aktyvumą per ramybės būseną lyginant su skirtingomis užduotimis (Liu et al., 2020; Seitzman et al., 2017; Zappasodi et al., 2019) ir susiejo šią mikrobūseną su NRT (Bréchet et al., 2019; Custo et al., 2017). Tikėtina, kad NRT ir lėmė neigiamą koreliaciją tarp tarp mikrobūsenos C dažnio ir ARBK Komforto domeno. Gebėjimas atsipalaiduoti ir jaustis patogiai yra susijęs su interocepciniais aspektais, kuriais siekiama palaikyti fizinę ir emocinę pusiausvyrą (Forkmann et al., 2019; Wei and Van Someren, 2020). Komforto domenas anksčiau buvo susietas su gebėjimu pereiti tarp užduočių (Simpraga et al., 2021), koreliavo su charakterio bruožais - savarankiškumu (siejamu su asmens gebėjimu valdyti elgesį pagal situacinius poreikius) (Diaz et al., 2014) ir psichiniu bei fiziniu gerbūviu (Diaz et al., 2013).

Reikia pažymėti, kad ARBK Komforto domenas taip pat teigiamai koreliavo su mikrobūsenų E ir G trukme. Tačiau dėl to, kad nebuvo iškeltos jokios prielaidos dėl kitų mikrobūsenų, išskyrus C ir F, šie ryšiai turėtų būti

laikomi tik tiriamaisiais. Nepaisant to, bandėme aptarti pastebėtas koreliacijas, remiantis turimomis funkcinėmis žiniomis apie šias mikrobūsenas.

Mikrobūsena E yra sąlyginai nauja ir yra pranešta tik keliuose nesenose tyrimuose. Brechet ir kt. (Bréchet et al., 2019) nustatė pagrindinius generavimo šaltinius dešiniojoje vidurinėje priekinėje žievėje, kuri yra NRT dalis, kuri dalyvauja minčių teorijoje ir protinėse simuliacijose (Chen et al., 2020), o Custo ir kt. (Custo et al., 2017) nustatė šaltinius priekinėje juostinėje žievėje, galinėje juostinėje žievėje ir priešpleistyje, šie regionai persidengia su NRT. Todėl priešingas ryšys tarp Komforto domeno ir mikrobūsenų C ir E greičiausiai atspindi skirtingus NRT veikimo aspektus (Andrews-Hanna, 2012).

Mikrobūsena G iki šiol buvo raportuota tik šešiose tyrimuose (Custo et al., 2017; Damborská et al., 2019a; Luo et al., 2020; Takarae et al., 2022; Tarailis et al., 2021; Zanesco et al., 2021b), tad funkciniai šios mikrobūsenos aspektai nėra gerai žinomi. Custo ir kt (2017) lokalizavo šaltinius dešinioje apatinėje skiltyje, viršutiniame smilkininiame vingyje ir smegenėlėse, dėl to, mikrobūsena G buvo susieta su sensomotoriniu smegenų tinklu. Stoffers ir kt. (Stoffers et al., 2015) raportavo teigimą koreliaciją tarp ARBK Komforto domeno ir funkcinio ryšio sensomotoriniame smegenų tinkle. Tad mūsų tyrime pastebėtas teigimas ryšys tarp mikrobūsenos G trukmės ir Komforto įverčių galimai atspindi geros fizinės savijautos aspektą, atsirandantį dėl tinkamo sensomotorinio tinklo aktyvumo.

Galiausiai ARBK Pats domenas teigiamai koreliavo su mikrobūsenos B dažniu, ir neigiamai koreliavo su su mikrobūsenos D trukme. Ankstesniuose tyrimuose mikrobūsena B buvo susieta su verbalizacija (Antonova et al., 2022; Milz et al., 2016) ir vizualinės informacijos apdorojimu (Antonova et al., 2022; D'Croz-Baron et al., 2021; Seitzman et al., 2017) ir susieta su aktyvumo vizualiniame smegenų tinkle (Britz et al., 2010; Custo et al., 2017), Brechet ir kt. (Bréchet et al., 2019) susiejo mikrobūseną B su autobiografine atmintimi, scenos vizualizacija ir savęs vizualizacija scenoje. Vellante ir kt. (Vellante et al., 2020) parodė neigiamą koreliaciją tarp šios mikrobūsenos ir disocijacijos ir nerimo būsenų bipolinio sutrikimo pacientuose, interpretuodami rezultatus kaip atspindinčius autobiografinės atminties sutrikimus ir padidėjusį susitelkimą į save. ARBK Pats domenas vertina šiuos teiginius: „Aš galvojau apie savo veiksmus", „Aš galvojau apie save", „Aš galvojau apie savo elgesį". Pastarieji du teiginiai ypač įdomūs Brechet ir kt. (2019) ir Vellente ir kt. (2020) tyrimų rezultatų kontekste, kadangi abu tiesiogiai susiję su autobiografine atmintimi ir savęs vizualizavimu konkrečioje scenoje.

Tad matomas ryšys tarp mikrobūsenos B ir Pats domeno atspindi savęs vizualizavimo aspektus. Nors Pats domenas yra orientuotas į vidinius išgyvenimus, mikrobūsena D siejama su į išorę orientuotos informacijos apdorojimu (Schiller et al., 2019). Keletas tyrimų parodė padidėjusį šios mikrobūsenos aktyvumą atliekant įvairias užduotis ir susiejo šią mikrobūseną su dėmesio, pažintinės veiklos ir darbinės atminties funkcijomis. (Bréchet et al., 2019; D'Croz-Baron et al., 2021; Seitzman et al., 2017; Zappasodi et al., 2019) ir fronto-parietaliniu tinklu (Britz et al., 2010; Custo et al., 2017). Mūsų rastas ryšys tarp Pats domeno ir mikrobūsenų B ir D galimai atspindi atsiskyrimą nuo išorinės aplinkos esant ramybės būsenoje užmerktomis akimis.

4.4 Bendrinė diskusija

EEG signalas savyje turi informaciją apie galią, fazę, globalius erdvinius ir laikinius paternus. Visa ši informacija yra reikšminga siekiant suprasti ryšį tarp smegenų aktyvumo ir subjektyvių potyrių. Topografinė analizė atspindi momentinį neuroninių tinklų aktyvumą, kuris yra nepriklausomas nuo dažnių diapazonų (Férat et al., 2022). Dažnių analizė suteikia informacijos apie tai, kuris dažnis ar dažnių diapazonas yra optimaliausias tam tikros kognityvinės ar sensorinės informacijos apdorojimui. Fazės vertinimas suteikia informacijos apie tai kaip skirtingos smegenų sritys komunikuoja skirtinguose dažniuose.

Kai buvo parodyta šiame darbe, skirtingai to paties signalo aspektai yra susiję tiek su skirtingais, tiek su tais pačiais ramybės būsenos domenais. Pavyzdžiui, EEG signalo galia, naudojant dažnių pagrindinių komponenčių analizę parodė, kad aktyvumas teta dažnių diapazone (5.5 Hz) yra susijęs su mieguistumo domeno individualiais vertinimais, o globalios fazės sinchronizacija – ne. Kita vertus, globalios fazės sinchronizacija beta dažnių diapazone koreliuoja su Komforto vertinimais, bet ne šio diapazono galios vertinimo parametrai. Galiausiai, tiek galia, tiek fazės sinchronizacija alfa dažnių diapazone koreliuoja su Komforto domeno vertinimais, kas rodo, kad abu šie signalo aspektai gali būti jautrūs šiam subjektyviam vertinimui. Galiausiai EEG mikrobūsenos C, E ir G buvo susijusios su Komforto domenu. Tai rodo, kad skirtingi subjektyvūs komforto vertinimai yra jautrūs skirtingiems EEG parametrams.

Reikia pažymėti, kad gautos koreliacijos nebuvo stiprios, tačiau atitiko fiziologinių ir psichologinių kintamųjų sąsajų stiprumo intervalą. Taip pat yra žinoma, kad koreliacijos stipriai varijuoja tarp tyrimų su mažmis imtimis ($n < 250$) (Schönbrodt and Perugini, 2013). Imtis naudota šiame darbe yra iki šiol

didžiausia, kurioje buvo naudotas Amsterdamo ramybės būsenos klausimynas. Vis dėlto svarbu, kad ateityje atliekant individualių skirtumų tyrimus apimtų didesnes imtis, kad jose būtų galima aptikti nedideles ar vidutinio dydžio koreliacijas tarp ARSQ vertinimų ir EEG parametrų.

IŠVADOS

1. Individualūs frontalinės T1 komponentės įverčiai, kurios pikas buvo ties 5.5 Hz, teigiamai koreliavo su subjektyviais Mieguistumo vertinimais.
2. Individualūs alfa komponentės įverčiai, kurios pikas buvo ties 9 Hz, teigiamai koreliavo su subjektyviais Komforto vertinimais.
3. Globalios fazės sinchronizacijos vertės alfa (8 – 13 Hz) ir beta (14 - 30 Hz) teigiami koreliavo su subjektyviais Komforto vertinimais.
4. Mikrobūsenos F indėlis neigiamai koreliavo su subjektyviais Somatinio suvokimo įvertinimais.
5. Mikrobūsenos B dažnis ir mikrobūsenos D trukmė koreliavo su subjektyviais domeno Pats vertinimais.
6. Mikrobūsenos C dažnis neigiamai koreliavo su Komforto domenu; Mikrobūsenų E ir G trukmės teigiamai koreliavo su subjektyviais Komforto vertinimais.

NOTES

NOTES

NOTES

Vilniaus universiteto leidykla
Saulėtekio al. 9, III rūmai, LT-10222 Vilnius
El. p. info@leidykla.vu.lt, www.leidykla.vu.lt
bookshop.vu.lt, journals.vu.lt
Tiražas 12 egz.